An-Najah National University
Faculty of Graduate Studies

THE IMPACT OF DEMAND SIDE MANAGEMENT ON THE UTILITY ACTIONS FOR IMPROVING THE OPERATION OF DISTRIBUTION SYSTEMS CONSISTING PV GENERATORS

By
Malaka Mustafa Abdel Raheem Hanhan

Supervisor
Dr. Moien A. Omar

This Thesis is Submitted in Partial Fulfillment of the Requirements for the Degree of Master of Electrical Power Engineering, Faculty of Graduate Studies, An-Najah National University, Nablus - Palestine.

2025

THE IMPACT OF DEMAND SIDE MANAGEMENT ON THE UTILITY ACTIONS FOR IMPROVING THE OPERATION OF DISTRIBUTION SYSTEMS CONSISTING PV GENERATORS

By

Malaka Mustafa Abdel Rahim Hanhan

This Thesis was Defended Successfully on 04/02/024 and approved by:

Dr. Moien A. Omar Supervisor	 Signature
Dr. Jafar Saif-Aldin External Examiner	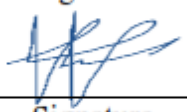 Signature
Dr. Maher Khammash Internal Examiner	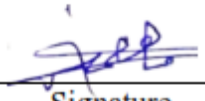 Signature

Dedication

I dedicate this work to all my fellow countrymen, to the martyrs of Palestine, to our courageous prisoners, to the wounded and their suffering, to my homeland and our holy sites, to our just cause, and to everything Palestinian, both within and beyond our borders.

To my parents, family, friends, and everyone believes in me.

To my dear paternal uncle who always supported me (Ibrahim Hanhan).

I dedicate this thesis.

Acknowledgment

I would like to express my deep gratitude to my supervisor for his great efforts in completing this work and for providing all the valuable advice and guidance throughout the preparation period of this work. His deep experience was the reason for developing my ideas and achieving my goals. All thanks and appreciation, my dear supervisor: Dr. Moien A. Omar.

Great thanks and gratitude to my parents for their support and encouragement always. They have been a source of inspiration to me throughout my life. Their prayers and pride in me have been a motivation to achieve my dreams. Mom and Dad, I am very grateful to you.

To my dear paternal uncle (Ibrahim Hanhan) who supported me greatly throughout my life and has always been there for me. For this, I would like to sincerely thank him. His encouragement and support have helped me accomplish my goals and deal resolutely with life's challenges. I'm grateful for your love and support, for being there for me no matter what, and for always being my source of confidence, pride, and happiness.

To my dear brothers and sisters, I would like to express my heartfelt thanks. Thank you for standing by my side through every circumstance, and for your love, which is priceless.

I would like to express my sincere thanks and gratitude to my dear family members. You are the family I prize. Thank you for your constant presence in my life, for your understanding and care, and for every moment you have shared with me.

My great veteran friends. Thank you for your support and trust. Thank you for standing by my side in joy and sorrow. Thank you for always being there for me.

Declaration

I, the undersigned, declare that I submitted the thesis entitled:

THE IMPACT OF DEMAND SIDE MANAGEMENT ON THE UTILITY ACTIONS FOR IMPROVING THE OPERATION OF DISTRIBUTION SYSTEMS CONSISTING PV GENERATORS

I declare that the work provided in this thesis, unless otherwise referenced, is the researcher's own work, and has not been submitted elsewhere for any other degree or qualification.

Student's Name: Malaka Mustafa Abdel Raheem Hanhan

Signature: *Malaka Hanhan*

Date: 04/02/2025

Table of Contents

List of Tables

List of Figures

List of Schemes

List of Appendices

THE IMPACT OF DEMAND SIDE MANAGEMENT ON THE UTILITY ACTIONS FOR IMPROVING THE OPERATION OF DISTRIBUTION SYSTEMS CONSISTING PV GENERATORS

By
Malaka Mustafa Abdel Raheem Hanhan
Supervisor
Dr. Moien A. Omar

Abstract

This thesis investigates the impact of demand-side management (DSM) strategies on utility actions for improving the operation of distribution systems with high photovoltaic (PV) penetration. A case study was conducted using OpenDSS software, applying the IEEE 30-bus test network. A 50 MW PV system was integrated into bus 21, demonstrating its ability to reduce total electrical losses in transmission lines from 9308.34 kW to 7742.83 kW.

Meanwhile, the study examined the application of various DSM strategies to further enhance network performance after hosting the PV system. Direct Load Control (DLC) reduced network losses to 5365.5 kW, while the Time-of-Use (TOU) tariff strategy significantly reduced losses to 3736.9 kW. Additionally, the Conservation Voltage Reduction (CVR) strategy improved overall network voltage profiles, particularly decreasing the voltage at bus 21 from 1.0524 p.u. to 1.0442 p.u. and at bus 11 from 1.0819 p.u. to 1.0748 p.u.

The hosting capacity analysis revealed that increasing PV penetration initially reduced electrical losses, with significant reductions observed at penetration levels of 15 MW, 30 MW, 50 MW, and 70 MW, corresponding to losses of approximately 9830 kW, 8000 kW, 7000 kW, and 5800 kW, respectively. However, beyond a hosting capacity of 70 MW, further increases in PV penetration led to a rise in losses, reaching 7900 kW at 150 MW and exceeding 12,200 kW at 200 MW. The use of DSM strategies effectively mitigated these losses even at higher penetration levels. For instance, DLC reduced losses to approximately 6000 kW, and TOU reduced them further to 5000 kW at a 200 MW PV hosting capacity. These findings highlight the critical role of DSM strategies in enhancing the operational efficiency and reliability of distribution systems with high PV integration.

Keywords: Demand Side Management (DSM); photovoltaic (PV); Direct Load Control (DLC); Conservation Voltage Reduction (CVR); Time-of-Use (TOU) tariff.

Chapter One

Introduction and Literature Review

1.1 Background of power system and distribution resources

The electrical power system is defined as the most complex human-made system, consisting of various electrical components such as generators, loads, transmission lines, transformers, buses, and circuit breakers[1]. This system primarily produces energy, transmits it through power lines, and facilitates consumption. When this system serves a large area, including industries, it is referred to as the electrical grid.

Generation stations are typically located in a central area, relatively distance from the consumption site. These stations convert energy from various sources into electrical energy, which is transmitted through high-voltage transmission lines to distribution stations. At these stations, the voltage is reduced by sub-distributed voltage transformers to levels suitable for residential, industrial, and commercial use. The voltage is further reduced to reach the end user at low voltage. These electrical networks are often single-source, but multiple networks can be interconnected to enhance reliability and security [2].

Conventional electricity distribution networks operate in a radial mode, with power moving from the main generator to consumer end loads at low voltage as in Figure 1 [3]. These networks are easily reconfigurable and consist of separate feeders connected to a single substation.

Figure 1

Conventional radial power system configuration

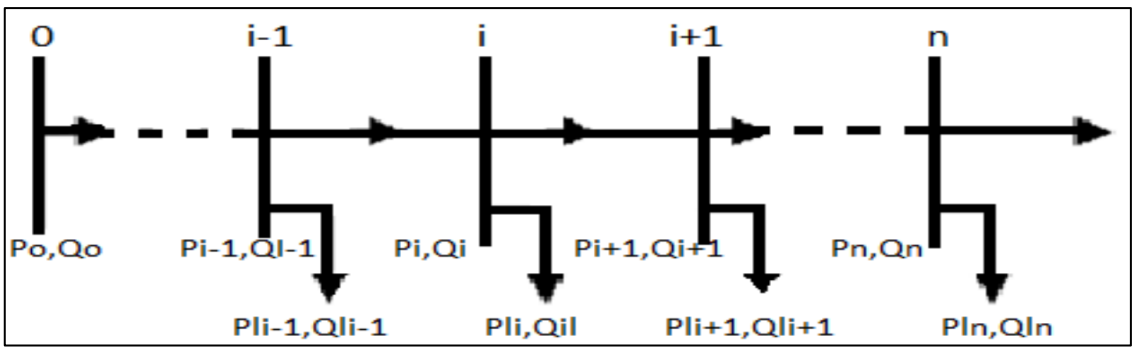

The conventional Power system can divided into three subsystems: generation system, transmission system, and distribution system as shown in Figure 2 [4]. Power plants use nuclear energy, fossil fuels, or hydroelectric power to generate electricity. The produced energy is then sent over the transmission lines. Before sending, this energy is magnified to a higher voltage, after passing through the transmission system, the energy is delivered to various users via the distribution system where the voltage is lowered [4].

Figure 2

Electrical power subsystem

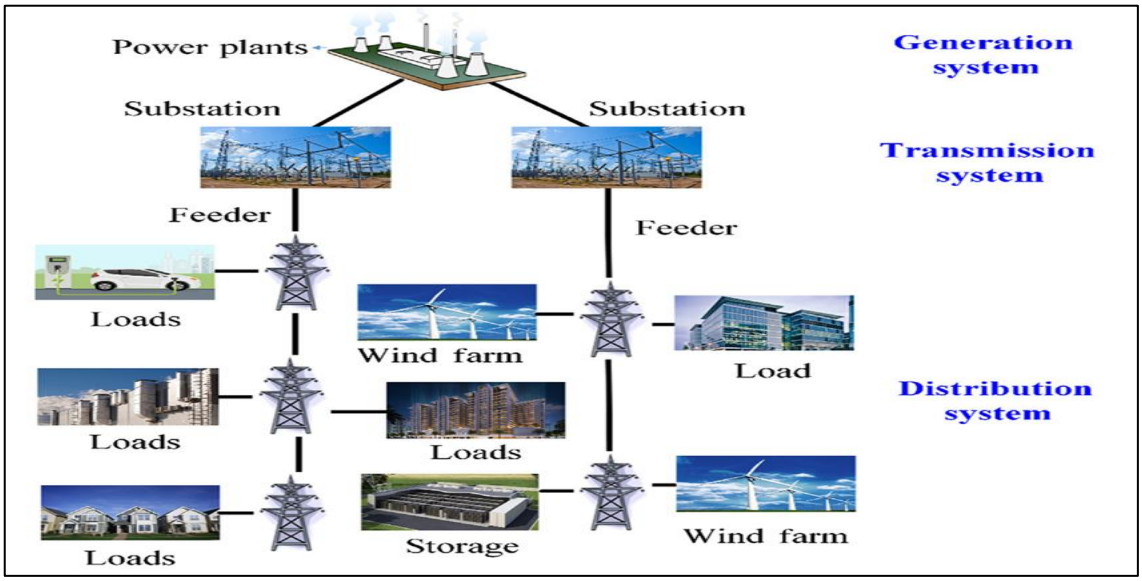

Electricity in conventional power grids is centralized and only flows from generators to consumers (high voltage to low voltage). Wind, solar, batteries, biomass, micro-turbines, fuel cells, and other distributed energy resource (DER) units are being developed in response to technological and environmental challenges, along with control systems and demand response capabilities, these microgrids incorporate DER units for power generation and storage. Microgrid studies are being improved by advanced power electronics, data management, control theory, renewable energy, wireless networks, interconnected systems, and high-performance computing. A typical Microgrid prototype consists of PV panels, batteries, controllers, and power electronics equipment that can function in both off-grid mode and on-grid mode [5].

Distributed power generation (DG), often referred to as alternative energy systems, it is expected to significantly affect future power grids. DG units are increasingly being

integrated into electricity distribution networks because of their benefits, playing a crucial role in smart grid technologies and can help maintain power supply during power outages.

The electrical system is one of the most complicated and biggest systems in the world, encompassing many complex components from electrical generators to the smallest devices used by consumers. The operations, planning, and predictions within this system are highly intricate. Until a few decades ago, these systems were simpler than today, primarily consisting of controllable generators with predictable operating times with semi-fixed loads or recurring during a particular period.

The current complexity arises from the integration of renewable energy sources, which are difficult to predict, as well as the introduction of unexpected loads, such as electric vehicles and storage battery chargers. These developments have exacerbated the challenges and difficulties facing the electrical system in general [6]. These developments to the traditional system are evident in the Figure 3 [7].

Figure 3

Structural distinctions between conventional grids and distributed generator

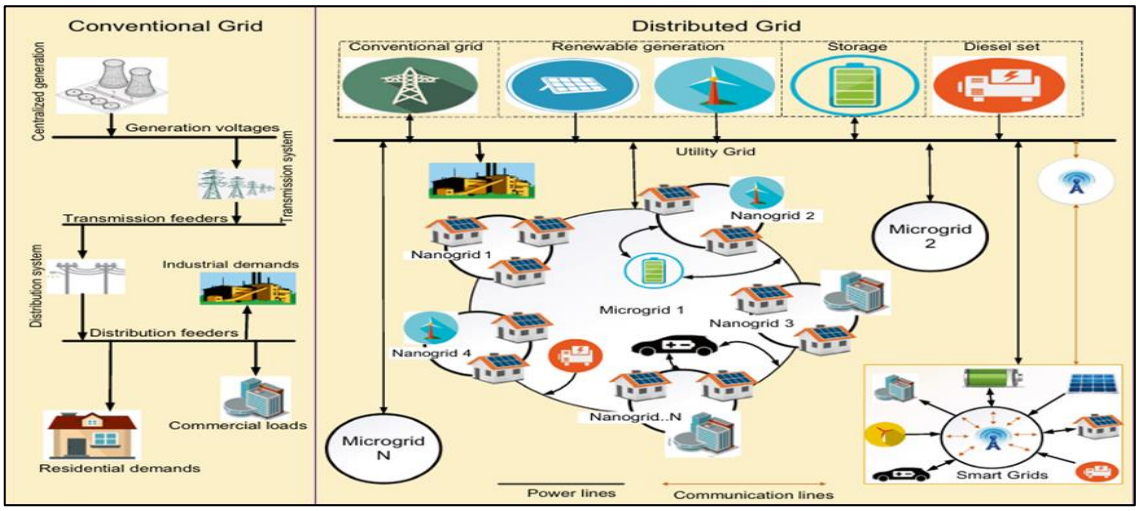

1.2 Background of smart grid and smart meter

In recent decades, conventional energy systems have undergone a significant transformation as they evolve into smart grids. This transition has brought numerous advantages to various aspects of power supply, including generation, transmission, distribution, and consumption. To fully embrace the smart grid concept, comprehensive

and efficient reforms have been necessary in all these areas to adapt to the innovative smart structure.

One noteworthy Energy generation is one area that has seen a significant shift. Conventional power grid units have historically been largely responsible for energy generation. On the other hand, new technologies, especially renewable energy sources, are integrated into smart energy systems. Solar and wind power generation systems are among the most popular, even though the smart power grid offers an environment that is conducive to the integration of several kinds of renewable energy resources. However, when compared to traditional dispatchable power generation units, the stochastic nature of solar and wind energy resources introduces fluctuation in power generation. Power produced by solar and wind energy systems is heavily reliant on weather. This unpredictability in the power generation from renewable systems can bring challenges to system flexibility.

The smart grid represents a digital revolution in the distribution system. It's essentially a comprehensive "system of systems" designed to enhance the electrical current system, particularly for long transmission lines, to reduce losses. The introduction of the new smart grid incorporates techniques like "real-time consumption estimation," which is expected to reduce high electricity bills for consumers. An electricity network that can economically integrate the behavior and actions of all users connected to it—generators, consumers, and those who do both— It aims to optimize economic efficiency, a sustainable power system with minimum losses and high quality, supply security, and safety is known as a smart grid.

This transformation has been made possible by adopting new technologies such as SCADA sensors, enabling two-way communication, and the implementation of intelligent autonomous controllers. These advancements have created unprecedented opportunities. While there are various definitions of the smart grid, it is important to note that it is not limited to specific applications based on individual preferences. Instead, it represents an evolution from the traditional one-directional power flow, which goes from production plants through transmission lines to distribution systems and end consumers (residential, commercial, and industrial).

The smart grid is a forward-looking, improved version that facilitates bi-directional energy transfers, along with data communication and power network control. It is crucial to identify and address any shortcomings in the system to further its development [8].

The vital goal of Smart Grids operation includes the use of software, hardware, and technologies that help electricity companies to identify and instantly correct imbalances between generations and demand to improve service quality, increase energy reliability, and reduce costs. There are several ways to represent the Smart Grids operating scheme. The Smart Grid Interoperability Panel (SGIP) and the National Institute for Standards and Technology (NIST) designed an algorithm or methodology for organizing and/or planning the different interconnections of a Smart Grid network, describing their seven main domains: service providers, transmission, generation, customer, distribution, market, and operators [9].

Finally, we can say that in the era of automation, the smart grid holds immense potential not only for the power system but also for the entire country. It represents a substantial enhancement to the electrical infrastructure, delivering improvements in efficiency, reliability, economic viability, and environmental sustainability in the distribution system. It is widely acknowledged that the smart grid is the future of power generation, transmission, and distribution, ultimately leading to more satisfied consumers.

The emergence of renewable energy sources as we know can introduce fluctuations into the power system, but the overall performance is expected to be outstanding in the future power network. The incorporation of information technology (IT) into the electric power system brings an added layer of security through its self-healing capabilities. This means that the grid can detect and respond to issues autonomously, ensuring a more resilient and reliable power supply.

In summary, the smart grid represents a transformative force that not only modernizes our power systems but also paves the way for a more sustainable, efficient, and consumer-centric energy future.

Absolutely, the advent of the smart grid system has brought smart meters into the spotlight. These meters, equipped with technologies like SCADA (Supervisory Control

and Data Acquisition), have revolutionized the way we measure and monitor energy consumption in real time. This is indeed a significant benefit for consumers.

Smart meters are crucial tools for utilities, providing real-time power consumption and price information to consumers. They are part of Advanced Metering Infrastructure (AMI), which combines electronic meters with two-way communication technology for information sharing, monitoring, and control [10]. They play a crucial role in integrating distributed generation sources like solar panels and wind turbines into the grid, enabling real-time monitoring and control of these resources. Smart meters are essential to accomplishing a smart grid (SG). They help balance renewable energy sources, enable customer operations, aid in peak load management, reduce commercial losses, detect energy theft, improve grid reliability, introduce innovative tariff structures, and generate accurate bills.

1.3 Demand Side Management (DSM) in Modern Power Grids

Most developed countries flow current electrical grid infrastructure that is built using designs that date back more than 50 years. This outdated electrical grid infrastructure uses transmission and distribution networks to distribute power to customers after it is generated centrally. In order to coordinate new generation technologies; including distributed energy resources (such as renewable energy), energy storage technologies (such as plug-in electric vehicles), and micro-grids, this outdated electrical grid must rapidly change. Modern Smart Grid technologies, like the communications network for sharing data between different agents that will also be necessary to integrate with the current grid infrastructure as shown Figure 4 [11].

Figure 4

Smart grid and energy management

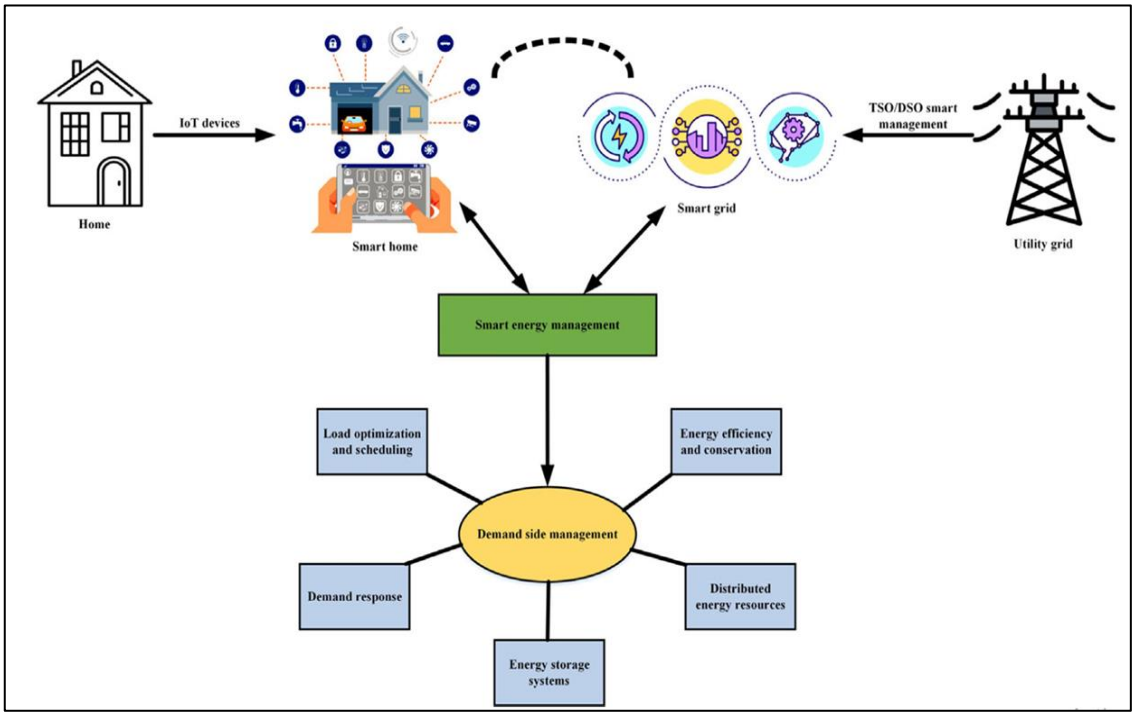

Matching power supply and demand, regardless of demand, at a set price is the traditional method of power delivery. This implies, however, that the generation capacity and the load profile, which peaks at specific times of the day, must coincide. More significantly, a high peak-to-average demand ratio (PAR) results from the critical peaks in the load profile over a year typically occurring less than 5% of the time. This implies that in order to meet these peaks, significant capacity investment is required, which significantly lowers system efficiency and capacity utilization. This is where demand-side management comes into play; it is essential to enhance the capacity of the existing grid. DSM encompasses a wide range of actions on the demand side of the power system, ranging from simple measures like replacing incandescent light bulbs with fluorescent ones to employing sophisticated controllers for dynamic load management [12].

The management of energy consumption in the electrical grid system's current load profile is a major concern. Due to the introduction of increasingly intelligent and efficient devices, a standard energy management strategy is required at the supplier and consumer levels.

This management is made possible by implementing several effective approaches and loss-reduction techniques in the load appliances and on the smart grid system. Both consumers and energy production companies partaking in the market will get a great deal from such an enhancement in the load profile. By executing such standardized efficiency and exhaustion management techniques, serious problems like reliance on fossil fuel consumption, emanations, energy cost, and other sustainability factors can be somewhat resolved. As the conventional grid, the system is transformed into smart grids, different communication, and the Internet of Things [11].

DSM can be significantly classified into four classes: Energy Efficiency (EE), Demand Response (DR), Spinning Reserve (SR), and Virtual Power Plants (VPP).

Demand Side Management (DSM) is defined as “One of the core contemporary strategies to control energy consumption in the developing world with inadequate electrical capacity, rising fuel prices, and environmental pollution issues.

It can be defined as “The economical method of electricity network management that aims to lower costs and capacity requirements, increase the use of renewable energy sources, and lower emissions from power systems” [13].

To achieve sustainable energy, which seeks to optimize energy use and reduce emissions, demand-side management, or DSM, is essential. Therefore, DSM uses a variety of techniques to increase the power system's operational flexibility as shown in Figure 5 below [14]:

- Load curtailment: the utility can turn off some of the loads in order to reduce the power consumed when high consumption is experienced by the user while maintaining the loads with the highest priority active.
- Valley filling or load shifting aims to alter load curves to achieve higher load factors within predetermined time margins. This can be done by either changing the load demand distribution plan throughout the day or by incentivizing end users to use energy during off-peak hours when tariffs are lower.
- Peak clipping is also aimed to reduce the demand during peak hours, particularly when installed capacity is insufficient to meet peak demand. Distributed generation can be used in peak hours in order to reduce the utility peak demand, Storage device

also can be used to the same purpose and it will increase the reliability of the overall system.

- Strategic conservation is aims to minimize the overall energy consumption; it may be achieved by adopting more efficient equipment and appliances, which is particularly essential at the global level.
- Load shifting is a technique for managing electrical loads that involves shifting demand for electricity from peak to off-peak hours of the day; in other words, load shifting is just shifting electricity consumption to a new period while keeping overall consumption constant.
- Strategic load growth programs aim to increase market share, improve customer productivity, and increase utility per kWh energy sales, similar to valley filling but with higher sales levels.
- Flexible load shape involves strategic additions beyond valley filling, using intelligent systems and efficient equipment, and promoting customer acceptance of variations in electricity service quality for specific incentives.

Figure 5

Demand side management strategies

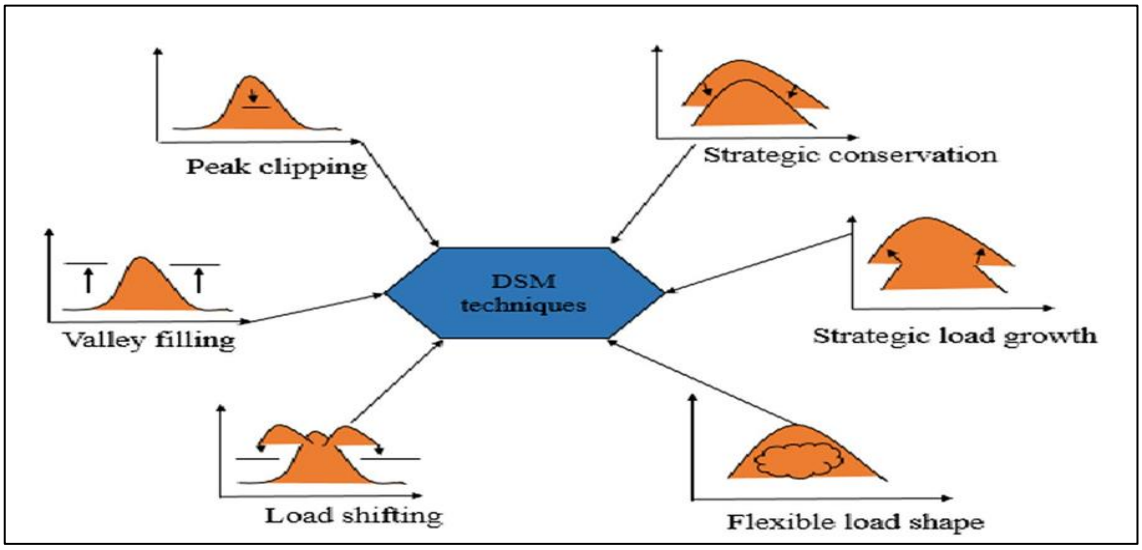

1.4 Challenges and Opportunities of PV Integration

An electrical system that converts sunlight into electrical energy is called a photovoltaic system. The sun is the most well-known renewable and limitless source of energy.

1.4.1 PV Integration Opportunities

Solar energy technologies are among the least carbon-intensive ways to generate electricity in a world where carbon emissions are becoming more and more limited. Life-cycle assessments unequivocally show that solar power has a lower carbon footprint from "cradle to grave" than fossil fuels, and it emits no emissions during generation.

So solar power is a rapidly growing, environmentally friendly, and rapidly growing energy source expected to provide over 33% of the world's energy supply in the next decades. Its CO2 emissions are 5% of gas-fired plant emissions and 10% compared to coal-fired plants. Governments are backing photovoltaic research and development programs, as it has the potential to contribute to sustainable energy supplies and mitigate greenhouse gas emissions. To achieve its potential, photovoltaic technology must achieve an acceptable cost-to-performance ratio and a net energy yield greater than zero.

Therefore, the solar photovoltaic system opens the door to a more sustainable society, but it has also a major problem the power supply from renewable energy sources is intermittent. This leads to uncertainty in keeping the balance between production and consumption. A problem also opens the door to the demand side management by trying to oblige the end-users to adapt their consumption to the existing production to avoid power outages that may happen when unbalanced happens.

1.4.2 PV integration challenges

PV generation variability

- PV power output exhibits variable patterns, leading to larger peak-to-valley differences in daily load profiles and increased ramping requirements. Real-time PV power can also experience significant fluctuations due to local weather conditions. These fluctuations can create challenges in load balancing and voltage control within power systems [15].

- Sharp fluctuations in PV power are often caused by moving clouds or precipitation temporarily blocking sunlight. While solar irradiance at a single point may fluctuate considerably during such events, the overall solar irradiance over a broader area remains relatively stable. This phenomenon has been evidenced by distributed PV power data collected from different regions [16] [17].
- Inconsistency with Demand Patterns: PV systems usually produce electricity during the day، but evenings are when demand is at its highest. In order to balance the grid, this leads to a mismatch between generation and demand, necessitating high ramp rates and additional reserve capacity.

Adaptability Issues

- Traditional large-scale generation systems, such as thermal steam power plants, struggle to adapt to rapid changes in electricity demand. In contrast, solar PV production is inherently intermittent due to factors like weather and cloud cover.
- Distributed PV systems show diurnal and seasonal production patterns, with peak generation typically occurring during midday and in summer months. As mentioned before cloud cover can cause sudden rapid and substantial fluctuations in solar power output, sometimes reaching 50% to 60% within minutes or seconds. These challenges result in fundamental costs, as PV-generated power may not always be reliable, and traditional energy systems might have to maintain high backup supply levels or rapidly respond to changing conditions [18].
- On the other hand, on a sunny day, it is common for all PV units in a region to generate nearly their maximum output at the same time. As a result, the planning and design of distribution grid infrastructure are increasingly influenced by the feed-in of electricity from high PV systems [19].

1.5 Role of IEEE 30-Bus System in Power System Research

The IEEE-30 bus test System represents a portion of the American standard Electric Power System (in the Midwestern US). This standard, along with other IEEE n-Bus Test Systems is primarily used by researchers and scholars to implement new ideas and concepts and tackle various problems, It is also used to validate new algorithms and methodologies, providing a common reference point for evaluating performance and

accuracy. This facilitates comparisons across different studies and ensures consistency of results.

The system is widely adopted in academic curricula for teaching power systems analysis and design. It provides students with hands-on experience in modeling, simulation, and problem solving, enhancing their understanding of complex power system dynamics.

This test systems simulate real-world electricity networks, it is a miniature network that contains all the components of electricity networks, including generators, transformers, transmission lines, loads, and capacitors. Globally, they have been utilized in many different research efforts on load flow analysis, fault analysis, and stability studies; they can be easily modified or expanded to include more buses, generators, and loads So that researchers can study more complex and larger systems.

The system is frequently used in optimization research, such as optimal power flow (OPF) studies. Researchers use various optimization techniques, including genetic algorithms and particle swarm optimization, to reduce operating costs, minimize losses, and optimize voltage profiles, making it a key resource for developing smart grid solutions.

IEEE30-Bus system has played avital role in the modern approaches that related to adding distributed generation sources such as PV, wind, and others, Researchers can simulate scenarios involving solar panels, wind turbines, and other renewable resources, and evaluate their impacts on grid stability, reliability, and overall performance.

The role of the IEEE 30-Bus system is to provide a unified platform for comparing results across different studies, facilitating collaboration and knowledge sharing in the research community.

In conclusion, the IEEE 30-Bus system is an invaluable asset in power systems research. Its role as a standard, testbed, educational tool, and resource for evaluating new technologies enhances its importance in advancing the field of electrical engineering and addressing contemporary energy challenges.

1.6 Problem Statement

The problem of our thesis is the increase in carbon dioxide emissions in the atmosphere, as well as other key greenhouse gases such as methane and nitrous oxide, and the consequences of that; CO2 is emitted into the atmosphere in many ways. The largest source of natural carbon emissions is the exchange of carbon dioxide between the oceans and the atmosphere. Animals and plants also emit CO2 through the process of breathing (breathe in oxygen; breathe out CO2). In addition, when these plants and animals decompose, organisms within the soil breathe to produce energy and emit more CO2 into the atmosphere.

Nature generally keeps most of these emissions in balance. Plants absorb CO2 through photosynthesis, and oceans absorb just about as much carbon dioxide as they let off. Carbon cycles through our air, water, and soil in a continuous process that supports life on earth.

Many recently researches show increasing in global energy demand and consumption. As a result, levels of carbon dioxide in the atmosphere and other key greenhouse gases such as methane and nitrous oxide are all rising. If no action is happen against that, the problems are compounded including the changes in climatic conditions and the melting of glaciers and ice caps and the planet Earth will eventually turn into an inhabitable place.

To avoid this Catastrophe, a global solution is needed to reduce the energy consumption by making strenuous attempts to reduce the per capita consumption of energy and so decrease the burning of fossil fuels, which are the main source of carbon dioxide emissions. All recent research has shown that there is an urgent need to take a global decision to reform consumption patterns, which is the synonymous concept of DSM.

Hence, the importance of DSM in power systems crystallized, the researchers dealt with it with great interest, it began to come into reality in many countries of the world, and it showed remarkable results in many of them. Summarized in fuel efficiency; DSM should minimize fossil fuel utilization and CO2 emission through using alternative energy sources such as solar energy, so reduce visual and noise pollution.

Over that it reduces the need of new resources by Make a schedule for the loads of final consumers and manipulate the load running time so as to maintain a balance between

demand and the available generated capacity. In another words demand-side management (DSM) is indeed a powerful tool for optimizing energy usage in various systems. It involves controlling and adjusting energy consumption patterns to improve efficiency and reduce costs.

Bottom line, several key factors come into play when addressing electrical demand. First, it is essential to maintain a balance between generation and demand at all times. Second, it is important to note that the electrical grid does not have the capacity to store electricity. Third, the integration of renewable energy sources necessitates the presence of flexible power plants. Smart grids play a central role in a future characterized by reduced carbon emissions and intermittent energy sources, as well as increased energy trading across borders.

In this vision, flexible consumers will play a vital role by having a clear understanding of their power consumption According to this perspective; the future smart grid will heavily rely on flexible consumers who possess the knowledge and tools to manage their power consumption actively. These consumers will have the capability to monitor their energy usage, proactively switch off appliances during peak times, and independently manage their demand with the assistance of automated controllers and energy aggregators and this is the main object of demand side management [20].

1.7 Research Objectives

The objectives of this thesis are summarized as follows:

1. Make a survey of demand side management; explain its definition, techniques, and benefits.
2. Model the tested electrical systems in suitable programmer.
3. Implementation of DSM programs (DLC, CVR, TOU) and Perform simulation of tested power system to achieve the expected goals.
4. In order to effectively model CVR, DLC, TOU as well as most distribution level behaviors, we aim in this study to perform time series simulations.
5. This thesis highlights the benefit of DSM in reducing the peak demand in the peak time of the electrical system by shifting some loads to the off peak hours; the utilities

can achieve that by using dynamic electricity price which must have high values in the peak time (TOU).

6. It demonstrates the impact of DSM in improving the quality of electrical services in smart grid including high PV penetration.
7. It will show that the benefits from applying DSM in many PV penetration levels through a case study.

1.8 Scope of the study

This thesis aims to investigate the impact of demand management strategies on improving the performance and quality of electrical networks in the presence and absence of solar energy systems. These strategies included CVR, DLC, and TOU. This study also conducted a PV hosting capacity analysis and its impact on the electrical network and the effect of the previous demand management strategies on reducing these effects. A case study was taken for the previous verification on the OpenDss program using the IEEE-30 Bus network.

This thesis was carried out by taking only the steady state of the network and did not take the case of transient system like faults or harmonic distortion.

1.9 Structure of the Thesis

Chapter 1: Introduction: This chapter gives the reader a first impression of DSM definition and strategies, then talks about modern power systems and smart grids, and then moves on to talk about the role of the IEEE-30 bus system in power system research. Finally, it includes the PV system integrating challenges and opportunities. This chapter also talks deeply about DSM taking into consideration DSM's birth, concepts, objectives, techniques, and recent development, and finally talks about its strategies and application (CVR, DLC, TOU) in previous studies, it also talking about hosting capacity and its impact on voltage stability and the power system in general, lastly it touches the earlier studies of IEEE-30 bus system.

Chapter 2: Methodology: This chapter talks about the IEEE-30 bus system in detail, its components, loads, transmission lines, generators, and the one-line diagram of the test network. It also talks about applying the DLC, CVR, TOU charts and algorithms. It gives an idea about how to make hosting capacity analysis.

Chapter 3: Simulation and Application of DSM Strategies on IEEE 30-Bus System: this chapter shows the simulation results of the DSM strategies and the base case simulation result and compare the voltage profile and losses in each strategies with the base case and with the addition of PV in each steps of penetration.

Chapter 4: Hosting capacity analysis: this chapter examine the effect of hosting PV on the network at many penetration levels.

Chapter 5: conclusion: This chapter explains the core of the topic in light of the results of the case study; these chapters are summarized as in figure 6.

Figure 6

Thesis structure diagram

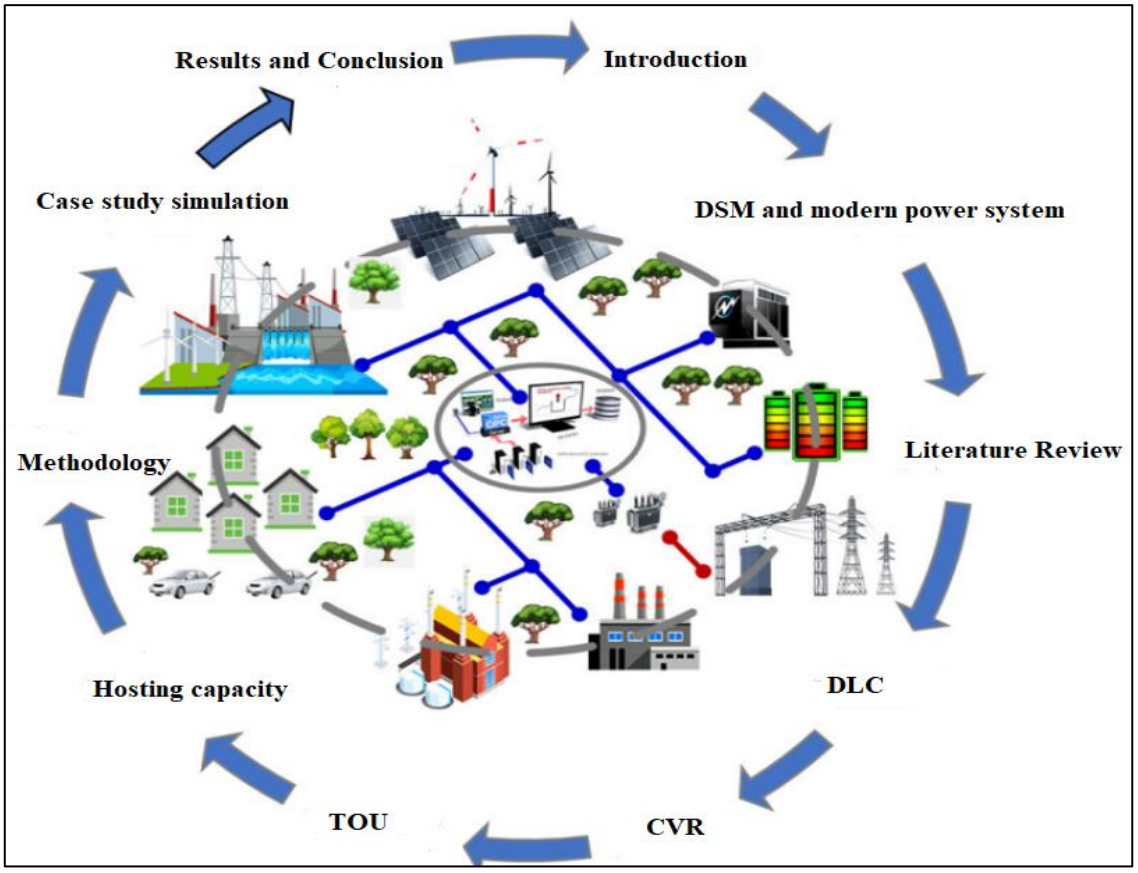

1.10 Overview of Demand Side Management (DSM) in Distributed Energy Resource (DER) Integration

1.10.1 The Birth of DSM

The emergence of Demand Side Management (DSM) can be traced back to global crises, the first of which was the oil crisis in 1973 [20]. In that year, the Organization of Petroleum Exporting Countries (OPEC) imposed an oil embargo against the United States, which significantly raised world crude oil prices.

This embargo caused turmoil in global petroleum markets and resulted in a five-fold increase in oil prices by 1985. By 1977, oil imports accounted for 50% of U.S. oil consumption, and there was a consensus that the U.S. faced an energy crisis.

Achieving greater energy self-sufficiency was seen as crucial for national security, given concerns about potential disruptions in oil supplies, and thus, President Carter introduced the National Energy Plan (NEP) in 1977, which proposed various demand-side and supply-side measures initiatives to these energy challenges [21].

The concept of DSM saw the light of reality in the Electric Power Research Institute (EPRI) during the 1980s [22]. Later, the California electricity crisis of 2001 served as a global wake-up call, emphasizing the importance of DSM, especially within electricity markets [23].

DSM gained further popularity with the U.S. Energy Independence and Security Act of 2007, which defined it as programs utilizing advanced metering, dynamic pricing, and enabling technologies to control peak demand [24].

1.10.2 Concept of DSM

The traditional approach to supplying electricity to consumers relied on a limited number of power plants to meet consumer demand. However, this approach faced challenges due to the introduction of volatile renewable energy sources and developments in electro-mobility, which transformed electricity supply into a two-way process, requiring advanced control methods for monitoring both electricity generation and consumption.

The idea of converting static electrical loads into dynamic ones has existed for some time, but its implementation only became feasible with the emergence of affordable global

communication networks and embedded systems. These technologies allowed for the integration of "smart" functionality to be integrated into electrical loads. Meanwhile, the growing demand for electricity continued despite improvements in the efficiency of electrical devices.

Electricity demand expanded due to industrialization and the transition to smart grid systems. The ascent of microgrids, renewable energy sources, plug-in electric vehicles, and energy storage systems necessitated the redesign of future grids to accommodate increased load levels. DSM programs offer promising solutions to enhance the reliability and financial performance of electrical power systems. DSM plays a vital role in sustainable energy, optimizing energy utilization, reducing emissions, and improving system flexibility, which is key to the low-carbon transition in electricity generation.

Renewable energy sources such as solar, and wind power frequently produce electricity in unpredictable and intermittent ways. Demand Side Management (DSM) consists of actions that change the amount or pattern of consumption. DSM can therefore assist in addressing the problems of unpredictability and intermittency, encourage the growth of renewable energy production, and reduce greenhouse gas emissions from the production of electricity. Furthermore, ensuring that peak electricity demand stays within improves the function of transmission businesses and individual consumers. Distribution infrastructure ensures it stays within the capacity limits of transmission and distribution infrastructure, which helps extend the lifespan of system components and reduces electricity distribution costs for both businesses and consumers [13].

A study on DSM dealt with the theoretical framework of DSM and highlighted that its main objective is to match the load demand with supply capacity, to how this objective is achieved, the study categorized DSM into two different types: static DSM and dynamic DSM. It showed that either increasing efficiency (dynamic DSM), such as load shifting, or decreasing consumption (static DSM), for example, then the goal is accomplished [25].

In agent-based control systems, the power balance between sources and loads alone is insufficient to ensure proper power flow in electric power distribution networks. The concept of power management in smart grids has been improved by the introduction of a virtual agent. Because DSM has a long response time, short-term energy storage may be

necessary to maintain power quality and achieve power balance across time scales with little additional energy storage [26].

1.10.3 Objectives and Techniques in DSM

The primary goal of DSM is to encourage users to consume less power during peak times or to shift energy use to off-peak hours to flatten the demand curve. In some cases, following the generation pattern may be preferred rather than flattening the curve. In each scenario, control over consumer energy use is necessary. A new technique proposed an algorithm where only time-insensitive devices are considered deferrable. The utility learns how customers respond to price changes, thus enabling it to send the correct price signal to achieve the desired demand pattern [27].

DSM has significant financial, environmental, and technical impacts on electrical power systems. Implementing DSM improves the performance and reliability of power systems [28][29]. It is economically viable, provides grid stability, improves demand and supply-side efficiency, and it is environmentally friendly [30]. DSM in a smart grid can manage load patterns effectively, reduce peak demand, enhance grid stability, lower carbon emissions, reduce operational costs, and decrease electricity expenses [31].

In cases of transmission line constraints and limited power supply, DSM programs can mitigate market power. They also lower market risk as well as the price volatility for both suppliers and consumers [28]. Heuristic optimization algorithms, like load shifting, can be used to reduce peak demand by allowing consumers to adjust appliance usage times or remotely turn appliances on/off [32].

1.10.4 Challenges in DSM Implementation

DSM faces five main categories of challenges:

1. Communication Network and Infrastructure: One of the primary challenges in implementing DSM is the need for a reliable two-way communication network. This is particularly important for smart grids, where the lack of reliable communication between energy sources and consumers is a major obstacle.

   As one study noted, the absence of reliable communication infrastructure is one of the most significant barriers to DSM implementation [31]. Furthermore, the integration of distributed generation into smart grids requires robust communication

systems. This includes sensors, control devices, advanced metering infrastructure, and the communication layers that connect these devices to enable effective DSM solutions [12].

2. Security and Privacy: Security and privacy concerns are critical in any communication network, including those involved in DSM systems. As DSM systems involve the collection and exchange of sensitive data between consumers, utilities, and grid operators, ensuring the security of this data is paramount. Privacy issues, such as consumer behavior data, must be handled with care to gain trust and participation in DSM programs. Thus, secure communication and transparent data handling are essential for the success of DSM programs [33].

3. Consumer Participation: A successful DSM program relies heavily on active consumer participation. Engaging consumers in DSM efforts requires a fair and transparent system that motivates them to alter their energy consumption behavior. The transition from a passive energy consumption model to an active participation model is crucial for DSM's success. Without consumer buy-in, DSM initiatives may struggle to achieve their goals [33].

4. Behavioral and Predictive Challenges: Another challenge in DSM is the difficulty in developing a universal optimization method or forecasting system for power consumption. The load profile of appliances is influenced by various factors, including consumer behavior patterns and environmental conditions, making it difficult to predict and manage energy consumption accurately. Moreover, the constant and irregular energy demands of consumers add complexity to real-time grid management. To obtain an effective power flow, DSM strategies are employed, but the unpredictability of consumer behavior can still make real-time energy balancing and forecasting challenging [34].

5. Flexibility of the Demand-Side: With the restructuring of electricity markets, the supply-side quickly adapted to the new environment. In contrast, the demand-side struggled due to its limited flexibility. Historically, electricity was viewed as a commodity available as needed, but with the increasing need for demand-side flexibility, DSM programs offer a suitable strategy. These programs can enhance flexibility on the demand side, helping to balance consumption with available supply and contribute to grid stability [35].

1.10.5 Recent Developments in DSM

With the increasing penetration of distributed energy resources (DERs) and the rise of smart grids, DSM techniques and methods have evolved, reshaping the electricity system. A comprehensive review of DSM evolution and methods was conducted, providing a classification of DSM approaches [25].

Recent innovations in DSM include the integration of hybrid genetic algorithms (HGAC) and artificial neural networks (ANNs) for forecasting and optimizing DSM in residential buildings. These models can predict external signals like load, temperature, solar irradiance, and Real-Time Price Demand Response Programs (RTPDRP) [36].

1.10.6 Technological Innovations and Applications in DSM

Modern DSM applications revolve around intelligent systems, advanced technologies such as Advanced Metering Infrastructure (AMI), and secure Internet of Things (IoT) networks. Models based on machine learning, deep learning, and data analytics are being proposed to improve load forecasting and achieve a balance between energy supply and demand. [37] .

1.11 Overview of Demand Side Management Strategies

The most common strategies of DSM in the modern electrical power system and smart grid is:

1.11.1 Conservation Voltage Reduction (CVR)

CVR is an energy-saving strategy employed by utilities to reduce energy consumption and peak demand by lowering voltage levels within certain bounds; it depends on the relationship between power demand and voltage. The fundamental idea is that power demand decreases proportionately when voltage is lowered within reasonable bounds. A 1% drop in voltage is assumed to result in a 1% decrease in power demand and, thus, in energy consumption.

CVR is an inexpensive technique that can assist utilities in delaying infrastructure expansion, reducing transmission line congestion, and increasing grid capacity during times of high demand [38]. CVR is a method that allows utilities to reduce the voltages

at the end of feeders to save energy, particularly when the most of loads are constant-impedance loads [39].

The assessment of the energy efficiency advantages of the combination of Voltage/VAR Optimization (VVO) and (CVR) technologies is covered by a vital study. By reducing voltage within reasonable bounds, these economical techniques seek to lower customer energy consumption. Depending on initial deployments, potential savings could be anywhere between 1% and 4%. The type of customer load, system characteristics, and voltage reduction used all affect how effective CVR/VVO is. CVR/VVO strategies are a flexible tool in the pursuit of energy efficiency and sustainability because they not only optimize the grid but can also help low-income households find affordable energy solutions [40].

As the penetration of Renewable Energy Sources (RES) increases, challenges such as unpredictable power flows, voltage swings, and reactive power management emerge. A study suggests that active distribution networks with advanced control features, such as the integration of distributed generation (DG), can help resolve these challenges and improve the integration of RES. The goal is to ensure the safe, reliable, and cost-effective operation of the distribution system as the share of renewable energy continues to grow [41].

The presence of DERs and load characteristics have a significant impact on CVR's efficacy. While constant Z loads are more responsive, constant PQ loads do not benefit much from voltage reduction. The incorporation of DERs makes voltage control more difficult because their variable outputs may result in voltage variations, which, if not properly controlled, could negate the advantages of CVR. Although voltage regulation devices aid in preserving acceptable voltage levels, systems with a high penetration of DERs may find that, their efficacy is diminished, particularly in high PV penetration levels [42].

A study examining the impacts of increasing solar PV penetration on voltage profiles and the efficiency of CVR in a distribution system in the Midwest of the United States. It examines different PV penetration levels, allocations, and inverter control modes using comprehensive simulations. The findings demonstrate that the best results for CVR are provided by voltage-reactive power mode (VRP) mode and dispersed PV allocation,

which allow for deeper voltage reductions and higher energy savings while lowering system losses. It is important to carefully manage the relationship between CVR and solar PV, particularly as solar PV penetration increases in distribution networks [43].

To enhance the scheduling and functioning of active distribution networks that integrate high penetration levels of renewable energy generation, a paper suggests an advanced optimization technique. The system can lower energy consumption, incorporate more renewable energy, and enhance the grid's overall dependability and economy by employing CVR and actively managing distributed generation. Based on a two-stage stochastic model, the method accounts for uncertainties in energy generation and demand by optimizing energy flow and voltage control [41]. In addition, a paper suggests a two-timescale control system to maximize voltage control and accomplish the CVR goal, combining a centralized controller with a local one. While local controllers work on a faster timescale to reduce local voltage fluctuations brought on by abrupt changes in PV generation, the centralized controller coordinates conventional devices (such as voltage regulators, capacitor banks, etc.) and smart inverters on a slower timescale. The method uses minimal computational resources, reduces communication overhead, and it is successful in achieving CVR goals while managing local PV generation variability, making it scalable for big distribution networks [44].

Finally, in grids with high photovoltaic penetration, a study shows how well Advanced Distribution Management Systems (ADMS) and Distributed Energy Resource Management Systems (DERMS) can be coordinated. While the DERMS controls PV smart inverters, the ADMS modifies Load Tap Changer (LTC) taps to reduce system voltages. With reduced PV energy curtailment, enhanced voltage profiles, and energy savings of up to 4.7%, this shows a very effective method of incorporating renewable energy without endangering grid stability [45].

In modern distribution grids, particularly those with high penetration levels of renewable energy sources like photovoltaic, the suggested multilevel CVR control and optimization methodology provides an advanced method for managing voltage and energy. This methodology tackles several issues, such as voltage violations, cloud-induced fluctuations, and renewable energy variability, by fusing centralized optimization with decentralized control and real-time voltage adjustment.

This strategy is flexible and resilient due to the incorporation of real-time frameworks and the assessment of uncertainties. It provides notable reductions in peak demand and energy consumption while maintaining grid stability and dependability. This makes it a viable option for smart grids that aim to sustainably and fairly integrate renewable energy with conventional power sources [46].

A recent study investigates the application of CVR in a smart grid (SG) to save energy and lower peak electricity demand. An Arduino-based SG that uses a real-time clock (RTC) and Wi-Fi module to monitor and control electricity consumption in real-time is presented, along with an experimental and simulation-based methodology. By modifying the firing angle of a TRIAC, the system maximizes the voltage delivered to the load during peak hours, resulting in lower energy consumption. Demand management is aided by transmitting energy data to the Thing Speak cloud for remote monitoring and analysis. The results demonstrate the potential of the CVR technique for energy conservation in developing nations, as it can reduce energy consumption by 8.33% with an optimized firing delay [47].

1.11.2 Demand response (DR)

Demand Response (DR) and demand-side management (DSM) have nearly the same meaning and they overlap in many points; the goal of demand-side management is to change the load curve by influencing consumer behavior. In particular, DR seeks to modify or shape customers' load curves by modifying their electricity consumption in response to price signals or other incentives. So it can be classified under the heading of DSM [48].

DR refers to the variation in electricity consumption patterns by end-use consumers in response to changes in electricity prices over time. It encompasses alterations in the timing of electricity consumption proposed by end-use consumers. It can also be defined as “Changes in electric usage by end-use customers from their normal consumption patterns in response to changes in the price of electricity over time, or to incentive payments designed to induce lower electricity use at times of high wholesale market prices or when system reliability is jeopardized” [49].

DR provides an opportunity for consumers to actively participate in the operation of the electric grid by shifting or reducing their electricity usage during peak hours in exchange for financial incentives. Electric operators and system planners utilize DR programs as a means to balance the supply and demand of electricity. These programs can lower electricity costs in wholesale markets, which ultimately results in reduced retail rates.

It presents various methods to engage customers based on real-time pricing, including real-time pricing, variable peak pricing, critical peak pricing, critical peak rebates, and time-of-use pricing. In the electric power industry, DR is considered a valuable resource due to its potential impacts and its role in grid modernization efforts. Recently, there has been a significant focus on DR programs aimed at improving market liquidity, reducing electricity prices, addressing transmission line congestion, and enhancing overall grid security [50]. These elements may include available incentives, agreements to directly manage or decrease a consumer's load, or even consumers participating in electricity trading through bid submissions. Typically, rigid fixed price levels can hinder the flexibility of demand, and this is recognized as a fundamental challenge in the electricity market [51].

The Electric Power Research Institute estimated that in the U.S., DR has the potential to reduce peak demand by as much as 45,000 MW. However, the adoption of DR remains relatively low due to inadequate marketing strategies and insufficient awareness of promoting energy and cost savings [51].

In contrast to earlier demand response (DR) programs, current ones provide utility customers with incentives to lower their electricity consumption during times of peak demand. Because peaking generation is more profitable, customers are paid more than usual for short-duration shutdowns a few times a year. Current DR Programs are a Pareto improvement, benefiting both utilities and customers. The value of flexibility resources in grid management is demonstrated by the fact that, for instance, the capital cost of DR is substantially lower than that of installing new peaking generation, with estimates of $165/kW versus $600–800/kW for new generation [52].

Demand response can be categorized into:

In incentive-based

In incentive-base DR programs, consumers enter into agreements by signing contracts that outline the rules of participation. Typically, these contracts include provisions for penalties if consumers fail to meet their contractual obligations.

Price-based

Price-based demand response programs operate by adjusting energy prices and observing how consumers respond to these price changes. This approach can introduce more variability in consumer behavior compared to incentive-based programs, where predefined response behaviors are determined by contractual rules. Nevertheless, active consumers in price-based programs retain the freedom to choose how they respond, including the option to disconnect appliances. In price-based programs, active consumers can potentially receive discounts by voluntarily reducing their energy demand during critical peak periods.

Both incentive and price-based

When analyzing the combination of both incentive-based and price-based DR programs in a dataset, it can be concluded that two key factors stand out: performance and reliability. These two factors are likely critical considerations when assessing the effectiveness and success of a mixed approach to DR programs. Performance would relate to how well consumers respond to both types of programs and how their actions contribute to grid load regulation and peak reduction. Reliability, on the other hand, would address the consistency and dependability of consumer responses under this combined approach [53].

Indeed, DR plays a crucial role in demand-side management by enabling consumers to provide reliable responses to changes in energy demand. It allows consumers to actively adjust their electricity usage in response to price signals, grid conditions, or other incentives. This flexibility in managing energy consumption not only benefits individual consumers but also contributes to the overall stability and efficiency of the electrical grid. In essence, DR is a valuable means of DSM, helping to balance supply and demand while ensuring reliability in energy consumption.

Although DR shows promise in increasing demand flexibility, the potential peak reduction achieved through DR programs in the US in 2015 was only 6.6% of the peak demand [[54]. This can be attributed to the fact that electricity is a resource with a much higher value to consumers than its price reflects. For instance, many articles show that in a one-hour power outage, residential consumers were willing to pay ten times higher than the actual price. Commercial and industrial consumers were even more willing to pay a premium for electricity.

Consequently, electricity consumers are generally reluctant to compromise their comfort or satisfaction to reduce their electricity bills. Therefore, the success and scalability of DR in the future depend on its ability to generate more significant economic savings for consumers than dissatisfaction. Key factors that contribute to dissatisfaction among residential consumers include:

Requiring consumers to alter their preferred electricity consumption patterns, such as delaying the use of home appliances. Imposing potentially undesirable temperature set points in buildings. The effort consumers need to invest in acquiring information about electricity prices and making consumption decisions accordingly.

Many scholarly articles have included human comfort and satisfaction as aspects of the control problem. However, a significant portion of these articles has concentrated on single-agent systems, where electricity prices remain unaffected by variations in energy demand [55].

DR includes many strategies and activities that fall under it, as shown in Figure 7 [56]. We will take DLC, TOU in more detail.

Figure 7

Demand Response Strategies

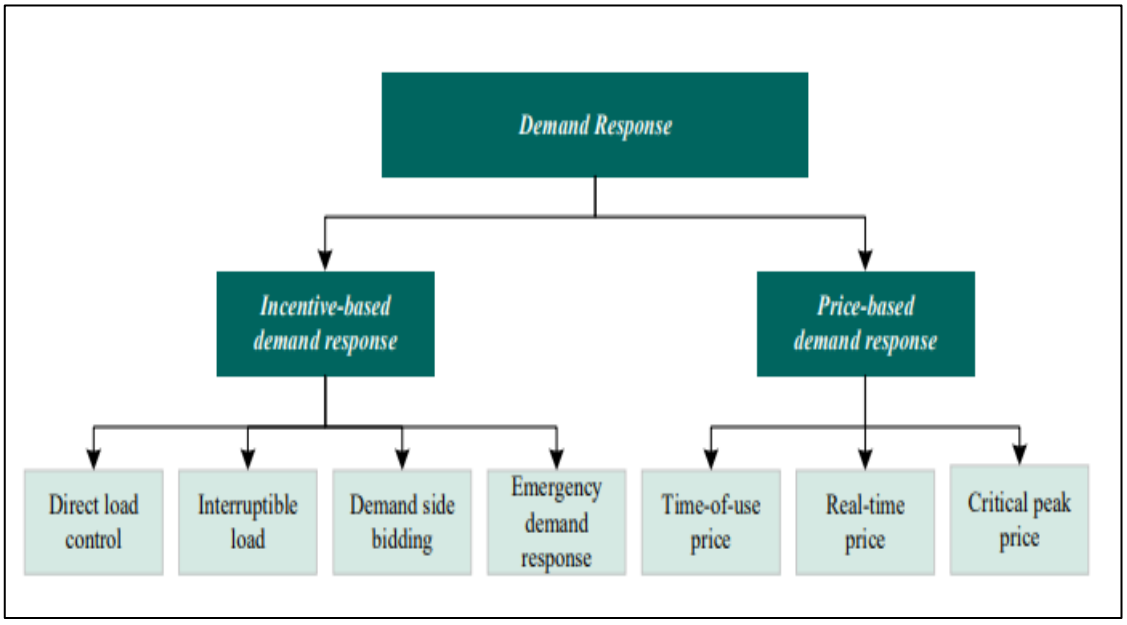

Direct Load Control (DLC)

Direct load control is a technique employed by utilities to remotely manage certain appliances of customers, such as air conditioners and water heaters. This technique helps stabilize the grid by reducing peak demand and ensuring a balanced distribution of electricity. Advance notices are usually given before any operation takes place. To participate in this program, customers must have a remote control switch system installed, allowing utilities to adjust, turn on, or turn off these appliances. Direct load control is mainly used in residential and small-scale commercial settings, as it may not be suitable for the industrial sector due to its requirement for precise processes [57].

DLC involves third-party entities controlling customer loads in response to DR events on the electric grid. Examples include utilities, ISO, Aggregators, and control companies [58]. DLC includes easier DSM for customers and more precise load reduction estimates during peak hours [59].

In the DLC method, DSM is implemented through partial load curtailment. The consumed load is continuously monitored to ensure it does not exceed the threshold power. If it does, DLC curtails 10–30% of the load, prioritizing the loads with the highest importance. If consumption drops below a specified threshold (PTH), the curtailment is reduced [60].

DLC programs have the potential to address challenges in distribution networks by balancing intermittent renewable energy sources. However, in many countries, these programs face low enrollment rates. Two key findings from studies on DLC programs are:

1. Acceptance Rates: The acceptance of DLC programs varies significantly among different socioeconomic groups, ranging from 33% to 71%. This suggests that there are differences in willingness to participate in these programs based on people's economic and social backgrounds.
2. Preferred Attributes: Multinomial logit results indicate that financial incentives are the most preferred attribute when it comes to heat pumps and is a major motivator for other appliances to participate in DLC programs. Offering financial incentives can significantly increase enrollment rates and enhance the effectiveness of DLC programs in addressing challenges related to renewable energy sources [61].

The electric utility is implementing the DLC to automate external control of shedding customer load. However, the growing number of customers in the DLC program has made it difficult for operators to manage customer load. The conventional DLCS requires continuous operator involvement to control load on/off status, which may lead to mistakes in decisions. This system had been developed into automatic load control after the emergence of the smart grid improving efficiency and reducing errors [62].

By reaching places where physical connections are challenging, wireless technologies provide greater flexibility to enable effective participation in DR programs; DLC for example. However, their range is limited because they are more prone to signal loss. To prevent unwanted access, stronger security measures are also required. For DR-enabled smart grid operations, ZigBee, Z-Wave, Wi-Fi, Wi-MAX, cognitive radio, and newer cellular technologies are essential wireless communication technologies. Conversely, wired technologies—like Ethernet, fiber optics, and power line communication—transmit signals by utilizing pre-existing infrastructure. To ensure successful DLC implementation, factors like scalability, replicability, availability, reliability, and security should be carefully examined regardless of whether wired or wireless technologies are used [61].

The term DLC describes how utilities or third-party aggregators manage customer-end devices, turning them off or lowering their consumption level in response to market conditions. Numerous DR resources are available for use by DLC programs. Water heaters, pumps, refrigerator defrost cycles, electronic battery chargers, washing machines, lights, and stoves are examples of residential DLC resources. Air conditioners, heat pumps, electric water heaters, dual-fuel boilers, refrigerated warehouses, HVAC systems with thermal storage, and lighting are examples of commercial DLC resources. DLC resources in industrial settings include apparatus like air liquefaction facilities, induction and metallurgy furnaces, gas and water pumps, agricultural irrigation systems, aluminum smelting, and different electrolysis processes (e.g., potassium hydroxide, magnesium, sodium chlorate, chlor-alkali [52].

DLC helps balance demand with generated energy and reduces electrical power flow during peak periods. However, to ensure the success of the program, it is crucial to understand customer preferences and the social and psychological factors that influence their willingness to participate. A study conducted in Switzerland on 556 participants in the DLC program focusing on electric cars and heat pumps revealed that most participants were motivated by financial incentives [63].

A study aimed to find out the preferences and motivations of participants in Finland towards DLC to determine the influence of economic, social, and demographic factors on participants. The results indicated that gender, education level, living conditions, and income level are strong factors determining the motivations of DLC [64].

A survey of 31 European countries examined the factors influencing acceptance of DLC programs; the findings reveal that attitudes and beliefs regarding direct load control programs—such as their perceived efficacy and the moral need to use them—are the most significant predictors of acceptance. Whereas socioeconomic factors and more general environmental attitudes—such as age, income, or education—have little to no bearing. Thus, encouraging environmental responsibility may lead to more participants [65].

A recent study investigated how consumers view (DLC) programs, specifically as they relate to residential heat pumps. It found that social and psychological factors like trust, privacy concerns, and a sense of control have a big impact on consumer acceptance, even though financial incentives remain a strong motivator. The study identifies many

participation barriers and facilitators based on in-depth interviews with participants in a Swedish DLC program. Customers must have faith in service providers; they must believe that the utility can efficiently control their energy usage maintain control over their loads and can withdraw whenever they want. Consumer control over the program is also crucial because many people are willing to take part if they can control the remote control of their [66].

Rapid increases in demand for air conditioning could destabilize the electrical grid and result in outages. DLC, which enables utilities to automatically regulate electricity consumption by managing consumer appliances like air conditioners without consumer intervention, was developed to address this issue. Wireless communication networks or the internet are used to accomplish this control [67].

An important study suggests a DLC approach for residential DR programs. If a utility needs to reduce electrical load consumption, the DLC signal is sent to a smart meter (SM) via the utility's communication infrastructure. The SM then communicates with a group of smart plugs attached to specific domestic appliances to individually reduce the output voltage, reducing the electrical consumption of those appliances without turning them off. This allows the peak demand of a residential home to be reduced without turning off specific power-intensive loads, as is the case with a classic DLC approach used by several electric utilities. To prevent any disadvantages to household appliances, the suggested dynamic voltage control is operated within a specific range established by international standards. According to the study findings, the suggested DLC could use both voltage control and renewable energy to cut the peak demand for electricity by about 32%. It is anticipated that the suggested strategy will allow utilities more latitude in managing residential electrical consumption while guaranteeing attendees' comfort during a DR event [68].

The industrial sector is one of the largest electricity consumers, and it is essential to optimize energy consumption to reduce costs and enhance energy efficiency. DR is a strategy that aims to manage and reduce peak electricity demand by shifting energy consumption to off-peak hours or reducing energy consumption during Peak demand periods. Smart meters are a promising technology for implementing DR programs in the industrial micro grid, as they enable real-time monitoring and control of energy usage,

providing customers with accurate information about their energy consumption patterns. That study presents an integrated approach to enhance the efficiency of direct load control demand response (DLC-DR) in industrial settings by leveraging smart meter technology. The primary objective is to concurrently lower energy consumption and associated expenses while reinforcing grid stability. The optimization is formulated as Mixed Integer Linear Programming (MILP). The case study Simulated in the plastic industry shows that direct load control Demand response in an industrial micro grid with Renewable Energy Resources (RES) and a battery energy storage system (BESS) can effectively utilize the reliability and flexibility of the power grid by reducing peak demand as well as the electricity cost [69].

Time Of Use Tariff

TOU tariffs on electricity pricing by introducing distinct electricity prices for peak and off-peak hours, the TOU tariff encourages customers to switch from high-priced peak hours to low-priced base periods, thereby lowering peak demand. A key aspect of TOU tariffs is how consumer behavior responds to the pricing structure. A study using a two-level model shows that consumers adjust their energy usage based on the price signals they receive from the TOU tariffs. This interaction between producers, who set the tariffs, and consumers, who adapt their consumption, is crucial for the success of TOU schemes.

Many studies show that TOU tariffs can benefit both sides: consumers can lower their electricity bills, and producers can boost profits by reducing the cost of generation during peak hours. Another study looks at how consumer behavior, such as moving electricity utilization to off-peak hours, can improve grid reliability and lower peak demand.

Furthermore, optimization models, such as the quadratic transfer cost model and multi-objective optimization techniques, illustrate that well-designed TOU tariffs can reduce peak demand and save costs for both consumers and energy producers [70,71].

To better understand and forecast consumers' responsiveness to TOU power tariffs—a crucial component of DSM programs— a more sophisticated approach suggests an interaction-aware framework. How diverse customer attributes—such as psychological, socioeconomic, and load profiles—interact affects how consumers react to certain tariffs. By identifying and evaluating these connections through data-mining tools, the suggested

framework increases the precision of customer behavior prediction; such an approach will allow the utilities to apply the TOU system with more reliability and efficiency [72].

To better understand customer attitudes toward TOU tariffs, a systematic literature review highlights the critical role of consumer awareness and behavioral responses to market cues. The review suggests that customized, context-specific solutions are essential to boost participation among different consumer groups, such as residential and industrial users [53].

In a complementary study a meta-analysis of 66 studies on consumer demand for (TOU) electricity tariffs from six different countries. The review states that how TOU tariffs are implemented has a significant impact on consumer adoption; opt-out systems may see nearly 100% uptake, while opt-in enrollment may see as low as 1%. National surveys tend to overestimate the demand, and the willingness to switch is significantly higher than actual enrollment. It also highlights the popularity of static TOU tariffs with predetermined peak and off-peak rates over real-time pricing tariffs. The review found that tactics like bill protection, automation, and small upfront payments could increase opt-in enrollment to bridge the gap between intention and action [73].

In addition to understanding consumer behavior, recent advancements in smart grid technologies and the (IoT) offer new ways to optimize TOU tariffs. These technologies enable more responsive and flexible energy usage, particularly in the context of EVs, as explored in several recent studies.

In general, DSM with EVs is still in its early stages and depends on sophisticated metering systems. The most widely used plan is the TOU price-based mechanism. A novel approach to TOU tariff estimation that makes use of big data technology is put forth. Peak and off-peak contribution coefficients from EVs are used in a mathematical model to determine tariff rates, and the NoSQL database enables the accumulation of historical and real-time data. Multiple EVs charging simultaneously is mitigated by conditional prioritization. The findings indicate a 6%–7% decrease in peak consumption [74]. In addition, another study's results demonstrated that while EV charging load can be shifted by TOU tariffs, a sizable price differential is necessary to achieve desired load shifts. Furthermore, TOU pricing in conjunction with the thoughtful placement of charging infrastructure can successfully shift the EV charging load, reducing RE

curtailments by 22.14% and carbon emissions by 10.12% when compared to the Business-as-Usual (BAU) scenario with current tariff rates [75].

Despite the many benefits of recent developments in electricity networks, the discrepancy between intermittent RE generation and EV charging load was a challenge and an obstacle that needed a modern solution. With the emergence of the (IoT) and DSM programs, most of these obstacles have been solved. The latest research on that obstacle was this year, where a solution was presented as an out-of-the-box idea called environmental time-of-use (E-TOU), which combines time-varying electricity prices with GHG intensity signals to encourage eco-friendly EV charging practices.

This strategy offers both monetary and environmental incentives by using GHG intensity as a "nudge" to change drivers' charging habits. The study demonstrates that charging costs and GHG intensity have an impact on EV users' charging decisions through conjoint-based choice experiments with 1,220 South Korean drivers. E-TOU reduced charging costs by 14.1% and GHG emissions from EV charging by 15.7% by enabling charging during periods of abundant renewable energy. Additionally, it decreased GHG emissions, decreased generation costs, and minimized renewable energy curtailments in the overall power system. E-TOU outperformed flat rate or conventional TOU pricing in every metric, indicating that a combination of financial and environmental incentives could help the transportation and power industries and promote a more sustainable future [76].

In practical applications, TOU tariffs have shown promising results in various case studies, in Cyprus; residential prosumers have been developed as part of a study to encourage demand-side management and reduce grid congestion. To minimize grid stress and peak demand, the tariffs promote moving electricity consumption from peak to off-peak times. The study's results of a successful decrease in peak consumption and an increase in load factor demonstrate how TOU tariffs can reduce electricity costs and encourage the use of renewable energy [77].

Similarly, a study in Ireland examines demand response control algorithms for a smart-grid-enabled all-electric residential building. The study uses an Energy Plus building simulation model to assess the impact of TOU tariffs and zone thermal control on energy consumption, costs, and carbon emissions. Results show that implementing DR measures

can reduce residential energy costs, electricity consumption, and carbon emissions by 16.5%, and 45.3% for utilities [78]. These case studies highlight the potential of TOU tariffs to promote demand-side management and drive more sustainable energy consumption patterns.

A three-stage optimization model for TOU tariffs is presented in a new study, which tackles problems such as irregular period divisions, irrational pricing, and inadequate seasonal adjustments. The K-means++ technique is used in the study to cluster load curves using data from the northwest region of China in 2022. The model enhances clustering performance by 4.27-26.70%. In comparison to traditional TOU structures, the model lowers monthly net load costs by 10.36% and decreases peak-to-valley variations and renewable energy abandonment [56].

Finally, the future success of TOU tariffs depends on how well utilities and policymakers address consumer engagement, tariff design, and emerging technologies integration. Strategies like automation, consumer education, and targeted incentives can help close the gap between willingness and actual adoption. The adoption of TOU tariffs should be considered within the energy transition context.

1.12 Hosting capacity and grid stability

The growing global demand for electricity, combined with the need to reduce carbon emissions, presents a significant challenge for power grids. One of the most promising solution to this dilemma is the significant increase in renewable energy recourses especially PV systems [79]. In 2023 alone, global renewable energy capacity grow by 473 GW with PV systems contributing 346 GW of this total, marking an all-time high. Wind energy added an additional 116 GW. This shift toward renewable is not only environmentally crucial but also economically significant, as evidenced by countries like Indonesia, which aims for 23% of their energy mix to come from renewable sources by 2025 [80].

Despite the environmental benefits, the integration of RESs into existing power systems poses challenges. While these new technologies are free from pollution, some types of RESs, such as PV and wind generation, can cause oscillation in the power system's voltage and frequency that potentially leads to stability issues. This is due to the

intermittent nature of these types of RESs. As the penetration of PV energy increases, maintaining grid stability with exceeding hosting capacity becomes increasingly difficult [81].

Grid operators will encounter more fluctuating net loads and steeper ramping demands as PV penetration increases, underscoring the significance of accommodating these variations. To maximize PV system integration without sacrificing grid reliability, a vital paper highlights the importance of carefully evaluating PV curtailment without compromising grid reliability; this paper also highlights the importance of frequency stability and hosting capacity planning especially in high PV penetration levels. The researchers noted that Excessive use of photovoltaic energy significantly impacts frequency, with a 50% penetration rate reaching its lowest and highest values (59.37-60.54) Hz, and it was recommended to reduce it in the case study conducted in Riyadh [82].

A key factor in integrating PV systems into the grid is determining the hosting capacity of the distribution system. Hosting capacity refers to the maximum amount of PV generation that can be integrated into the grid without violating operational constraints such as voltage limits, transformer ratings, and circuit overloads. It can also be defined as the ratio of consumers equipped with PV, Or the rated power of the photovoltaic power as a percentage of the total connected load or transformer rating, or peak current demand on the feeder. The concept of hosting capacity is central to defining the safe operational limits of the grid and ensuring that PV integration does not compromise system stability [83]. A simple formula for calculating the maximum penetrated power of DERs in low voltage distribution systems is derived in an important article as in equation (1.1) [84]:

$$P_{DERs} = 2 \times P_{load} + (1 - S_{load}) \quad (1.1)$$

Where: P_{DERs}: the distributed energy resources power in P.U.

P_{load}, S_{load}: the load real power, apparent power in P.U.

As PV systems are deployed alongside other distributed energy resources (DERs) like (EVs) and energy storage systems (ESSs), the pressure on grid stability and the variable nature of these technologies make it critical to assess the optimal deployment of these resources without overwhelming the grid or causing significant instability. To address

them, the HC concept is used to determine the ideal location and maximum capacity of DERs, EVs, and ESSs [85]. Based on recent industry reports and existing literature in the last few years (2014–2023) which deals with integrating, a recent review examines the difficulties and novel approaches for hosting capacity analysis in the distribution network. Active network management, flexible operating limits, demand response, ideal placement techniques, and network reconfiguration are recognized as viable solutions for hosting capacity enhancement [86].

Several strategies are being explored to enhance hosting capacity and ensure grid stability with high levels of PV penetration. One of the primary approaches is the use of advanced modeling techniques to more accurately predict the grid's ability to integrate PV systems, it used the more popular method to calculate PV hosting capacity called Monte Carlo simulation with real feeders from both urban and rural areas, in contrast to previous research that usually relied on supposition or oversimplified models. The study found that urban areas with many industrial and business customers have a higher hosting capacity (31% of full load) compared to rural areas hosting capacity (18% of full load) [80].

Another recent paper introduced a different approach to measuring the hosting capacity of low-voltage networks. It was applied to 14 low-voltage networks in Austria where they were able to fully exploit the potential of rooftop solar and then gradually reduce the installed PV capacity in order to minimize the effects of violations such as overvoltage at nodes, overcurrent in lines, and overloading of transformers. This approach provided a larger hosting capacity and lower computational costs compared to previous random methods [87].

In addition to modeling, the key solution is Smart grids, voltage control solutions, and coordinated operations of multiple technologies like on-load tap changers and reactive power control from inverters offer quicker and more affordable ways to increase hosting capacity grid stability than traditional grid reinforcement, which is slow and costly [88].

Another promising solution is DSM, in which the distribution system operator (DSO) communicates with consumers to modify their electricity usage in reaction to overvoltage situations. A new study that suggested a load-shifting plan based on Residential Demand Response (RDR) which incentivizes consumers to modify their electricity usage during peak PV generation periods, reducing grid stress and increasing hosting capacity.

According to case studies, the RDR scheme can increase hosting capacity almost as much as DLC, but it is less expensive and raises fewer privacy issues [89].

In addition to these techniques, the high relation between peak load and the rate of solar insulation has prompted recent interest in DSM applications of PV. PV-DSM applications are focused on maximization of the electrical energy, especially at peak demand periods, and these applications could be valuable to commercial customers because they typically pay higher demand charges compared to energy charges. A PV-DSM system with storage can help maximize their earnings. Utility companies can also profit from PV-DSM systems' contribution to peak shaving [90]. Incorporating ESSs into the grid is another vital strategy to enhance both hosting capacity and stability. ESSs, such as battery storage, can mitigate the intermittent nature of PV generation by storing excess energy during periods of high solar output and releasing it when generation is low. This flattens the fluctuations and reduces the risk of overvoltage or under-frequency events that could destabilize the grid. Studies, such as those conducted in Malaysia, have shown that integrating ESSs can help manage reverse power flows from distribution networks to transmission networks, which could otherwise cause significant stability issues [91].

In low-voltage networks, the researchers have created an enhanced version of the Voltage-Dependent Marginal Balance (VMB) technique to measure the grid PV hosting capacity. By adding voltage and current sensitivity matrices, that aid in estimating the required power reductions to prevent voltage and current violations, this improvement increases computational efficiency. In comparison to the original method, the new approach improves the hosting capacity values by an average of 4% while reducing the number of iterations needed for the calculation from 1764 to just 7 [92].

In conclusion, the successful integration of renewable energy into contemporary power grids depends on optimizing photovoltaic systems' hosting capacity. PV systems have a lot to offer the environment, but because they are intermittent, they pose serious grid stability issues. These difficulties can be lessened, though, by integrating energy storage systems, demand-side management, smart grid technologies, and sophisticated modeling techniques. The creation of a more robust, stable, and effective grid that can support large amounts of renewable energy while maintaining system reliability will depend on ongoing research and innovation in these areas as the global energy transition quickens.

1.13 PV impacts on the distribution network

In recent years, the installation of solar photovoltaic (PV) systems has seen a significant surge in popularity. This growth can be attributed to various factors such as the increasing energy demand, the growing emphasis on green and efficient energy production, and the need to effectively manage electricity costs.

Solar PV systems have a profound impact on both individuals and the environment. For homeowners or businesses, installing a solar PV system can lead to substantial cost savings on energy bills over time. By harnessing sunlight and converting it into electricity, these systems offer a renewable and sustainable alternative to traditional energy sources.

Moreover, the adoption of solar PV systems contributes to reducing carbon emissions and lessening dependence on fossil fuels. This aligns with global efforts to combat climate change by promoting clean energy solutions.

As technology advances and economies of scale drive down costs, solar PV systems are becoming more accessible to a wider range of consumers. This trend is expected to continue as governments implement incentives and policies that support renewable energy adoption. The widespread adoption of solar photovoltaic systems holds great promise for transforming how we produce and consume energy more sustainably while also reaping financial benefits for individuals and businesses alike [93].

Although photovoltaic systems, have a significant benefit on the way we generate and consume energy; the integration of PV systems into power grids presents various challenges due to the distinctive features of PV technology. These hurdles include its decentralized deployment, limited generation during daylight hours, dependence on converters, and intermittent output, it can be classified as follows:

Reverse Power Flow and Voltage Imbalances

Reverse Power Flow: PV systems are typically installed in small-scale units directly at the load, reducing power losses and making them non-dispatchable. However, this dispersed setup can lead to issues like reverse power flow and voltage imbalances, especially when connected to low-voltage distribution networks. The grid was designed for power flow unidirectional from high to low-voltage networks. PV generation primarily occurs during the day, which may not align with peak demand periods,

necessitating high ramp rates and reserves to manage the transition from low daytime to high evening loads. This can lead to challenges like reverse power flow, especially in residential networks with low daytime loads. In a scenario of no load but maximum solar power generation, negative energy flow could be substantially greater, causing the voltage at the PV connection to rise [94], [95].

Voltage Imbalances: unbalanced installations of distributed PV systems across phases can also cause voltage imbalances in the low-voltage network, Transformers and induction motors may overheat as a result of imbalance [95].

Voltage issues

The intermittent nature of PV output, which can fluctuate rapidly due to factors like cloud movements, poses challenges such as voltage flickers and harmonic distortions, particularly at high penetration levels. A main significant impact is the total loss improvement; we can say that when the power generated from PV sources surpasses the load demand, the surplus power is exported to the grid. Conversely, if the load demand exceeds the PV-generated power, the grid supplies the additional power required. A vital approach finding indicates that employing PV systems enhances the voltage profile, with the degree of improvement contingent upon PV production levels. The most optimal voltage stability is achieved when PV production closely matches the load demand. High PV penetration levels, which exceed 100%, and power losses, tend to increase [96].

One of the key challenges with PV systems is the fluctuations in active power generation, which can lead to variations in bus voltages within distribution networks because distribution networks have a high R/X ratio, these variations can lead the system to instability, which also can lead to equipment damage, power outages, and interruptions.

The fluctuations often require frequent tap-change operations of voltage regulation devices to maintain stability [97]; these tap modifications, particularly when coupled with a substantial disconnection of PV systems, can induce voltage fluctuations that deviate from standard steady-state voltage criteria. Such significant disconnections of PV installations may also precipitate power quality issues, notably voltage variations, particularly under conditions of high PV power generation and maximum system loading [98].

Vital studies demonstrate that, on a cloudy day, PV fluctuations can result in more tap changes than load variations. About one-third of the tap changes on cloudy days are caused by PV fluctuations on partially cloudy days. However, tap operations are only slightly impacted by PV power fluctuations on the other two types of days (i.e., Clear Sky Day and Overcast Day).

The link to investigate how power fluctuations, voltage variations, and tap changes interact is voltage sensitivity [99].

$$\vec{V_{load}} = \vec{V_{bus}} + \vec{I_{load}}(R_{line} + JX_{line}) \quad (1.2)$$

Certain utility-connected PV systems run at DC voltages greater than 300 volts before switching to conventional alternating current (AC), depending on the system design. Because DC arcs are more difficult to put out than AC arcs at the same voltage, DC poses a higher fire risk than AC at these voltages. However, the risks connected with DC power can be greatly reduced with appropriate wiring and safety precautions [100].

Power Quality Issues

Power quality addresses problems like transient voltage fluctuations and harmonic distortion by ensuring that sensitive equipment has enough power and grounding. Power quality is typically improved by on-site power generation, such as PV systems; however, connecting to the grid can result in problems like harmonics, voltage flickers, and strain on distribution transformers. Significant issues are also raised by distributed generation's reversed power flow and altered voltage profiles. The main source of current harmonics, voltage harmonics, and overall harmonic distortion in the network is the inverters of PV systems [101].

- Harmonics and Inverter Issues: The nonlinear operation of inverters, which convert DC to AC power, can introduce harmonics into the grid. These harmonics can distort the waveform of the electricity supply, negatively affecting sensitive electronic equipment and other components.
- Lack of Inertia: PV systems do not have the kinetic energy or inertia that conventional generators do, which is necessary to keep frequency and stability stable during disruptions. Inverters' nonlinear operation can also lower power quality and

introduce harmonics. This makes the grid more vulnerable to frequency fluctuations, especially during large-scale disturbances or rapid changes in load [102].

- Power fluctuation: the overall functioning of the network has been significantly impacted by the integration of photovoltaic systems into the power grid. One major impact is the fluctuations in net power flow, deterioration in power factor, and increased network power losses. Solar PV generation is intermittent, which can cause power fluctuations in lines. The grid's stability and dependability could be influenced by these variations [103].

Protection System Failures

- Impact on Fault Currents: Reverse power flow and protection problems may arise when Distributed Generation's (DG) power output surpasses local demand. The magnitude and direction of fault currents can be changed by high DG penetration, raising the possibility of protection system failures. In particular, DG sources that are connected to radial sections of the distribution network may cause issues like protection systems that trip incorrectly or fail to trip at normal conditions [104]. Relay protection issues become more apparent as PV generation penetration levels increase. For dynamic and efficient pick-up current settings, PV-induced intermittent and random variations in fault currents require effective signal tracking and logical decision-making [105]. Addressing these issues is crucial to ensuring a seamless transition to cleaner energy in the future as renewable energy sources.
- Low-resistance grounding or solidly grounded DERs: Low-resistance grounding has an impact on a distribution network's initial grounding technique, which alters neutral voltage and zero-sequence fault current and compromises system protection. Selecting the appropriate DER grounding is essential, particularly for high penetration levels. Undervoltage can lead to DER disconnection, which compromises system security and stability [106].
- Increased Risk of Overcurrent Events: Overcurrent conditions can occur when the PV current exceeds the rated capacity of cables or transformers. This can lead to equipment failures or service disruptions [107].

Ampacity And Thermal overloading problems

As the DERs integration increased in modern power systems, it is essential to estimate and control the current carrying capacity (ampacity) and thermal overload risks of critical equipment, such as cables, circuit breakers (CBs), and transformers. The experience and standards of Distribution System Operators (DSOs) are among the variables that affect these capacities, which are not fixed. Reverse power flow and voltage deviations are the main causes of problems, particularly during off-peak hours or when peak loads are not balanced. Equipment damaging and overheating may result from such conditions, to avoid operational failures, it is crucial to accurately evaluate and maximize these components' capacity limits [85].

Another study found that the increased use of PV generation presented a risk of overcurrent. A case study found that solar photovoltaic currents could surpass installed cables' capacity during the summer months when photovoltaic systems are producing high amounts of energy and the system is experiencing low loads. Events involving overcurrent can put stress on distribution equipment and cause power delivery interruptions [107].

Overall, photovoltaic systems play a crucial role in transitioning towards a more sustainable energy future. By understanding the impacts of these systems on distribution networks and implementing innovative solutions, we can harness the full potential of solar power while ensuring grid stability and reliability [39]. When integrating solar PV systems into low-voltage (LV) distribution networks, there are significant technical impacts that can affect the operation performance of the network:

Firstly, advancements in technology are being made to improve the efficiency and reliability of PV systems. For example, smart inverters with grid-support functions are being developed to help stabilize grid voltage and frequency levels during periods of high solar generation.

Secondly, as more solar PV systems are connected to distribution networks, there is a need for advanced monitoring and control mechanisms to mitigate any potential negative impacts on network operation such as protection of plants and the grid (G/P protection). This safeguard keeps an eye on all pertinent grid parameters and, if required, cuts the

plant off from the grid. Proper planning and coordination are essential to optimize the integration of photovoltaic systems while maintaining power quality standards [39].

Thirdly: Energy storage systems integration: It is essential to balance solar energy with grid stability in order to guarantee grid dependability and stability. Batteries and other energy storage devices can help balance supply and demand; reduce grid load, and solar energy fluctuations. When excess solar energy is produced, these gadgets store it and release it when required.

Finally, efforts are being made to mitigate these impacts through advanced grid management techniques and technologies. By incorporating smart grid solutions and energy storage systems, which permit a range of demand-side management and flexible load applications, they can better manage the variability of solar PV generation and maintain grid stability [91].

1.14 Previous Studies on the IEEE 30-Bus System

The IEEE-30 bus test System represents a portion of the American standard Electric Power System (in the Midwestern US). This standard, along with other IEEE n-Bus Test Systems is primarily used by researchers and scholars to implement new ideas and concepts and tackle various problems. Because this test system simulates real-world electricity networks, it is a miniature network that contains all the components of electricity networks, including generators, transformers, transmission lines, loads, and capacitors. Globally, they have been utilized in many different research efforts on load flow analysis and modern approaches related to adding distributed generation sources such as PV, wind, and others.

One notable study analyzed load flow using Gauss-Seidel (GS) and Newton-Raphson (NR) Methods revealing differences between the two techniques. While the Newton-Raphson method is proven more complicated computationally, it requires fewer iterations for large power systems [108].

IEEE30-Bus Test System was also studied and discussed in another experiment using the NR Method alongside Fast decoupled load flow (FDLF). The results confirm that raising the number of buses reduces the power losses but the main difference is that the FDLF method is more reliable and convergence faster than the NR method [109].

A further analytical study was carried out on this circuit specifically to analyze the sensitivity of this standard network to minimize the probability of cascading effects in the system. This is achieved by concluding which transmission lines are more critical and whose failure poses a significant risk potentially leading to the blackout of the network as a whole or in a specific zone [110].

Another research effort applied genetic algorithm technique to the standard IEEE 30-bus system. Achieving power flow analysis aimed at minimizing the overall system cost with the same maximum and minimum control variable limits [111].

An intriguing article explored optimization algorithms in the context of the IEEE30-Bus system with the presence of distribution sources, which were mainly aimed at reducing losses and improving the voltage profile. This study tested an advanced algorithm that combined the genetic algorithm (GA) with the improved particle swam optimization (IPSO) algorithm to determine optimal locations and sizes for distribution generation resources while maintaining the rating voltages of all the elements in the network nearly (1 P.U). Results indicated that the proposed hybrid algorithm HGAIPSO was an efficient and promising optimization solution for distribution network reconfiguration problems [3].

Finally, a case study investigated the Predestination of Particles Wavering Search (PPS) algorithm test on the IEEE30-Bus System, along with other standard test networks, to address optimal reactive power issues. This research demonstrates significant success, with results indicating a notable reduction in losses [112].

Chapter Two

Methodology

2.1 Overview of the IEEE 30-Bus System

2.1.1 System Layout and Components

The test system consists of 30 buses and 41 transmission lines and many transformers and synchronous generators, the system has a 100 MVA apparent power base and three voltage bases of 132, 33 and 11 kV, the other detailed shown in tables 1, 2, and 3 and the rest in appendix D. The IEEE30-Bus System can be implemented as a one line diagram in Figure 8:

Figure 8

IEEE-30 Bus system one line diagram

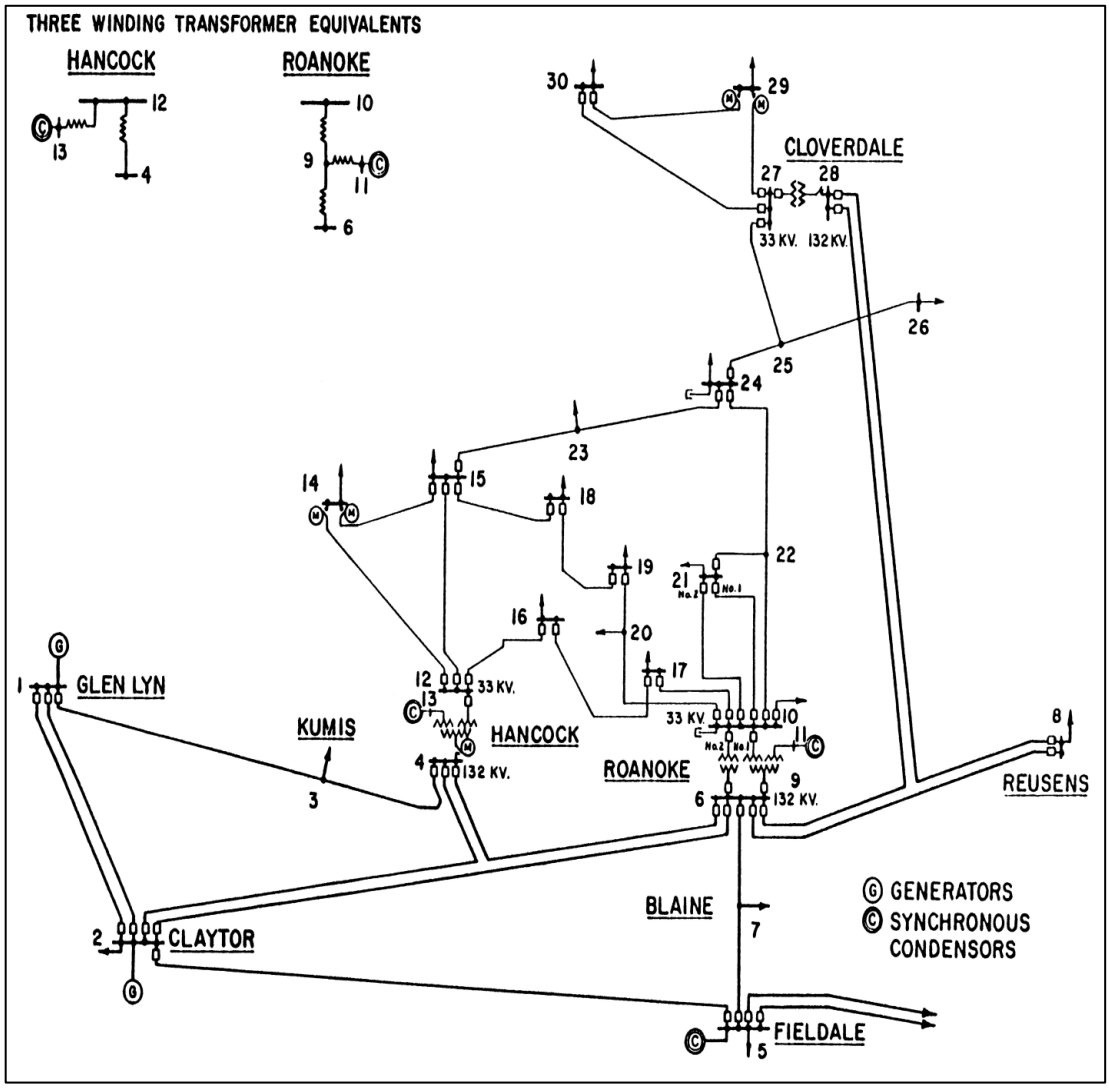

Table 1

Reactive Power Limit of IEEE30-Bus System

Bus	Qmin(p.u.)	Qmax(p.u.)	Bus	Qmin(p.u.)	Qmax(p.u.)
1	-0.2	0.0	16		
2	-0.2	0.2	17	-0.05	0.05
3			18	0.00	0.055
4			19		
5	-0.15	0.15	20		
6			21		
7			22		
8	-0.15	0.15	23	-0.05	0.055
9			24		
10			25		
11	-0.1	0.1	26		
12			27	-0.055	0.055
13	-0.15	0.15	28		
14			29		
15			30		

Table 2

Constraints of Control Variables of IEEE30-Bus

System	Variable	Min (P.U.)	Max (P.U,)
IEEE30-Bus	Generator Voltages	0.9	1.1
	Transformer Tap	0.9	1.1
	VAR Source	0.00	0.2

Table 3

Shunt Capacitor Data for IEEE30- Bus System

Bus Number#	Susceptance
10	19
24	4

2.1.2 Generation, Loads, and Transmission Lines in the 30-Bus System

The implemented algorithms are solely concerned with the 33-kV region, which has the most loads in the test system, these loads are illustrated in Table 5, each generator is represented as a voltage source, its source impedance is set arbitrarily as 10 Ohms, and its rated capacity is 100 MVA. Table 4 represents the characteristics of each source:

Table 4

Generator characteristics of IEEE30-Bus System

Bus	V (KV)	δ (deg)	P (p.u.)	Q (p.u.)
1	139.9200	98.4316	206095	-0.1679
2	137.6932	93.0798	0.4000	0.5000
5	133.4520	84.2658	0.0000	0.3685
8	133.3200	86.6183	0.0000	0.3714
11	35.7060	84.3227	0.0000	0.1617
13	35.3430	83.4883	0.0000	0.1062

Table 5

IEEE30-Bus power Loads

Bus number#	Load (MW)	Bus number#	Load (MW)
1	0.0	16	3.5
2	21.7	17	9.0
3	2.4	18	3.2
4	67.6	19	9.5
5	34.2	20	2.2
6	0.0	21	17.5
7	22.8	22	0.0
8	30.0	23	3.2
9	0.0	24	8.7
10	5.8	25	0.0
11	0.0	26	3.5
12	11.2	27	0
13	0.0	28	0
14	6.2	29	2.4
15	8.2	30	10.6

2.2 Simulation Tools and Software Used

OpenDSS programmer load flow software

The open-source distribution system simulator (OpenDSS), which is a thorough electrical power system simulation with a primary focus on power distribution in electric utility networks, is used for all modeling. Numerous frequency domain (sinusoidal steady state) analyses that are frequently carried out in power distribution systems are made easier by it. Beyond traditional analysis, it also encourages creative studies that meet future needs in the areas of renewable energy research, smart grids, and grid modernization.

The OpenDSS has been used for distribution system analysis in numerous research and consulting projects since its launch in 1997.

It was initially created to analyze distributed generation that is integrated into utility distribution systems, and it still does so today. It also has tools for evaluating power delivery energy efficiency and examining harmonic current.

Notably, OpenDSS is made to be readily expanded, guaranteeing flexibility in response to changing requirements. The Distribution System Simulator (DSS) represents circuits using nodal admittance equations, which many electrical engineers learned to write in their first university courses. This method uses a "primitive" nodal admittance (Y) matrix to express each component of the system. Although this is usually simple, some components of the power system, such as transformers, may find it difficult. One complete system Y matrix is then created by combining these primitive Y matrices. Sparse matrix solvers are used to solve the distribution system's equations.

One notable feature is how some devices, like specific load models, handle nonlinear behaviors. Current source injections, also known as "compensation" currents, are used to simulate these behaviors. In essence, an external injection is used to compensate for the current predicted by the linear portion of the model within the system Y matrix, and the adjustment is made iteratively to reach the correct current. In distribution system analysis tools, this method is frequently used to represent loads. One benefit is the adaptability it offers for integrating various load models, which is essential for some analyses, such as those carried out in energy efficiency research.

Compared to a traditional power flow program, the program's origin is more in line with a harmonic flow analysis program or even a dynamics program. This design decision offers remarkable modeling flexibility, particularly for accommodating different load models and non-traditional circuit configurations, even though it may appear unusual for a tool primarily used for power flow studies. The reasoning behind this is that creating a simulation program for harmonic flow is simpler than creating one for power flow.

The default circuit model is a full 3-phase model, but it can also be a simplified positive-sequence model or a full multi-phase model. Users may need to define a single-phase model of the circuit in order to generate positive-sequence models outside of the DSS due to the intricacy of multi-phase models with multiple unbalances. Although it is not always successful, the "MakePosSeq" command tries to transform a multi-phase model into a positive-sequence model.

The standard single Snapshot mode, Daily mode, Duty cycle mode, Monte Carlo mode, and modes where the load changes over time are among the different solution modes that the power flow execution supports. Following the completion of a power flow, data is available for the entire system, individual components, and designated areas, including losses, voltages, flows, and more. Models of energy meters can be used to provide overload and loss information or to integrate power over time.

Both network (meshed) systems and radial distribution (MV) circuits are supported in the power flow calculation. The radial nature of the circuit model may affect the accuracy of some algorithms, but the power flow solution is widely applicable and performs well on radial circuits and meshed networks. It works best in systems that have at least one rigid source.

Radial circuits, which are a common problem with some conventional Newton-Raphson formulations, have not been difficult for OpenDSS to solve. Iterative power flow and direct solution are the two main categories of power flow solutions. Nonlinear components such as distributed generators and loads are regarded as injection sources in iterative power flow, the direct solution, which solves them without iteration and includes them as admittances in the system admittance matrix.

Two algorithms are available in the iterative power flow: "Normal" current injection mode (which is faster by default) and "Newton" mode (which is a little more reliable for difficult circuits). The Normal mode is the recommended approach for lengthy sequential-time simulations because of its speed and robustness; the choice between these modes is contingent upon the particular simulation requirements. Fault studies employ a direct solution with linear load models, whereas power flow calculations usually use an iterative solution with nonlinear load models. Linear or a combination of linear and nonlinear load models can be used in dynamics mode simulations.

Direct solution, which solves them without iteration and includes them as admittances in the system admittance matrix. Two algorithms are available in the iterative power flow: "Normal" current injection mode (which is faster by default) and "Newton" mode (which is a little more reliable for difficult circuits).

The Normal mode is the recommended approach for lengthy sequential-time simulations because of its speed and robustness; the choice between these modes is contingent upon the particular simulation requirements. Fault studies employ a direct solution with linear load models, whereas power flow calculations usually use an iterative solution with nonlinear load models. Linear or a combination of linear and nonlinear load models can be used in dynamics mode simulations.

Parallel processing has been a feature of OpenDSS since 2016 when version 8 was introduced. The parallel processing suite was improved in this version and is now a crucial component of the OpenDSS foundation. OpenDSS currently offers several parallel execution features, such as:

1. The ability to perform long-term series simulations by splitting time (for example, a year) into discrete periods and allocating a distinct CPU to each temporal segment.
2. Dividing large circuits into smaller circuits and allocating a distinct CPU to each to implement dichoptic parallelization.
3. Managing several circuits at once. Notably, the OpenDSS scripting language enables users to directly control these parallel processes, doing away with the necessity for external software to manage parallel processing. This improvement gives users more control and flexibility.

2.3 Load flow analysis

It is noteworthy that power flow analysis serves as the basis for both preliminary research and design of power systems. Planning, operation, economical scheduling, and the sharing of power among utilities all depend mainly on them. Finding the voltage magnitude and phase angle at each bus as well as the real and reactive power flowing through each transmission line are the main facts pertaining to power flow analysis.

Furthermore, it offers data on line and transformer loading (along with losses) across the system and voltages at various system locations for power system performance assessment and control [113].

Important facts regarding load flow include:

1. The steady state analysis of the power system network is known as a load flow study.
2. A load flow study establishes the system's operating condition for a specific loading.
3. At every node in a system, load flow solves a set of simultaneous nonlinear algebraic power equations for the two unknown variables (|V| and ∠δ).
4. Accurate, quick, and efficient numerical algorithms are essential for solving nonlinear algebraic equations.
5. The voltage and phase angle, real and reactive power (both sides in each line), line losses, and slack bus power are the results of the load flow analysis.

Bus classification

One or more transmission lines, loads, and generators are connected to a bus, which is a point or node. Each bus in a power system study is linked to four different quantities: active power (P), reactive power (Q), the phase angle of voltage (δ), and voltage magnitude (|V|), it can be sorted as in Figure 9 [3] and the different between them is summarized as in Table 6:

1. Slack bus: A reference bus that keeps the network's power balance This generating unit, usually identified as bus 1, has two known variables: |V| and δ. It can be adjusted to account for losses.
2. Generator bus: This voltage control bus connects to a generator unit, allowing output power and voltage control. It adjusts prime mover, generator excitation, with limits

on reactive power based on machine characteristics, the known variable in this bus is P and |V|, and the unknown is Q and δ.

3. Load bus: This bus, derived from historical data, measures, or forecasts, is a non-generator that supplies positive real and reactive power to a power system, while consuming negative power, meeting consumer power, The known variable for this bus is P and Q and the unknown variable is |V| and δ [114].

Figure 9

Bus classification

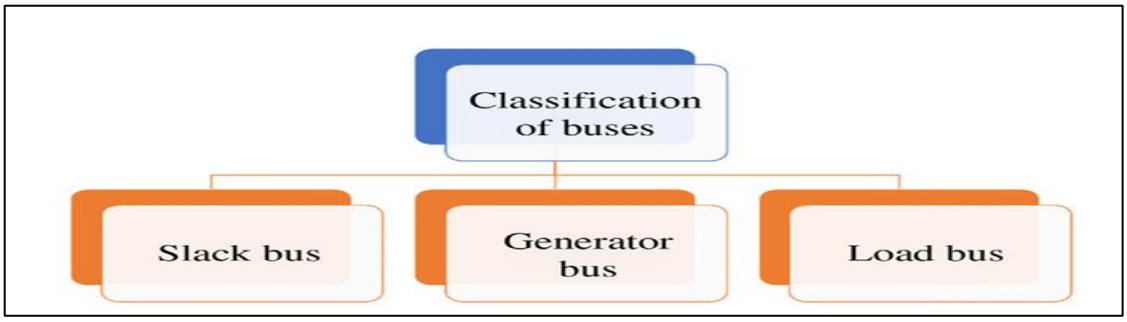

Table 6

Bus classification characterization

Bus type	P	Q	|V|	Δ
Slack bus	Unknown	Unknown	Known	Known
Generator bus	Known	Unknown	Known	Unknown
Load bus	Known	Known	Unknown	Unknown

The main steps of the load flow analysis:

1. Modeling of power system components and the total network.
2. Development and construction of load flow equations.
3. Applying numerical methods to solve the load flow equations.

The nodal equation can be written as:

$$I_1 = V_1Y_{11} + V_2Y_{12} + V_3Y_{13}$$

$$I_2 = V_1Y_{21} + V_2Y_{22} + V_3Y_{23}$$

$$I_3 = V_1Y_{31} + V_2Y_{32} + V_3Y_{33} \qquad (2.1)$$

The nodal equation in general form can be written as:

$$I_i = \sum_{j=1}^{n} Y_{ij} V_j \quad for\ i = 1,2,3.... n \qquad (2.2)$$

Real and reactive power (complex power S) delivered to bus i can be calculated in the following equations:

$$P_i + jQ_i = V_i I_i^* \qquad (2.3)$$

$$I_i = \frac{P_i - j\,Q_I}{V_I^*} \qquad (2.4)$$

Substituting for Ii in terms of Pi & Qi, the equation will be:

$$\frac{P_i - j\,Q_I}{V_I^*} = V_I \sum_{j=1}^{n} Y_{ij} + \sum_{j=1}^{n} Y_{ij} V_j \qquad (2.5)$$

The opendss program mainly classifies all devices and elements in the electrical network into power conversion elements and power transmission elements, then models and integrates them into the program, then finds the appropriate solution for the voltage and current distributions efficiently.

- Power Delivery Elements: These elements transport energy in the system, they often consist of two terminals or more (like lines and transformers) as in Figure 10 [8], they are typically represented by linear impedance models (Yprim matrices) that define their behavior in steady-state conditions.

Figure 10

Power delivery, power conversion elements representation in opendss

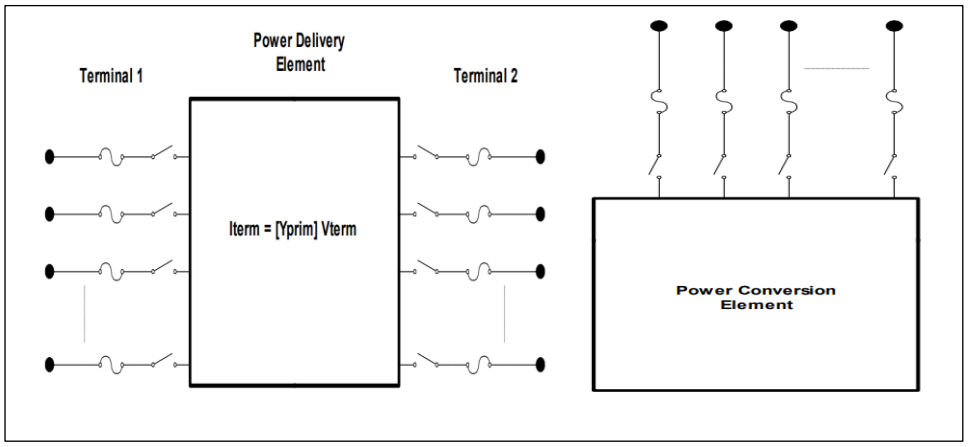

- Power Conversion Elements: These elements convert electrical power to other forms or store it temporarily, often they have one connection to the power system as shown in Figure 10 (such as loads and generators).

These elements often have nonlinear characteristics, and OpenDSS uses models like compensation currents to represent these nonlinearities as shown in Figure B.1 in Appendix B. The compensation current is the current that is added to the injection current vector in the main solver, where the current injected into the system depends on the voltage and the type of load (e.g., constant power, impedance, or exponential).

OpenDSS put the PC and PD elements together in the main solver as in Figure B.2 in Appendix B, it performs power flow calculations using a nodal admittance formulation, where it iteratively solves for system voltages and currents using the primitive admittance matrix, (Yprim), which is computed for each circuit element in the model. These small nodal admittance matrices are used to construct the main system admittance matrix, (Ysystem) by the sparse matrix solver, this solution process involves solving nonlinear equations in many iterations to get the final solution:

$$I_{inj}\,(V) \;=\; Y_{system} \times V \tag{2.6}$$

$$V_{n+1} \;= [Y_{system}\,]^{-1}\, I_{inj}\,(V_n) \qquad n = 0,1,2,.. \tag{2.7}$$

Where I inj(v) is the compensation current of PC elements, it may be nonlinear.

The initial guess of voltage gain from performing a direct solution of I=YV where loads and generators are modeled by their linear equivalents with no injection currents, this initial voltages are often quite close to the final converged voltages. The currents from power conversion elements are updated in each iteration based on voltage estimates, and added into the injection current vector, the sparse set is then solved for the next guess at the voltages. The cycle repeats until the voltages converge to typically 0.0001 p.u.

2.4 Power Flow Sensitivity

The sensitivity of system flow indicates whether power flowing through a distribution or transmission line connecting two buses, like buses J and I, varies in the case of varying in input factors. The link to investigate how power fluctuations, voltage variations, and tap changes interact is voltage sensitivity [8].

The complex power injected into the ith bus of the system is given* by equation (2.8):

$$S_i = P_i + Q_i = V_i I_i^* \quad , i = 1,2,\ldots . n \tag{2.8}$$

Where the real power and the reactive power in each bus is given by the following equations depending on the busses shown in Figure B.3 in Appendix B:

$$P_i = Re\left\{V_i * \sum_{j=1}^{n} Y_i V_J\right\} \tag{2.9}$$

$$Q_i = Im\left\{V_i * \sum_{j=1}^{n} Y_i V_J\right\} \tag{2.10}$$

$$P_i = |V_i| \sum_{j=1}^{n} |Y_{ij}| \cos\left(\theta_{ij} + \delta_{ij}\right) \quad ; i = 1,2\ldots\ldots . n \tag{2.11}$$

$$Q_i = -|V_i| \sum_{j=1}^{n} |Y_{ij}| \sin\left(\theta_{ij} + \delta_{ij}\right) \quad ; i = 1,2\ldots\ldots . n \tag{2.12}$$

Where: Vi and Vj are the voltage magnitudes at buses i and j, respectively, and vi and vj are the voltage angles at buses i and j, respectively.

Further, Yij is the magnitude of the ij element of the Y BUS matrix, which is summarized in equation (2.13), and θij is the angle of the ij element of the Y BUS matrix.

$$Y_{ij} = \begin{cases} -y_{ij} & , if\ j \neq i \\ y_{ii} + \sum_{k=1,k\neq i}^{n} y_{ik} & , if\ j = i \end{cases} \tag{2.13}$$

Then the real power sensitivity is written as:

$$P_{ij} = V_i V_j Y_{ij} \cos\left(\theta_{ij} + \delta_{ij}\right) - V_i^* V_{ij} \cos\left(\theta_{ij}\right) \tag{2.14}$$

The amount of change in the magnitude and angle of the voltage in the distribution network concerning the change in real and reactive power is given by:

$$\begin{bmatrix} \sigma_{P\delta} & \sigma_{P|V|} \\ \sigma_{Q\delta} & \sigma_{Q|V|} \end{bmatrix} \begin{bmatrix} \Delta\delta \\ \Delta|V| \end{bmatrix} = \begin{bmatrix} \Delta P \\ \Delta Q \end{bmatrix} \tag{2.15}$$

Where σPδ , σP|v| , σQδ ,σQ|v|: are the sensitivity matrices of active and reactive power concerning the magnitude and angle of voltage, respectively.

Based on the inversion of the Jacobian matrix, the sensitivity matrix can be obtained as shown:

$$J^{-1} = \begin{bmatrix} \frac{\Delta\delta^{abc}}{\Delta P^{abc}} & \frac{\Delta\delta^{abc}}{\Delta Q^{abc}} \\ \frac{\Delta V_{l-n}^{abc}}{\Delta P^{abc}} & \frac{\Delta V_{l-n}^{abc}}{\Delta Q^{abc}} \end{bmatrix} \tag{2.16}$$

2.5 Demand Side Management Strategies Implementation

2.5.1 Conservation Voltage Reduction (CVR)

In the Conservation Voltage Reduction (CVR) method, Demand-Side Management (DSM) is implemented through load curtailment. The primary objective of CVR is to decrease the voltage on the consumer side while ensuring it remains above the minimum allowable voltage. The flowchart illustrated in Figure B.4 in appendix B [57] utilizes an assigned Voltage Set Point (Vs) and the minimum allowable voltage (Vmin) based on voltage standards.

The process involves continuously measuring voltages at customer buses and adjusting the taps of tap-changing transformers to increase or decrease until all bus voltages fall within the range of Vmin and Vs. Δt represents the time interval between different voltage measurements. We can apply the CVR algorithm by using the existing CVR OpenDSS Script as the code shown below, which regulates the voltage so that it does not exceed a sit point value and does not fall below a minimum value through control of the tap changer of the autotransformer as stated in the CVR algorithm:

The regulator was added at bus 12 with a voltage set point (250v). Pt ratio (60) multiplied by Vreg (300) gives the nominal bus voltage =~ (33/√3=19.400 kV) and the minimum voltage is the minimum allowable voltage which is .9 V=.9*(33/√3 kV) = 17.500Kv as illustrated in the CVR implementation in appendix D. The nominal voltage regulation range is from –10% to +10% over 32 taps, which means 0.00625pu/tap.

2.5.2 Direct Load Control (DLC)

In the (DLC) method, (DSM) is applied by selectively reducing partial loads. The primary objective of DLC is to minimize power consumption during periods of high demand.

The consumer's load can be classified as follows:

1. Manageable loads (low priority loads): These loads have the control ability maybe by the end users or utilities without affecting the comfort of to motivate the power system conditions, they are separated into shiftable and adjustable loads:

- Adjustable loads: Depending on the required level of comfort, these loads' energy consumption can be directly changed and decreased or in some cases shut down. Air conditioners and space heaters fall under this category.
- Shiftable loads: The end-user can program the start time of these loads and change it over time. Electrical vehicles, dishwashers, and washing machines fall under this category.

2. Non-manageable loads (high priority loads): These loads run constantly, and there is not much that can be done to change or lower their power usage such as lights, freezers, and in particular medical devices.

The flowchart depicted in Figure B.5 in Appendix B [60] assesses the power usage of individual loads. The process begins by comparing each load with its predetermined threshold (PTH) within a 30-minute interval (Δt). When the power consumed by the loads or users surpasses this threshold, load control mechanisms are activated. DLC involves curtailing 10–30% of the load while ensuring that loads with the highest priority remain active. Subsequently, if the consumption drops below the PTH, the algorithm re-establishes the curtailed percentage for the load.

We applied this algorithm manually by decreasing some of the existing loads assumed to be low-priority loads (about 10-30% reduction), which is required to not exceed the threshold P_{THN}.

2.5.3 Time-of-Use (TOU) Pricing

Here we assumed that the utility imposed a special electricity price that is characterized by the fact that the price of electricity is more expensive during the peak time load and less during off-peak times. We imposed an actual customer response, which led to the transfer of the peak load from peak time to other times so that the load pattern became almost constant and its size averaged at all times by approximately 0.6 Load factor.

2.6 Hosting Capacity Analysis

“ A PV system consists of one or more solar cell modules or panels, that take insulation from the sun (direct and indirect) and convert that into a DC signal which is passed on to an input filter capacitor. Following the input filter capacitor, a DC to AC inverter transforms the current from the DC stage into an AC signal that is synchronized with the grid. In the OpenDSS modeling program, most of these components are represented in a simplified manner in the PV System device class. The present version of the PV System model is useful for simulations generally greater than 1s time steps. The model assumes the inverter can find the max power point (mpp) of the panel quickly. This simplifies the modeling of the individual components (PV panel(s) and inverter) and should be adequate for most interconnection impact studies.

The interface to the circuit model is the same as any Power Conversion (PC) element in the OpenDSS program. It appears the same to the circuit model as a Generator or Load or Storage device would, producing or consuming power according to some function. In this case, the active power, P, is a function of the Irradiance (insolation from the sun), temperature (T), and rated power at the maximum power point, Pmpp, at a selected temperature and an irradiance of 1.0 kW/m2. In addition, the efficiency of the inverter at the operating power and voltage is applied. The PV system model uses XYcurve objects to describe certain characteristics of the PV panels and inverters. XYcurve objects are new to this version of OpenDSS. The user may enter x-y curves as either an array of points or as separate arrays of x and y values. The following two examples are equivalent:

// curve in separate x, y array New XYCurve. MyEff npts=4 xarray=[0.1 0.2 0.4 1.0] Yarray=[1 1 1 1].

XYcurve objects are interpolated linearly between defined points to determine the actual value. For curves used in the PVsystem model, it is usually sufficient to enter only 4 or 5

points because the curves are relatively smooth and monotonic. An array of points is entered to describe how the Pmpp varies with T relative to the temperature chosen for the rated Pmpp at 1 kW/m2. This is a per unit factor for discounting the panel power output for temperature. The factor is 1.0 for the temperature for which the Pmpp is defined. This curve normally declines for higher temperatures and increases for lower temperatures as shown in Figure B.6 in appendix B. An array of points is also used to represent the efficiency curve for the inverter. While this is a family of curves depending on the dc bus voltage, the model uses only a single curve at this time, using a curve near the typical operating voltage of a given array. An InvControl device works with PVsystem objects by controlling them in a manner to provide three main advanced inverter functions.

!new loadingshape.myirrad npt=24 interval=1

! ~ mult = { 0 0 0 0 0 0 .1 .2 .3 .5 .8 .9 1.0 1.0 .99 .9 .7 .4 .1 0 0 0 0 0}

!new tshape.myirrad npt=24 interval=1

! ~ temp = { 25 25 25 25 25 25 25 25 35 40 45 60 60 55 40 30 25 25 25 25 25 25 } [115].

In this section, we increased the PV penetration by several percentages of the total maximum load and made an analysis and comparisons between them. We use 15 MW 30 MW 50 MW 70 MW 100 MW 150 MW 200 MW PV systems; which is added also in the same bus (B21).

2.7 Data Collection and Analysis Methodology

The researcher collected the data from the test circuits attached in the programmer files. The initial run of the load flow programmer was on the test circuit without any adjustment. Secondly we applied the previous tools (CVR, DLC, TOU) without adding PV, later adding PV system with these tools and finally examines the hosting capacity of the PV at many penetrations levels before and after DSM tools addition and compare the results.

2.8 Assumptions and Limitations

The researcher assume that the consumers encouraged to use electrical devices at off-Peake time as the electricity price reduced at these times, so that the resultant load shape was nearly constant, despite that, the practical consumers reaction may be different, it is unexpected because it relays on individual consumers behavior.

DSM limitation can be summarized in two points: in one hand, it needs advanced communication to be practically implemented and this need a technical revolution in the electrical power system and conventional grid infrastructure. In the other hand, it depend on the consumers comfort and many of DSM strategies relayed on the consumer sharing and confirming.

Chapter Three

Simulation and Application of DSM Strategies on IEEE 30-Bus System

3.1 Baseline Scenario: IEEE 30-Bus System without DSM

3.1.1 Voltage Profiles

We can first execute the program without making any modifications to the test network except change the execution mode to daily, run the basic circuit give us the voltages (P.U) for each busses that summarized in this basic Figure B.7 in appendix B. We can see that the voltages are in the allowable range (.9 – 1.1 P.U) with the highest voltage at bus 11, 13 due to the determination of generators voltage constructed by the DSS programmer as 1.082, 1.071 P.U as shown in the DSS code below:

```
! Generator Definitions

New Generator.B2  Bus1=B2  kV= 132 kW=40000 Model=3 Vpu=1.045 Maxkvar=50000 Minkvar=-40000 !  kvar=50000

! The following buses just have a voltage target and kvar limits defined.
! The kW value is defined as zero, but this is illegal in the OpenDSS Generator model
! So we just put a small value (1 kW) here and use model 3 to regulate the bus.

New Generator.B5  Bus1=B5  kV= 132 kW=1    Model=3 Vpu=1.01  Maxkvar=40000 Minkvar=-40000 !  kvar=37000
New Generator.B8  Bus1=B8  kV= 132 kW=1    Model=3 Vpu=1.01  Maxkvar=40000 Minkvar=-10000 !  kvar=37300
New Generator.B11 Bus1=B11 kV= 11  kW=1    Model=3 Vpu=1.082 Maxkvar=24000 Minkvar=-6000  !  kvar=16200
New Generator.B13 Bus1=B13 kV= 11  kW=1    Model=3 Vpu=1.071 Maxkvar=24000 Minkvar=-6000  !  kvar=10600
```

In addition, we can monitor all the busses voltages but we monitor here only bus 30 in order to facilitate and reduce the number of figures, so we monitor bus 30 voltage each hour all over the day, the daily bus 30 voltage represented in Figure B.8 in appendix B.

3.1.2 System losses

The system total losses is (9.3+ j1.6) MVA with total real losses 9308.3 KW, the lines losses detailed in Table 7 as a base case losses. The daily load profile of bus 30 is represented in Figure B.9 in Appendix B, with maximum demand of each default load bus is 1 P.U. at the hour 17. The line losses can be calculated by this equation:

$$P_{Losses} = I^2 * R \tag{3.1}$$

$$Q_{Losses} = I^2 * X \tag{3.2}$$

Where: I: line current, R: line resistor, X: line reactance.

Table 7

Base case real and reactive losses in kW, kVar

Element	Total real losses(kW)	Total reactive losses(kvar)
Line.1-2	2469.098	1544.971
Line.1-3	1647.269	1576.127
Line.2-4	603.4138	-2080.77
Line.3-4	453.9005	424.1232
Line.2-5	1662.528	2569.631
Line.2-6	1127.828	-548.515
Line.4-6	336.8904	240.83
Line.5-7	76.92461	-1882.66
Line.6-7	214.5932	-1080.79
Line.16-17	3.656396	13.41841
Line.15-18	20.30557	41.34919
Line.18-19	2.444898	4.943362
Line.19-20	9.952073	19.90415
Line.10-20	46.77697	104.4486
Line.10-17	8.895319	23.19921
Line.10-21	61.8256	133.0672
Line.10-22	29.32303	60.4611
Line.21-22	0.319724	0.650474
Line.15-23	16.08475	32.4912
Line.22-24	25.79077	40.14389
Line.23-24	2.667692	5.456642
Line.24-25	10.99769	19.20657
Line.25-26	24.4061	36.45565
Line.25-27	12.73074	24.30837
Line.27-29	47.19159	89.16591
Line.27-30	88.6606	166.8824
Line.29-30	18.31002	34.59746

Table 8

Base case real and reactive buses power in kW, kVar

Load	Kw	KVar	PF
B2	21700	12700	0.863
B3	2400	1200	0.894
B4	7600	1600	0.979
B5	94200	19000	0.98
B7	22800	10900	0.902
B8	30000	30000	0.707
B10	5800	2000	0.945
B12	11200	7500	0.831
B14	6200	1600	0.968
B15	8200	2500	0.957
B16	3500	1800	0.889
B17	9000	5800	0.841
B18	3200	900	0.963
B19	9500	3400	0.942
B20	2200	700	0.953
B21	17500	11200	0.842
B23	3200	1600	0.894
B24	8700	6700	0.792
B26	3500	2300	0.836
B29	2400	900	0.936
B30	10600	1900	0.984

3.2 PV system integrating

The PV system can connected to the load bus as shown in the Figure B.10 in Appendix 19 [101]:

The load flow analysis and line losses in the case of the absent of PV system and the case of the existence of PV will be as follows:

Case 1: Losses without PV system:

The configuration of power system without PV is represented by Figure B.11 in Appendix B, then we can write this equation according to it:

$$I_i^K = \left(\frac{S_i}{V_i^K}\right)^* = \left(\frac{P_i + \mathrm{j}Q_i}{V_i^K}\right)^* \quad (3.3)$$

Substituting this in equation (1), (2) getting:

$$P_{Loss}(i,i+1) = \frac{R_i}{V_i^2}(P_i^2 + Q_i^2) \quad (3.4)$$

$$Q_{Loss}(i,i+1) = \frac{X_i}{V_i^2}(P_i^2 + Q_i^2) \quad (3.5)$$

$$P_{T,Loss} = \sum_{i=1}^{N} \frac{R_i}{V_i^2}(P_i^2 + Q_i^2) \quad (3.6)$$

$$Q_{T,Loss} = \sum_{i=1}^{N} \frac{X_i}{V_i^2}(P_i^2 + Q_i^2) \quad (3.7)$$

Case 2: Losses with PV system:

The configuration of power system with PV is represented by Figure B.12 in appendix B, then we can write these equations according to it:

$$P_{PV,Loss}(i,i+1) = \frac{(P_i - P_{PV})^2 + Q_i^2}{V_i^2} R_i \quad (3.8)$$

$$Q_{PV,Loss}(i,i+1) = \frac{(P_i - P_{PV})^2 + Q_i^2}{V_i^2} X_i \quad (3.9)$$

Integrating PV in the power system reduces the line losses as the previous equation illustrated through the subtraction of the PV power from the bus power ($P_i - P_{pv}$), which means lower power passing through the transmission lines. The results summary below shows a reduction of the total line losses from (9308.34KW) to (7742.83KW) after adding a PV system. All the lines losses is represented in the table 9 below.

Year = 0
Hour = 24
Max pu. voltage = 1.0819
Min pu. voltage = 1.0078
Total Active Power: 183.551 MW
Total Reactive Power: -7.32345 Mvar
Total Active Losses: 9.30834 MW (5.071 %)
Total Reactive Losses: 1.58566 Mvar

Year = 0
Hour = 24
Max pu. voltage = 1.0818
Min pu. voltage = 1.0087
Total Active Power: 163.398 MW
Total Reactive Power: -3.63911 Mvar
Total Active Losses: 7.74283 MW, (4.739 %)
Total Reactive Losses: -5.56839 Mvar

Table 9

Total line losses with and without the PV addition

Element	Base Total loss(kW)	PV addition Total loss(kW)
Line.1-2	2469.102	1964.843
Line.1-3	1647.272	1293.766
Line.2-4	603.4155	464.7985
Line.3-4	453.9015	354.5994
Line.2-5	1662.532	1533.528
Line.15-18	20.30563	11.09539
Line.18-19	2.444906	0.479369
Line.10-17	8.895315	16.13513
Line.10-21	61.82571	15.18638
Line.10-22	29.32308	8.230068
Line.21-22	0.319725	4.584133
Line.15-23	16.08481	8.34851
Line.23-24	2.667708	0.965207
Line.24-25	10.9977	9.276228

Integrating PV in the power system increase the feeder voltages as shown in the Figure B.13 in Appendix B which illustrate voltage increment near bus 21 where a 50 MW PV system connected in our case study.

Voltage regulation after adding PV system (Distributed generator)

Drop voltage representation without PV can be calculated from this basic one line diagram,

Scheme 1

Drop voltage representation without PV

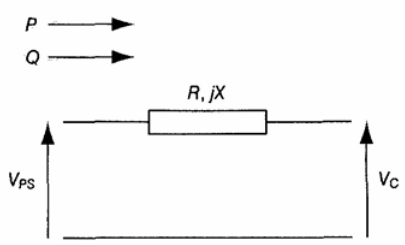

$$\Delta V = VPS - VC = \frac{RP+XQ}{VPS} \quad (3.10)$$

Where VPS is the substation voltage (sending voltage).

VC is the consumer point voltage.

R, X is the resistor and reactance of the transmission line.

P, Q is the real and reactive power carried by the transmission line transmitted from the substation.

Drop voltage representation with PV can also be derived from this basic one line diagram,

Scheme 2

Drop voltage representation witht PV

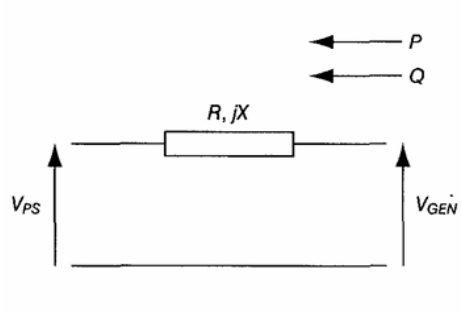

$$\Delta V = VGEN - VPS = \frac{RP+XQ}{VGEN} \qquad (3.11)$$

Where: VPS is the substation voltage (sending voltage).

VGEN is the distribution generator voltage.

R, X is the resistor and reactance of the transmission line.

P, Q is the real and reactive power transmitted by distribution generator.

3.3 Application of Direct Load Control (DLC)

We applied the chart manually by implicitly reduce some of the lower-priority loads from the page designated for loads in the opendss program by (10-30%) when loads exceed the threshold limit of power that was choose according to the capacity of the generators on the network., then applying them and monitoring the changes that occurred in the results. The power reduction in the loads is illustrated in the table 10 below; this reduction of loads will reduce the total bill of the consumers and also this will reduce the power losses in the grid from 9308.34 to 8220 kw after applying DLC system, the line losses in details is mentioned in table A.1 in appendix A; but it will slightly rise the voltages as shown in Figure B.16 in Appendix B.

Table 10

System with and without DLC real and reactive load power reduction

Load (#)	Active Power Without DLC (KW)	Active Power With DLC (kW)	Active Power Reduction (kW)
Bus # 3	604.805	423.365	181.44
Bus # 4	1915.21	1340.65	574.56
Bus # 10	1461.65	1315.48	146.17
Bus # 20	554.418	388.093	166.325
Bus # 21	4410.17	3528.13	882.04
Bus # 24	2192.48	1534.74	657.74
Bus # 26	882.025	617.419	264.606
Bus # 29	604.811	423.37	181.441
Bus # 30	2671.24	1869.88	801.36

Therefore, we can see a slight increase in the voltages of some buses due to the reduction of loads and the reduction of currents in the network in general. This is a symptom that can be ignored, provided that the permissible limit of the generated power is not exceeded and also the voltage constraint is not exceeded, because this is a bigger problem that leads to frequent power outages on all loads. The reduction of power can be observed by insert power monitor in any bus we need; we select arbitrary bus 23, compare the daily power after applying DLC and the power before, and represented in Figure B.15 in Appendix B.

3.4 Application of Direct Load Control (DLC) with (PV)

If we repeat the last run with the existent of PV, we get the Figure B.16 in Appendix B; we can note that DLC voltages will be affected by a bit decrease after added PV system and the grid losses also decreases from 8220 to 7742.83 kw, the line losses in detailed is enclosed in Table A.2 in appendix A.

3.5 Application of Conservation Voltage Reduction (CVR)

After Appling, the CVR techniques in the opendss as mentioned in Appendix E we get the following figure. We can notice the decrease in the voltages wither the bus voltages and the daily voltage profile of each bus; this will protect the network and the consumer's devices due to the voltage regulator achieved by the CVR autotransformer, which regulate the voltage to particular limits. This will improve the voltage stability of the grid, the

reduction of the voltage of the buses was as shown in Table A.3 in appendix A, and it can be demonstrated as in Figure B.17 in Appendix B, the daily voltage profile of bus 30 also represented in Figure B.18 in Appendix B, which also shows a reduction in voltage after applying CVR. The grid losses was slightly increased from 9308.34 to 9334.29 after applying CVR system due to the constant power nature of the loads, so any reduction in voltage followed by current increment so the total losses in the lines decreased.

3.6 Application of Conservation Voltage Reduction (CVR) with (PV)

Adding PV systems to the power system will introduce some raise in the voltage; these voltages will be regulated and reduced by applying CVR algorithm as shown in the Figure B.19 in Appendix B. Which gives us the opportunity to increase the hosting of the PV and not fear violating the voltage limits, which are considered the most important determinants of hosting the PV. Here lies the importance of the CVR in grids connected to the PV; CVR will mitigate the risk overvoltage conditions due to high levels of PV penetration that affect the network stability.

We can note that PV increase the voltages especially at bus 20, 21 where we add the PV system 1.063, 1.0524 pu, these voltages reduced after CVR to 1.055,1.044 P.U this reduction will be noticed also in the buses daily voltage profile as shown in Figure B.20 in appendix B.

The total line losses decreased after added PV system from 9334.29 to 6289.7 kW because the currents passed through the transmission lines decreased.

3.7 Application of Time-of-Use (TOU) Pricing

Here we assumed that the utility imposed a special electricity price that is characterized by the fact that the price of electricity is more expensive during the peak time load and less during off peak times. We imposed an actual customer response, which led to the transfer of the peak load from peak time to other times, so that the load pattern became almost constant and its size averaged at all times by approximately (0.6) Load factor as shown in Figure B.21 in Appendix B which monitor the load profile of bus 30 after applying TOU. When replacing the default load shape by smoothly load shape in the program, we obtain increasing in the voltages caused by the overall load reduction which

illustrated in Table A.4 in Appendix A, Figure B.22 in Appendix B shows the slight increase of the voltages for all the busses in our network,

Table A.5 in Appendix A represents the total line losses after applying TOU, it shows that the losses decreased at most of the lines, the total grid losses reduced from 9308.34 to 5779.78 kW after applying TOU.

3.8 Application of Time-of-Use (TOU) Pricing with (PV)

in this section; we find that applying TOU after adding the PV will slightly increase the voltages as shown in Figure B.23 in Appendix B; but to an acceptable degree; but it differs greatly in power losses as shown in Table A.6 in Appendix A; Here, this method differs from other DSM methods is that it aims to reduce the power generated by the generators in the network by decreasing the beak loads and control the load shape; as well as reduce losses in the cables, but in the case of not caring about the increase in voltage, but without exceeding the limits, in this case it will be more effective.

This figure shows that the buses voltages increased after applying TOU with the existence of PV due to the load pattern reduction as the price changes in each hour of the day. Table A.6 shows the reduction in the line losses in detail after applying TOU and also after adding PV due to the load pattern softening and the transmission line passing currents reduction due to the existence of distribution resources so the total grid losses reduced from 5779.78 to 3736.9 kW.

Chapter Four

Hosting Capacity for PV Integration and Conclusion

4.1 Hosting capacity analysis

The simulation after adding PV systems in many penetration levels, results shows that every increase in PV power will followed by a decrease in source power. We can note that at the 100 MW stage and above, the power generated by the PV system exceeds that generated by the source power; which means that there will be reverse power and more losses; but The biggest problem in such a case is that the power generated by solar cells is fluctuating and affected by weather, clouds, and sunlight. This harms the electrical grid in general and leads to frequent power outages, which affects electrical devices and eliminates the source security in the grid.

The power losses at every PV penetration scenario are represented in Figure B.24 in Appendix B; it is clear that losses decrease with the presence of PV because it reduces the power coming from the grid through the transmission lines, which reduces the current passing through them, which in turn reduces losses. We notice that the higher the value of PV penetrations, the lower the losses until it reaches a value of 100 MW or above. Here, the reverse power begins to appear and the currents of the solar cells begin to increase greatly, which increases losses significantly.

Also if we represent the voltage regulation of the line (14-15) as an example at these PV penetration levels, we can get Figure B.25 in Appendix B; which shows that the voltage regulation of that line decreases as we increase the PV power; It continues to decrease to the point where it turns and becomes negative at 100 and above. This indicates that the receiving voltage becomes higher than the sending voltage. Therefore, the power begins to pass from the high voltage to the lower one, which leads to the appearance of reverse power, which is the major problem of PV systems, as it changes the passage of electrical power from a unidirectional conventional electrical system to a bidirectional system.

$$\text{V.R} = \frac{VS-VR}{VR} * 100\% \quad = \frac{\Delta V}{VR} * 100\% \qquad (4.1)$$

Where: V.R: voltage regulation, VS: sending voltage, VR: receiving voltage.

The voltages are also affected by the change of the PV added to the system; we get some busses arbitrarily, represent their voltages, and compare them with the base voltage of that bus at every PV level as in Figures B.26-B.28 in Appendix B. From the figures, we can note that the busses voltages will rise as the PV power rises, and this leads to stability problems in the power systems if it exceeds the voltage constraint. In addition, the figures below show us the ampacity (current carrying capacity of cables) problem in some lines.

We can note that the currents in general decreased after adding PV, Figure B.29 in Appendix B illustrates that, with each increase in the PV hosting c, the current passing through the line B15-18 decreases until we reached 70, then the current began to increase significantly due to the reverse power flow. As for Figure B.30 in Appendix B, it dealt with a line close to the distributed generation source (line B19-20). Where the current began to increase with each addition of PV and continued to increase significantly so that it exceeded the cable rating current and caused the cable to heat up significantly, which led to the insulation collapsing in some cases where the penetration was very high.

4.2 Hosting capacity analysis with DSM techniques

We achieved this analysis by increasing the PV shared power to the system and then applying the DSM techniques (DLC, TOU) and noting the difference in the power, voltage, and losses at each of them, and then we summarize line 3-1 results is illustrated in Tables A.7-A.11 in Appendix A. We can note that the voltage drop, the power losses, and the voltage regulation will decrease after applying DSM techniques at all PV penetrations. So implementing the DSM techniques will increase the opportunity of increasing the hosting capacity of PV because it decreases the power losses of the network due to a decrease in currents passing through the transmission line; it can be represented in Figure B.31 in Appendix B; we can note that TOU will achieve the best results.

DSM techniques in general work to reduce the currents passed through the lines by decreasing the power delivered from the source; but in the case of huge PV penetration the currents of some lines will increase largely as we mentioned before, DSM reduces it as shown in Figure B.32 in Appendix B which represents the currents passed through line 10-20 at many penetration levels with and without implemented DSM techniques. We can note that the current when simulating PV 50 MW with TOU is equal to the 10 MW PV simulating without DSM (130 A) and also the current when simulating PV 50 MW

with DLC is equal to the current of 30 MW current without DSM(=~148A); So applying DSM will increase the opportunity to host much PV.

However, in the case of over 100 MW PV hosting capacity; it cannot reduce the current to its nominal voltage So that the possibility of cable insulation breakdown becomes certain. Therefore, it is preferable not to increase the percentage of hosting the PV to avoid this problem. The figure below shows the effect of the DSM on the current of one of the network cables close to the PV, in which the current increases with the increase in the value of the added PV. Unlike the large cables close to the source and designed to carry high currents, the current passing through them becomes very small with the increase in the size of the PV. Therefore, it is recommended not to exceed the permissible limit of the PV.

Running DLC, and TOU together simultaneously is better than running each one separately because, with each increase in the PV hosting capacity, the losses were reduced as shown in Figure B.33 in Appendix B. However there was a slight increase in the voltage at each increment of PV, and here the role of the CVR appeared in reducing and improving the voltage in each PV addition. Figure B.34 in Appendix B shows the important role of this strategy because the voltage in this case almost exceeded the upper limits of the voltage (1.1) at bus 21 when adding 250 MW PV to the same bus, but after applying it, the voltages became within the rang.

4.3 Conclusion

This study demonstrates the significant impact of (DSM) strategies on improving the performance and quality of electrical networks, both with and without photovoltaic (PV) integration. The results highlight the ability of DSM to optimize network operation, reduce losses, and enhance voltage profiles under various scenarios.

Firstly, the DLC strategy showed a slight increase in voltage levels, attributed to its ability to reduce the capacity required for loads, thereby decreasing the currents flowing through the network. This voltage increase, while minor, remained within acceptable limits. The most notable benefit of DLC is its effectiveness in reducing electrical losses in transmission lines and decreasing the capacity required from the utility to meet load demands. By prioritizing and automatically managing loads, DLC reduces the cost of

energy generation, aligning with its primary objective of minimizing operational expenses.

Secondly, the TOU tariff strategy proved effective in shifting loads from peak consumption periods to off-peak times. By incentivizing consumers to adjust their electricity usage through variable pricing, TOU reduces the need for generating additional electricity during peak demand. This not only decreases the investment required for new-generation units but also lowers the currents in transmission lines, leading to substantial reductions in network losses. Unlike DLC, TOU relies on consumer responsiveness to pricing signals, emphasizing the importance of consumer engagement in achieving optimal results.

The CVR strategy focused on regulating and reducing voltage levels. Results confirmed its ability to improve voltage stability across most network buses, particularly after integrating PV systems, which tend to slightly increase voltage in areas close to the generation source. The importance of CVR becomes particularly evident in networks where voltages exceed the global permissible limit of 1.1 p.u., as maintaining voltage within acceptable ranges is critical for system sensitivity and stability.

In the context of PV integration, the results showed that adding a 50 MW PV system to bus 21 reduced total transmission line losses from 9308.34 kW to 7742.83 kW. Additionally, the impact of DSM strategies was analyzed, with DLC reducing losses further to 5365.5 kW and TOU achieving an even greater reduction to 3736.9 kW. CVR, in turn, improved overall voltage profiles, reducing the voltage at bus 21 from 1.0524 p.u. to 1.0442 p.u. and at bus 11 from 1.0819 p.u. to 1.0748 p.u.

The hosting capacity analysis revealed that increasing PV penetration initially led to a steady reduction in losses. At penetration levels of 15 MW, 30 MW, 50 MW, and 70 MW, losses decreased from approximately 9830 kW to 8000 kW, 7000 kW, 6000 kW, and 5800 kW, respectively. However, beyond a hosting capacity of 70 MW, losses began to rise due to reverse power flow effects, increasing to 5900 kW, 7900 kW, and 12,200 kW at penetration levels of 100 MW, 150 MW, and 200 MW, respectively. This trend highlights the limitations of excessive PV penetration, as it can cause substantial losses and voltage instability.

Nevertheless, the use of DSM strategies mitigated these issues, even at high penetration levels. For instance, DLC reduced losses to approximately 6000 kW, while TOU achieved further reductions to 5000 kW at a 200 MW hosting capacity. These findings underscore the importance of combining DSM strategies with PV integration to optimize network performance, minimize losses, and enhance voltage stability.

In conclusion, this study establishes that DSM strategies, such as DLC, TOU, and CVR, play a crucial role in improving the operational efficiency of electrical networks, particularly in the context of PV integration. By reducing losses, enhancing voltage stability, and optimizing load distribution, these strategies contribute to the development of more resilient and cost-effective electrical systems.

List of Abbreviations

Abbreviation	Meaning
ADMS	Advanced Distribution Management Systems
AMI	Advanced Metering Infrastructure
CO2	carbon dioxide
CVR	Conservation Voltage Reduction
DER	Distributed Energy Resource
DERMS	Distributed Energy Resource Management Systems
DG	Distributed Generations
DLC	Direct Load Control
DSM	Demand Side Management
DR	Demand Response
EE	Energy Efficiency
EPS	Electrical Power Systems
EPRI	Electric Power Research Institute
IEEE	Institute of Electrical and Electronics Engineers
IT	Information Technology
IoT	Internet of Things
Kw	Kilowatt
KWh	kilowatt-hour
LTC	Load Tap Changer
MG	MicroGrid
NIST	National Institute for Standards and Technology
OPEC	Organization of Petroleum Exporting Countries
OPF	Optimal Power Flow
PAR	High Peak-to-average demand Ratio
P_peak	peak Watt produced
PV	Photovoltaic
RTC	Real-Time Clock
RTPDRP	Real-Time Price Demand Response Programs
SCADA	Supervisory Control and Data Acquisition
SG	Smart Grid
SGIP	Smart Grid Interoperability Panel
SM	Smart Meter
SR	Spinning Reserve
TOU	Time Of Use Tarrif
VPP	Virtual Power Plants
VVO	Voltage/VAR Optimization

References

[1] P.S.R. Murty, *Power System Analysis*. Elsevier, 2017.

[2] *Standalone Photovoltaic (PV) Systems for Disaster Relief and Remote Areas*. Elsevier, 2017. doi: 10.1016/C2014-0-03107-3.

[3] M. Ntombela, K. Musasa, and M. C. Leoaneka, "Power Loss Minimization and Voltage Profile Improvement by System Reconfiguration, DG Sizing, and Placement," *Computation*, vol. 10, no. 10, Oct. 2022, doi: 10.3390/computation10100180.

[4] Y. Li, C. Zhao, H. Jiang, Y. Zhang, and E. Muljadi, "Introduction," in *New Technologies for Power System Operation and Analysis*, Elsevier, 2021, pp. 1–21. doi: 10.1016/B978-0-12-820168-8.00001-8.

[5] K. Twaisan and N. Barışçı, "Integrated Distributed Energy Resources (DER) and Microgrids: Modeling and Optimization of DERs," *Electronics (Basel)*, vol. 11, no. 18, p. 2816, Sep. 2022, doi: 10.3390/electronics11182816.

[6] Jorge García, *Encyclopedia of Electrical and Electronic Power Engineering*. 2023.

[7] S. Tripathi, P. K. Verma, and G. Goswami, "A review on SMART GRID power system network," in *Proceedings of the 2020 9th International Conference on System Modeling and Advancement in Research Trends, SMART 2020*, Institute of Electrical and Electronics Engineers Inc., Dec. 2020, pp. 55–59. doi: 10.1109/SMART50582.2020.9337067.

[8] A. T. Dahiru, D. Daud, C. W. Tan, Z. T. Jagun, S. Samsudin, and A. M. Dobi, "A comprehensive review of demand side management in distributed grids based on real estate perspectives," *Environmental Science and Pollution Research*, vol. 30, no. 34, pp. 81984–82013, Jan. 2023, doi: 10.1007/s11356-023-25146-x.

[9] J. J. Moreno Escobar, O. Morales Matamoros, R. Tejeida Padilla, I. Lina Reyes, and H. Quintana Espinosa, "A Comprehensive Review on Smart Grids: Challenges and Opportunities," Oct. 21, 2021, *NLM (Medline)*. doi: 10.3390/s21216978.

[10] P. U. M and M. M. M, "A Review on Smart Meter System," *IJIREEICE*, vol. 3, no. 12, pp. 70–73, Dec. 2015, doi: 10.17148/ijireeice.2015.31215.

[11] S. Panda *et al.*, "Residential Demand Side Management model, optimization and future perspective: A review," Nov. 01, 2022, *Elsevier Ltd*. doi: 10.1016/j.egyr.2022.02.300.

[12] A. Adekunle Adeyemo and O. Taiwo Amusan, "Demand Side Management in Future Smart Grid: A Review of current state-of-the-art," in *Energy Proceedings*, Scanditale AB, 2021. doi: 10.46855/energy-proceedings-9185.

[13] B. Williams, D. Bishop, P. Gallardo, and J. G. Chase, “Demand Side Management in Industrial, Commercial, and Residential Sectors: A Review of Constraints and Considerations,” *Energies (Basel)*, vol. 16, no. 13, p. 5155, Jul. 2023, doi: 10.3390/en16135155.

[14] M. S. Bakare, A. Abdulkarim, M. Zeeshan, and A. N. Shuaibu, “A comprehensive overview on demand side energy management towards smart grids: challenges, solutions, and future direction,” *Energy Informatics*, vol. 6, no. 1, p. 4, Mar. 2023, doi: 10.1186/s42162-023-00262-7.

[15] Y. Tang, J. W. M. Cheng, Q. Duan, C. W. Lee, and J. Zhong, “Evaluating the variability of photovoltaics: A new stochastic method to generate site-specific synthetic solar data and applications to system studies,” *Renew Energy*, vol. 133, pp. 1099–1107, Apr. 2019, doi: 10.1016/j.renene.2018.10.102.

[16] H. A. H. Al-Hilfi, A. Abu-Siada, and F. Shahnia, “Estimating Generated Power of Photovoltaic Systems during Cloudy Days Using Gene Expression Programming,” *IEEE J Photovolt*, vol. 11, no. 1, pp. 185–194, Jan. 2021, doi: 10.1109/JPHOTOV.2020.3029217.

[17] E. Sarmas, E. Spiliotis, E. Stamatopoulos, V. Marinakis, and H. Doukas, “Short-term photovoltaic power forecasting using meta-learning and numerical weather prediction independent Long Short-Term Memory models,” *Renew Energy*, vol. 216, Nov. 2023, doi: 10.1016/j.renene.2023.118997.

[18] D. Assané, D. E. Konan, and P. C. Anukoolthamchote, “Assessing variability of photovoltaic load supply in Hawai‘i,” *Energy Policy*, vol. 132, pp. 290–298, Sep. 2019, doi: 10.1016/j.enpol.2019.05.007.

[19] P. Neetzow, R. Mendelevitch, and S. Siddiqui, “Modeling coordination between renewables and grid: Policies to mitigate distribution grid constraints using residential PV-battery systems,” *Energy Policy*, vol. 132, pp. 1017–1033, Sep. 2019, doi: 10.1016/j.enpol.2019.06.024.

[20] J. Torriti, *Peak Energy Demand and Demand Side Response*. Routledge, 2015. doi: 10.4324/9781315781099.

[21] J. Richardson and R. Nordhaus, “The National Energy Act of 1978,” 1995.

[22] V. S. K. Murthy Balijepalli, V. Pradhan, S. A. Khaparde, and R. M. Shereef, “Review of demand response under smart grid paradigm,” in *ISGT2011-India*, IEEE, Dec. 2011, pp. 236–243. doi: 10.1109/ISET-India.2011.6145388.

[23] H. Fraser, “The Importance of an Active Demand Side in the Electricity Industry,” *The Electricity Journal*, vol. 14, no. 9, pp. 52–73, Nov. 2001, doi: 10.1016/S1040-6190(01)00249-4.

[24] C. W. Gellings, “Evolving practice of demand-side management,” *Journal of Modern Power Systems and Clean Energy*, vol. 5, no. 1, pp. 1–9, Jan. 2017, doi: 10.1007/s40565-016-0252-1.

[25] A. F. Meyabadi and M. H. Deihimi, “A review of demand-side management: Reconsidering theoretical framework,” 2017, *Elsevier Ltd*. doi: 10.1016/j.rser.2017.05.207.

[26] “ARCHITECTURE AND PRINCIPLES OF SMART GRIDS FOR DISTRIBUTED POWER GENERATION AND DEMAND SIDE MANAGEMENT,” in *Proceedings of the 1st International Conference on Smart Grids and Green IT Systems*, SciTePress - Science and and Technology Publications, 2012, pp. 5–13. doi: 10.5220/0003949700050013.

[27] R. Sharifi, S. H. Fathi, and V. Vahidinasab, “A review on Demand-side tools in electricity market,” *Renewable and Sustainable Energy Reviews*, vol. 72, pp. 565–572, May 2017, doi: 10.1016/j.rser.2017.01.020.

[28] H. J. Jabir, J. Teh, D. Ishak, and H. Abunima, “Impacts of demand-side management on electrical power systems: A review,” 2018, *MDPI AG*. doi: 10.3390/en11051050.

[29] S. Kahrobaee and S. Asgarpoor, “The effect of demand side management on reliability of automated distribution systems,” in *2013 1st IEEE Conference on Technologies for Sustainability (SusTech)*, IEEE, Aug. 2013, pp. 179–183. doi: 10.1109/SusTech.2013.6617317.

[30] S. Iqbal *et al.*, “A Comprehensive Review on Residential Demand Side Management Strategies in Smart Grid Environment,” *Sustainability*, vol. 13, no. 13, p. 7170, Jun. 2021, doi: 10.3390/su13137170.

[31] E. Sarker *et al.*, “Progress on the demand side management in smart grid and optimization approaches,” *Int J Energy Res*, vol. 45, no. 1, pp. 36–64, Jan. 2021, doi: 10.1002/er.5631.

[32] M. N. Hafizah, A. Khiar, S. A. Farid, A. N. Ramani, M. Shamshiri, and C. K. Gan, “A REVIEW ON MICRO-GRID AND DEMAND SIDE MANAGEMENT AND THEIR RELATED STANDARDS,” 2012.

[33] Z. Baharlouei and M. Hashemi, “Demand Side Management challenges in smart grid: A review,” in *2013 Smart Grid Conference (SGC)*, IEEE, Dec. 2013, pp. 96–101. doi: 10.1109/SGC.2013.6733807.

[34] A. K. Muthria and L. Mathew, “A Review on Demand Side Management Schemes for Optimized Energy Utilization in Smart Grids.”

[35] L. Gelazanskas and K. A. A. Gamage, “Demand side management in smart grid: A review and proposals for future direction,” *Sustain Cities Soc*, vol. 11, pp. 22–30, Feb. 2014, doi: 10.1016/j.scs.2013.11.001.

[36] H. W. Khan *et al.*, “Intelligent Optimization Framework for Efficient Demand-Side Management in Renewable Energy Integrated Smart Grid,” *IEEE Access*, vol. 9, pp. 124235–124252, 2021, doi: 10.1109/ACCESS.2021.3109136.

[37] D. Kanakadhurga and N. Prabaharan, “Demand side management in microgrid: A critical review of key issues and recent trends,” *Renewable and Sustainable Energy Reviews*, vol. 156, p. 111915, Mar. 2022, doi: 10.1016/j.rser.2021.111915.

[38] I. F. Visconti, D. A. Lima, and J. V Milanovi, “Comprehensive analysis of Conservation Voltage Reduction: A real case study.”

[39] K. N. Nwaigwe, P. Mutabilwa, and E. Dintwa, “An overview of solar power (PV systems) integration into electricity grids,” *Mater Sci Energy Technol*, vol. 2, no. 3, pp. 629–633, Dec. 2019, doi: 10.1016/j.mset.2019.07.002.

[40] DanielLawlor, “Conservation Voltage Reduction / Volt VAR Optimization EM&V Practices.”

[41] D. A. Quijano and A. Padilha-Feltrin, “Optimal integration of distributed generation and conservation voltage reduction in active distribution networks,” *International Journal of Electrical Power and Energy Systems*, vol. 113, pp. 197–207, Dec. 2019, doi: 10.1016/j.ijepes.2019.05.039.

[42] T. Lawanson, R. Karandeh, V. Cecchi, and A. Kling, “Impacts of Distributed Energy Resources and Load Models on Conservation Voltage Reduction,” in *2018 Clemson University Power Systems Conference (PSC)*, IEEE, Sep. 2018, pp. 1–6. doi: 10.1109/PSC.2018.8664059.

[43] R. Cheng, Z. Wang, Y. Guo, and F. Bu, “Analyzing Photovoltaic’s Impact on Conservation Voltage Reduction in Distribution Networks,” Oct. 2021, [Online]. Available: http://arxiv.org/abs/2110.14777

[44] R. R. Jha, A. Dubey, and K. P. Schneider, “Conservation voltage reduction (CVR) via two-timescale control in unbalanced power distribution systems,” *IET Smart Grid*, vol. 3, no. 6, pp. 801–813, Dec. 2020, doi: 10.1049/iet-stg.2020.0051.

[45] H. Padullaparti *et al.*, “Conservation Voltage Reduction with Distributed Energy Resource Management System, Grid-Edge, and Legacy Devices,” in *2023 IEEE Power & Energy Society General Meeting (PESGM)*, IEEE, Jul. 2023, pp. 1–5. doi: 10.1109/PESGM52003.2023.10252669.

[46] S. Singh, S. Veda, S. P. Singh, and M. Baggu, “Maximizing the Benefits of Volt/VAR Optimization in the Presence of Community Energy Storage,” in *2018 IEEE International Conference on Power Electronics, Drives and Energy Systems (PEDES)*, IEEE, Dec. 2018, pp. 1–6. doi: 10.1109/PEDES.2018.8707524.

[47] M. M. Rahman *et al.*, “Energy Conservation of Smart Grid System Using Voltage Reduction Technique and Its Challenges,” 2022.

[48] K. Kostková, Ľ. Omelina, P. Kyčina, and P. Jamrich, “An introduction to load management,” *Electric Power Systems Research*, vol. 95, pp. 184–191, Feb. 2013, doi: 10.1016/j.epsr.2012.09.006.

[49] Ferc, “2008 Assessment of Demand Response and Advanced Metering Staff Report Federal Energy Regulatory Commission,” 2008.

[50] M. Saad, “Methods of Demand Site Management and Demand Response,” 2016.

[51] D. Stanelyte, N. Radziukyniene, and V. Radziukynas, “Overview of Demand-Response Services: A Review,” Mar. 01, 2022, *MDPI*. doi: 10.3390/en15051659.

[52] T. Hesser and S. Succar, “Renewables Integration Through Direct Load Control and Demand Response,” in *Smart Grid: Integrating Renewable, Distributed and Efficient Energy*, Elsevier, 2011, pp. 209–233. doi: 10.1016/B978-0-12-386452-9.00009-7.

[53] C. Silva, P. Faria, Z. Vale, and J. M. Corchado, “Demand response performance and uncertainty: A systematic literature review,” May 01, 2022, *Elsevier Ltd*. doi: 10.1016/j.esr.2022.100857.

[54] Ferc, “2016 Assessment of Demand Response and Advanced Metering Staff Report Federal Energy Regulatory Commission,” 2016.

[55] J. R. Vázquez-Canteli and Z. Nagy, “Reinforcement learning for demand response: A review of algorithms and modeling techniques,” *Appl Energy*, vol. 235, pp. 1072–1089, Feb. 2019, doi: 10.1016/j.apenergy.2018.11.002.

[56] P. You *et al.*, “Price-Based Demand Response: A Three-Stage Monthly Time-of-Use Tariff Optimization Model,” *Energies (Basel)*, vol. 16, no. 23, p. 7858, Nov. 2023, doi: 10.3390/en16237858.

[57] D. Li, W.-Y. Chiu, and H. Sun, “Demand Side Management in Microgrid Control Systems,” in *Microgrid*, Elsevier, 2017, pp. 203–230. doi: 10.1016/B978-0-08-101753-1.00007-3.

[58] E. Koch and A. M. A. Piette, “Direct versus Facility Centric Load Control for Automated Demand Response and published in the Proceedings,” 2009.

[59] S. Yilmaz, C. Chanez, P. Cuony, and M. K. Patel, “Analysing utility-based direct load control programmes for heat pumps and electric vehicles considering customer segmentation,” *Energy Policy*, vol. 164, May 2022, doi: 10.1016/j.enpol.2022.112900.

[60] J. A. Sa’ed, Z. Wari, F. Abughazaleh, J. Dawud, S. Favuzza, and G. Zizzo, “Effect of demand side management on the operation of pv-integrated distribution systems,” *Applied Sciences (Switzerland)*, vol. 10, no. 21, pp. 1–26, Nov. 2020, doi: 10.3390/app10217551.

[61] N. G. Paterakis, O. Erdinç, and J. P. S. Catalão, “An overview of Demand Response: Key-elements and international experience,” Mar. 01, 2017, *Elsevier Ltd*. doi: 10.1016/j.rser.2016.11.167.

[62] S. Y. Choi and K. Y. Lee, *Direct Load Control System Design Using Active Database*.

[63] S. Yilmaz, P. Cuony, and C. Chanez, “Prioritize your heat pump or electric vehicle? Analysing design preferences for Direct Load Control programmes in

Swiss households," *Energy Res Soc Sci*, vol. 82, Dec. 2021, doi: 10.1016/j.erss.2021.102319.

[64] A. Sridhar *et al.*, "Residential consumer preferences to demand response: Analysis of different motivators to enroll in direct load control demand response," *Energy Policy*, vol. 173, Feb. 2023, doi: 10.1016/j.enpol.2023.113420.

[65] S. Vesely and C. A. Klöckner, "Individual differences in acceptance of direct load control," *Energy Build*, vol. 325, Dec. 2024, doi: 10.1016/j.enbuild.2024.115009.

[66] A. Nilsson and C. Bartusch, "Empowered or enchained? Exploring consumer perspectives on Direct Load Control," *Energy Policy*, vol. 192, Sep. 2024, doi: 10.1016/j.enpol.2024.114248.

[67] I. Garniwa and N. S. Wardana, "Design of direct load control device and its effect on load reduction," in *IOP Conference Series: Materials Science and Engineering*, IOP Publishing Ltd, Dec. 2019. doi: 10.1088/1757-899X/673/1/012061.

[68] O. Elma, M. Kuzlu, and M. Pipattanasomporn, "A Smart Direct Load Control Approach Using Dynamic Voltage Control for Demand Response Programs," *Electric Power Components and Systems*, vol. 50, no. 13, pp. 738–750, Aug. 2022, doi: 10.1080/15325008.2022.2139869.

[69] A. Osman. M. Bahageel, G. I. Rashed, H. A. I. Gony, A. Badjan, and H. I. Shaheen, "Optimization of Direct Load Control Demand Response for Industrial Micro-Grid Using Smart Meter," in *2024 9th Asia Conference on Power and Electrical Engineering (ACPEE)*, IEEE, Apr. 2024, pp. 823–827. doi: 10.1109/ACPEE60788.2024.10532330.

[70] S. Datchanamoorthy, S. Kumar, Y. Ozturk, and G. Lee, "Optimal time-of-use pricing for residential load control," in *2011 IEEE International Conference on Smart Grid Communications (SmartGridComm)*, IEEE, Oct. 2011, pp. 375–380. doi: 10.1109/SmartGridComm.2011.6102350.

[71] L. Yang, C. Dong, C. L. J. Wan, and C. T. Ng, "Electricity time-of-use tariff with consumer behavior consideration," *Int J Prod Econ*, vol. 146, no. 2, pp. 402–410, Dec. 2013, doi: 10.1016/j.ijpe.2013.03.006.

[72] Q. Ma, R. Li, and F. Li, "Differential customer responsiveness to time-of-use tariffs," in *IEEE Power and Energy Society General Meeting*, IEEE Computer Society, Aug. 2020. doi: 10.1109/PESGM41954.2020.9281877.

[73] M. L. Nicolson, M. J. Fell, and G. M. Huebner, "Consumer demand for time of use electricity tariffs: A systematized review of the empirical evidence," Dec. 01, 2018, *Elsevier Ltd*. doi: 10.1016/j.rser.2018.08.040.

[74] A. P. Kaur and M. Singh, "Time-of-Use tariff rates estimation for optimal demand-side management using electric vehicles," *Energy*, vol. 273, p. 127243, Jun. 2023, doi: 10.1016/j.energy.2023.127243.

[75] S. Y. Yang, J. Woo, and W. Lee, “Assessing optimized time-of-use pricing for electric vehicle charging in deep vehicle-grid integration system,” *Energy Econ*, vol. 138, p. 107852, Oct. 2024, doi: 10.1016/j.eneco.2024.107852.

[76] W. Lee, Y. Koo, and Y. Kim, “Environmental time-of-use scheme: Strategic leveraging of financial and environmental incentives for greener electric vehicle charging,” *Energy*, vol. 309, p. 133174, Nov. 2024, doi: 10.1016/j.energy.2024.133174.

[77] V. Venizelou, N. Philippou, M. Hadjipanayi, G. Makrides, V. Efthymiou, and G. E. Georghiou, “Development of a novel time-of-use tariff algorithm for residential prosumer price-based demand side management,” *Energy*, vol. 142, pp. 633–646, Jan. 2018, doi: 10.1016/j.energy.2017.10.068.

[78] C. Eid, E. Koliou, M. Valles, J. Reneses, and R. Hakvoort, “Time-based pricing and electricity demand response: Existing barriers and next steps,” *Util Policy*, vol. 40, pp. 15–25, Jun. 2016, doi: 10.1016/j.jup.2016.04.001.

[79] J. A. Khan, “Grid connected PV systems and their growth in power system,” *International Journal of Trend in Scientific Research and Development*, vol. Volume-2, no. Issue-3, pp. 1791–1797, Apr. 2018, doi: 10.31142/ijtsrd11646.

[80] M. I. B. Setyonegoro *et al.*, “Study of rooftop PV hosting capacity in 20 kV systems in facing distributed generation penetration,” *Results in Engineering*, vol. 23, Sep. 2024, doi: 10.1016/j.rineng.2024.102517.

[81] B. Uzum, A. Onen, H. M. Hasanien, and S. M. Muyeen, “electronics Rooftop Solar PV Penetration Impacts on Distribution Network and Further Growth Factors-A Comprehensive Review,” 2020, doi: 10.3390/electronics.

[82] A. Alshahrani, S. Omer, and Y. Su, “An Investigation into the Potential of Hosting Capacity and the Frequency Stability of a Regional Grid with Increasing Penetration Level of Large-Scale PV Systems,” *Electronics (Basel)*, vol. 10, no. 11, p. 1254, May 2021, doi: 10.3390/electronics10111254.

[83] M. Bollen and S. Rönnberg, “Hosting Capacity of the Power Grid for Renewable Electricity Production and New Large Consumption Equipment,” *Energies (Basel)*, vol. 10, no. 9, p. 1325, Sep. 2017, doi: 10.3390/en10091325.

[84] R. A. Shayani and M. A. G. de Oliveira, “Photovoltaic Generation Penetration Limits in Radial Distribution Systems,” *IEEE Transactions on Power Systems*, vol. 26, no. 3, pp. 1625–1631, Aug. 2011, doi: 10.1109/TPWRS.2010.2077656.

[85] H. H. H. Mousa, K. Mahmoud, and M. Lehtonen, “A Comprehensive Review on Recent Developments of Hosting Capacity Estimation and Optimization for Active Distribution Networks,” *IEEE Access*, vol. 12, pp. 18545–18593, 2024, doi: 10.1109/ACCESS.2024.3359431.

[86] A. K. Karmaker, K. Prakash, M. N. I. Siddique, M. A. Hossain, and H. Pota, “Electric vehicle hosting capacity analysis: Challenges and solutions,” *Renewable*

and Sustainable Energy Reviews, vol. 189, p. 113916, Jan. 2024, doi: 10.1016/j.rser.2023.113916.

[87] R. Lliuyacc-Blas and P. Kepplinger, "Violation-mitigation-based method for PV hosting capacity quantification in low voltage grids," *International Journal of Electrical Power & Energy Systems*, vol. 142, p. 108318, Nov. 2022, doi: 10.1016/j.ijepes.2022.108318.

[88] J. Varela, N. Hatziargyriou, L. J. Puglisi, M. Rossi, A. Abart, and B. Bletterie, "The IGREENGrid Project: Increasing Hosting Capacity in Distribution Grids," *IEEE Power and Energy Magazine*, vol. 15, no. 3, pp. 30–40, May 2017, doi: 10.1109/MPE.2017.2662338.

[89] Y.-J. Son, S.-H. Lim, S.-G. Yoon, and P. P. Khargonekar, "Residential Demand Response-Based Load-Shifting Scheme to Increase Hosting Capacity in Distribution System," *IEEE Access*, vol. 10, pp. 18544–18556, 2022, doi: 10.1109/ACCESS.2022.3151172.

[90] J. Byrne, S. Letendre, C. Govindarajalu, Y.-D. Wang, and R. Nigro, "Evaluating the economics of photovoltaics in a demand-side management role," *Energy Policy*, vol. 24, no. 2, pp. 177–185, Feb. 1996, doi: 10.1016/0301-4215(95)00106-9.

[91] S. N. Md Saad and A. H. van der Weijde, "Evaluating the Potential of Hosting Capacity Enhancement Using Integrated Grid Planning modeling Methods," *Energies (Basel)*, vol. 12, no. 19, p. 3610, Sep. 2019, doi: 10.3390/en12193610.

[92] R. Lliuyacc-Blas, M. L. Kolhe, and P. Kepplinger, "Enhanced violation-mitigation-based method using voltage/current sensitivities for PV hosting capacity quantification in low-voltage grids," *Electric Power Systems Research*, vol. 232, p. 110430, Jul. 2024, doi: 10.1016/j.epsr.2024.110430.

[93] A. Gulraiz, N. E. Batool, R. Shaherbano, R. Hussain, and S. Haider Zaidi, "Impact of Photovoltaic Ingress on Power Distribution System," in *2023 International Conference on Emerging Power Technologies (ICEPT)*, IEEE, May 2023, pp. 1–6. doi: 10.1109/ICEPT58859.2023.10152398.

[94] J. Paoli, B. Brinkmann, and M. Negnevitsky, "Optimising Low-Voltage Transformer Tap Settings in Distribution Networks," in *2019 29th Australasian Universities Power Engineering Conference (AUPEC)*, IEEE, Nov. 2019, pp. 1–6. doi: 10.1109/AUPEC48547.2019.211792.

[95] O. Gandhi, D. S. Kumar, C. D. Rodríguez-Gallegos, and D. Srinivasan, "Review of power system impacts at high PV penetration Part I: Factors limiting PV penetration," *Solar Energy*, vol. 210, pp. 181–201, Nov. 2020, doi: 10.1016/j.solener.2020.06.097.

[96] T. Al Momani, A. Harb, and F. Amoura, "Impact of photovoltaic systems on voltage profile and power losses of distribution networks in Jordan," in *2017 8th International Renewable Energy Congress (IREC)*, IEEE, Mar. 2017, pp. 1–6. doi: 10.1109/IREC.2017.7925996.

[97] R. Aghatehrani and A. Golnas, “Reactive power control of photovoltaic systems based on the voltage sensitivity analysis,” in *2012 IEEE Power and Energy Society General Meeting*, IEEE, Jul. 2012, pp. 1–5. doi: 10.1109/PESGM.2012.6345477.

[98] Yining Hou, J. Magnusson, G. Engdahl, and L. Liljestrand, “Impact on voltage rise of PV generation in future swedish urban areas with high PV penetration,” in *2014 IEEE International Energy Conference (ENERGYCON)*, IEEE, May 2014, pp. 904–911. doi: 10.1109/ENERGYCON.2014.6850533.

[99] F. Bai, R. Yan, T. K. Saha, and D. Eghbal, “An Excessive Tap Operation Evaluation Approach for Unbalanced Distribution Networks With High PV Penetration,” *IEEE Trans Sustain Energy*, vol. 12, no. 1, pp. 169–178, Jan. 2021, doi: 10.1109/TSTE.2020.2988571.

[100] H. K. Khyani and J. Vajpai, “Integration of Solar PV Systems to the Grid: Issues and Challenges.” [Online]. Available: www.ijert.org

[101] A. Alshahrani, S. Omer, Y. Su, E. Mohamed, and S. Alotaibi, “The Technical Challenges Facing the Integration of Small-Scale and Large-scale PV Systems into the Grid: A Critical Review,” *Electronics (Basel)*, vol. 8, no. 12, p. 1443, Dec. 2019, doi: 10.3390/electronics8121443.

[102] B. Belcher, B. J. Petry, T. Davis, and K. Hatipoglu, “The effects of major solar integration on a 21-Bus system: Technology review and PSAT simulations,” in *SoutheastCon 2017*, IEEE, Mar. 2017, pp. 1–8. doi: 10.1109/SECON.2017.7925361.

[103] D. Chathurangi, U. Jayatunga, M. Rathnayake, A. Wickramasinghe, A. Agalgaonkar, and S. Perera, “Potential power quality impacts on LV distribution networks with high penetration levels of solar PV,” in *2018 18th International Conference on Harmonics and Quality of Power (ICHQP)*, IEEE, May 2018, pp. 1–6. doi: 10.1109/ICHQP.2018.8378890.

[104] S. M. Ismael, S. H. E. Abdel Aleem, A. Y. Abdelaziz, and A. F. Zobaa, “State-of-the-art of hosting capacity in modern power systems with distributed generation,” *Renew Energy*, vol. 130, pp. 1002–1020, Jan. 2019, doi: 10.1016/j.renene.2018.07.008.

[105] Z. Kailun, D. S. Kumar, D. Srinivasan, and A. Sharma, “An adaptive overcurrent protection scheme for microgrids based on real time digital simulation,” in *2017 IEEE Innovative Smart Grid Technologies - Asia (ISGT-Asia)*, IEEE, Dec. 2017, pp. 1–6. doi: 10.1109/ISGT-Asia.2017.8378368.

[106] R. Jain, Y. N. Velaga, K. Prabakar, M. Baggu, and K. Schneider, “Modern trends in power system protection for distribution grid with high DER penetration,” *e-Prime - Advances in Electrical Engineering, Electronics and Energy*, vol. 2, p. 100080, 2022, doi: 10.1016/j.prime.2022.100080.

[107] D. S. Nair and T. Rajeev, “Impact of Reverse Power Flow Due to High Solar PV Penetration on Distribution Protection System,” 2022, pp. 1–13. doi: 10.1007/978-981-16-9033-4_1.

[108] Dharamjit and D. K. Tanti, “Load Flow Analysis on IEEE 30 bus System,” *International Journal of Scientific and Research Publications*, vol. 2, no. 11, 2012, [Online]. Available: www.ijsrp.org

[109] P. Sharma, N. Batish, S. Khan, and S. Arya, “Power Flow Analysis for IEEE 30 Bus Distribution System.”

[110] I. Totonchi, H. Al Akash, A. Al Akash, and A. Faza, “Sensitivity analysis for the IEEE 30 bus system using load-flow studies,” in *2013 3rd International Conference on Electric Power and Energy Conversion Systems*, IEEE, Oct. 2013, pp. 1–6. doi: 10.1109/EPECS.2013.6713060.

[111] H. Om and S. Shukla, “Optimal Power Flow Analysis of IEEE-30 bus System using Genetic Algorithm Techniques”.

[112] K. Lenin, “Real power loss diminution by predestination of particles wavering search algorithm,” *International Journal of Informatics and Communication Technology (IJ-ICT)*, vol. 9, no. 2, p. 92, Aug. 2020, doi: 10.11591/ijict.v9i2.pp92-99.

[113] D. Kaur Mander and S. K. Saini, “Load Flow Analysis: A Review,” *International Journal of Advanced Research in Electrical, Electronics and Instrumentation Engineering (An ISO*, vol. 3297, 2007, doi: 10.15662/IJAREEIE.2016.0503009.

[114] O. A. Afolabi, W. H. Ali, P. Cofie, J. Fuller, P. Obiomon, and E. S. Kolawole, “Analysis of the Load Flow Problem in Power System Planning Studies,” *Energy Power Eng*, vol. 07, no. 10, pp. 509–523, 2015, doi: 10.4236/epe.2015.710048.

[115] R. C. Dugan and D. Montenegro, “Reference Guide The Open Distribution System Simulator™ (OpenDSS),” 2022.

Appendices

Appendix A

Tables

Table A.1

Total line losses before and after applying DLC

Element	Base Total LOSS(kW)	DLC Total LOSS(kW)
Line.1-2	2469.102	2420.069
Line.1-3	1647.272	1564.407
Line.2-4	603.4155	558.1023
Line.3-4	453.9015	437.5804
Line.2-5	1662.532	1673.427
Line.2-6	1127.832	1057.87
Line.4-6	336.8911	330.0853
Line.5-7	76.92282	94.32538
Line.6-7	214.5943	238.7174
Line.6-8	63.64129	63.64222
Line.12-14	40.54785	33.10873
Line.12-15	117.1775	112.0259
Line.12-16	27.78904	28.32296
Line.14-15	2.93875	5.004794
Line.19-20	9.952082	12.50544
Line.10-20	46.77703	51.24287
Line.10-17	8.895315	12.53889
Line.10-21	61.82571	51.92978
Line.10-22	29.32308	23.97574
Line.21-22	0.319725	0.456311
Line.15-23	16.08481	11.44758
Line.22-24	25.7908	16.25372
Line.23-24	2.667708	0.919773
Line.24-25	10.9977	15.7088
Line.25-26	24.40614	17.22933
Line.25-27	12.73076	14.50143
Line.27-30	88.66074	48.55173
Line.29-30	18.31005	9.762113

Table A.2

Total line losses with the PV addition and after applying DLC

Element	PV-case losses Total(kW)	DLC-PV losses Total(kW)
Line.1-2	1964.843	1932.05
Line.1-3	1293.766	1228.795
Line.2-4	464.7985	429.0758
Line.3-4	354.5994	342.5148
Line.2-5	1533.528	1545.86
Line.2-6	876.4755	820.9634
Line.4-6	268.3567	263.2842
Line.5-7	103.8628	123.1002
Line.6-7	252.3675	277.4339
Line.6-8	69.43427	69.36663
Line.14-15	1.287471	2.61487
Line.16-17	0.420708	0.746696
Line.15-18	11.09539	12.74307
Line.18-19	0.479369	0.566414
Line.19-20	14.24753	17.42422
Line.10-20	61.95224	67.40182
Line.10-17	16.13513	21.47532
Line.10-21	15.18638	18.73806
Line.10-22	8.230068	8.527612
Line.21-22	4.584133	4.116903
Line.15-23	8.34851	6.824156
Line.22-24	69.73098	49.54967
Line.23-24	0.965207	3.815814
Line.24-25	9.276228	7.081805
Line.25-26	24.31977	17.27824
Line.25-27	2.235668	3.173181
Line.27-29	47.14826	26.37596
Line.27-30	88.579	48.57037
Line.29-30	18.29311	9.765861

Table A.3

CVR voltage reduction

Bus#	V-pu1 BASE	CVR V- PU
B1	1.06	1.06
B2	1.0451	1.0417
B3	1.0272	1.0212
B4	1.0189	1.0116
B5	1.0101	1.0045
B6	1.0155	1.0083
B7	1.0078	1.0011
B8	1.0099	1.0027
B9	1.0591	1.0509
B10	1.0588	1.05
B11	1.0819	1.074
B12	1.0658	1.0541
B13	1.071	1.06
B14	1.0551	1.0433
B15	1.0519	1.0407
B16	1.0571	1.0467
B17	1.0545	1.0452
B18	1.0453	1.0348
B19	1.0437	1.0336
B20	1.0469	1.0372
B21	1.0496	1.0406
B22	1.05	1.0409
B23	1.0447	1.0341
B24	1.0414	1.0316
B25	1.0353	1.0265
B26	1.0223	1.0132
B27	1.0378	1.0298
B28	1.0127	1.0052
B29	1.0233	1.0149
B30	1.0148	1.0063

Table A.4

Load power reduction after applying TOU

Load (#)	Active Power Without TOU (KW)	Active Power With TOU (kW)	Active Power Reduction (kW)
B2	5468.3	4412.32	1055.98
B3	604.805	487.99	116.815
B4	1915.21	1545.29	369.92
B5	23737.3	19154	4583.3
B7	5745.54	4635.94	1109.6
B8	7560.2	6099.84	1460.45
B10	1461.65	1179.28	282.37
B12	2822.52	2277.24	545.28
B14	1562.45	1260.59	301.86
B15	2066.47	1667.24	399.23
B16	882.033	711.633	170.4
B17	2268.09	1829.93	438.16
B18	806.425	650.629	155.796
B19	2394.08	1931.56	462.52
B20	554.418	447.309	107.109
B21	4410.17	3558.19	851.98
B23	806.428	650.635	155.793
B24	2192.48	1768.94	423.54
B26	882.025	711.641	170.384
B29	604.811	487.98	116.831
B30	2671.24	2155.22	516.02

Table A.5

Total line losses with and without TOU

Element	baseTotal loss(kW)	TOU Total loss(kW)
Line.1-2	2469.102	1354.244
Line.1-3	1647.272	1011.397
Line.2-4	603.4155	411.5525
Line.3-4	453.9015	280.0325
Line.2-5	1662.532	1090.789
Line.2-6	1127.832	754.428
Line.4-6	336.8911	209.6743
Line.5-7	76.92282	41.70968
Line.6-7	214.5943	139.6762
Line.6-8	63.64129	62.29212
Line.16-17	3.65641	2.100787
Line.15-18	20.30563	12.37295
Line.18-19	2.444906	1.427913
Line.19-20	9.952082	6.674196
Line.10-20	46.77703	30.9885
Line.10-17	8.895315	6.35701
Line.10-21	61.82571	39.7682
Line.10-22	29.32308	18.90947
Line.21-22	0.319725	0.19932
Line.15-23	16.08481	9.636932
Line.22-24	25.7908	17.06796
Line.23-24	2.667708	1.449706
Line.24-25	10.9977	12.22985
Line.25-26	24.40614	15.50177
Line.25-27	12.73076	8.706737
Line.27-29	47.19167	29.99278
Line.27-30	88.66074	56.31559
Line.29-30	18.31005	11.6212

Table A.6

Total line losses with PV alone and system synchronized PV withTOU

Element	PV loss Total(kW)	PV-TOU losses Total(kW)
Line.1-2	1964.843	1003.399
Line.1-3	1293.766	746.41
Line.2-4	464.7985	301.4279
Line.3-4	354.5994	205.9612
Line.2-5	1533.528	991.4482
Line.2-6	876.4755	556.7183
Line.4-6	268.3567	158.0804
Line.5-7	103.8628	64.03629
Line.6-7	252.3675	169.7883
Line.6-8	69.43427	74.62686
Line.12-14	34.09698	20.52396
Line.12-15	84.92622	48.38914
Line.12-16	11.1861	4.643004
Line.14-15	1.287471	0.54423
Line.16-17	0.420708	0.190581
Line.15-18	11.09539	5.497435
Line.18-19	0.479369	0.114117
Line.19-20	14.24753	10.2235
Line.10-20	61.95224	43.44412
Line.10-17	16.13513	12.51874
Line.10-21	15.18638	9.422602
Line.10-22	8.230068	4.141691
Line.21-22	4.584133	4.893011
Line.15-23	8.34851	3.91386
Line.22-24	69.73098	55.55422
Line.23-24	0.965207	0.612931
Line.24-25	9.276228	11.97522
Line.25-26	24.31977	15.45846
Line.25-27	2.235668	1.06638
Line.27-29	47.14826	29.98459
Line.27-30	88.579	56.30021
Line.29-30	18.29311	11.61803

Table A.7

Power Losses and voltage drop of line 3-1 in 15 MW PV addition with DSM strategies

Case	Line Current	Line voltage Drop	Line Power Losses	V.R
Base Case	263.246	2500.4	1647.26	3.19%
PV 15 MW Addition	243.333	2472.9	1410.125	3.15%
PV 15 MW With DLC	222.75	2341.7	1183.18708	2.98%
PV 15 MW With TOU	188.11	2265.9	848.88551	2.88%

Table A.8

Power Losses and voltage drop of line 3-1 in 30 MW PV addition with DSM strategies

Case	Line Current	Line voltage Drop	Line Power Losses	V.R
Base Case	263.246	2500.4	1647.26	3.19%
PV 30 MW Addition	217.588	2381.4	1130.54709	3.03%
PV 30 MW With DLC	196.2	2249.5	921.32271	2.86%
PV 30 MW With TOU	161.705	2178.1	631.84487	2.77%

Table A.9

Power Losses and voltage drop of line 3-1 in 50 MW PV addition with DSM strategies

Case	Line Current	Line voltage Drop	Line Power Losses	V.R
Base Case	263.246	2500.4	1647.26	3.19%
PV 50 MW Addition	185.592	2277	827.06227	2.90%
PV 50 MW With DLC	138.159	2149.8	650.85966	2.73%
PV 50 MW With TOU	130.79	2132.5	420.02213	2.65%

Table A.10

Power Losses and voltage drop of line 3-1 in 70 MW PV addition with DSM strategies

Case	Line Current	Line voltage Drop	Line Power Losses	V.R
Base Case	263.246	2500.4	1647.26	3.19%
PV 70 MW Addition	153.481	2127	570.62679	2.70%
PV 70 MW With DLC	132.661	2008.9	430.18185	2.55%
PV 70 MW With TOU	102.153	1991.6	264.19078	2.53%

Table A.11

Power Losses and voltage drop of line 3-1 in 100 MW PV addition with DSM strategies

Case	Line Current	Line voltage Drop	Line Power Losses	V.R
Base Case	263.246	2500.4	1647.26	3.19%
PV 100 MW Addition	112.349	2089.4	316.24	2.66%
PV 100 MW With DLC	95.4645	1994.5	233.87	2.53%
PV 100 MW With TOU	65.5008	1850.6	121.86	2.34%

Note: Where Line Current in (A) , Line voltage Drop in (V), Line Power Losses in (kW).

Appendix B

Figures

Figure B.1

Compensation Current Model of PC Elements (one-line) in opendss.

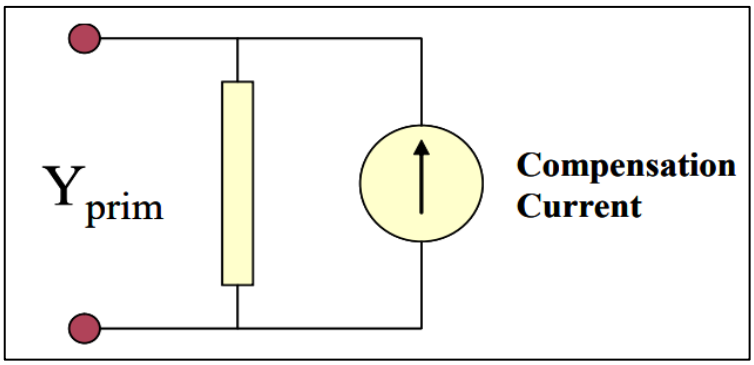

Figure B.2

Opendss solution loop

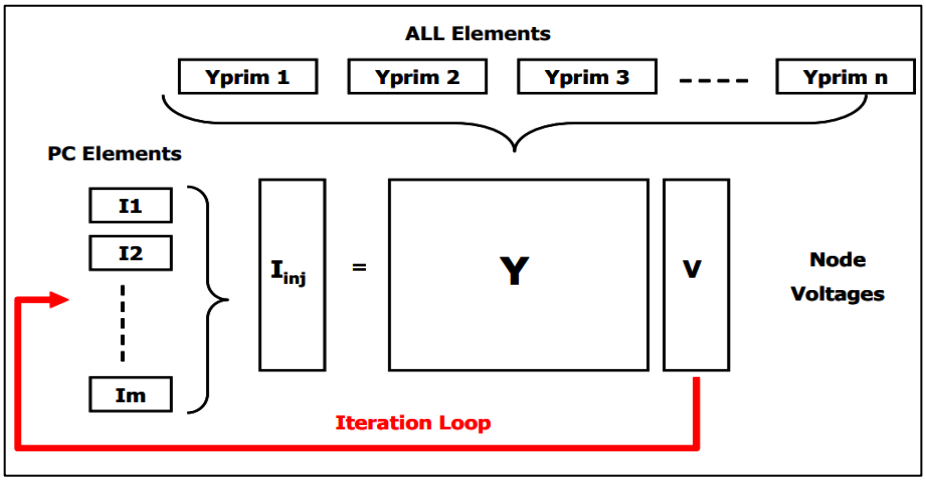

Figure B.3

Buses i, j represented in the power flow equations

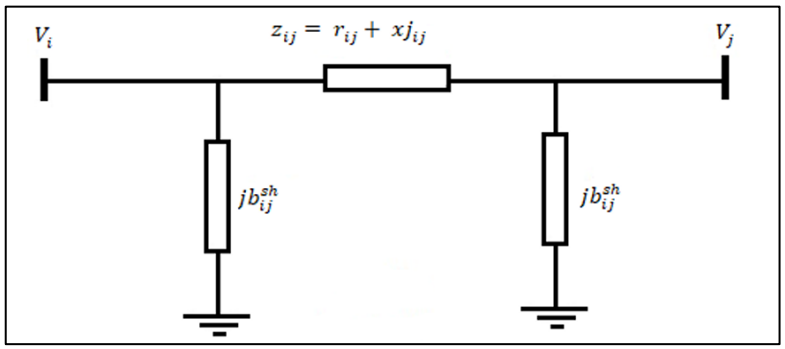

Figure B.4

CVR implementation algorithm

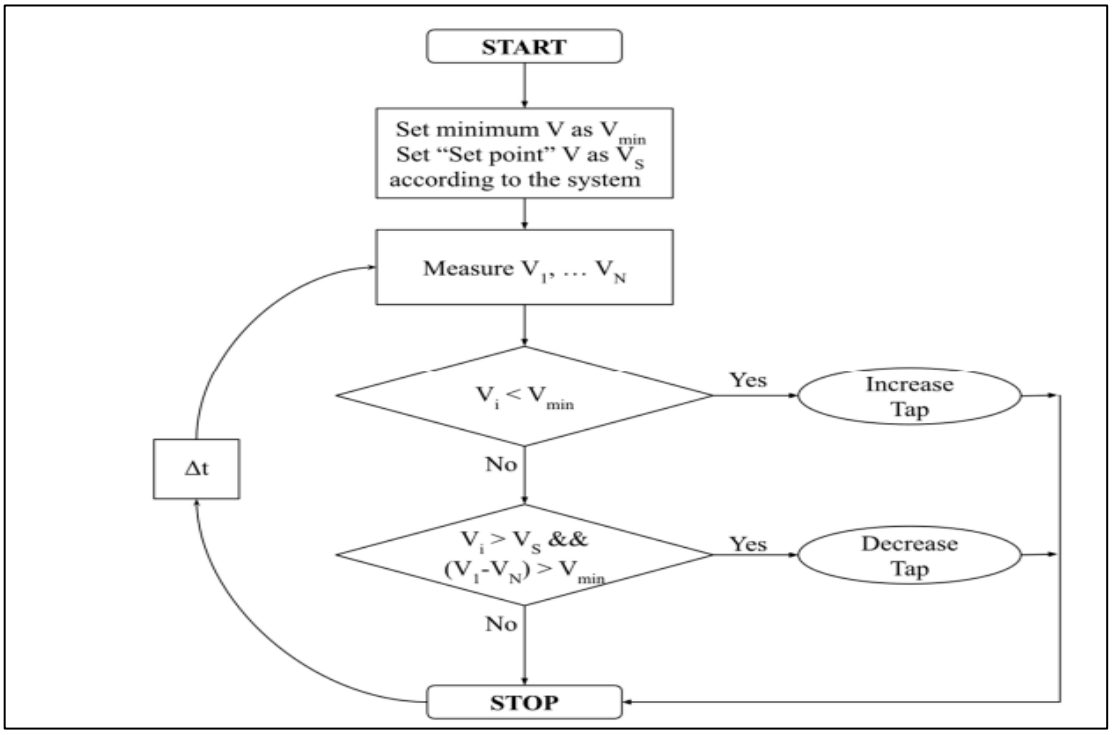

Figure B.5

DLC implementation chart

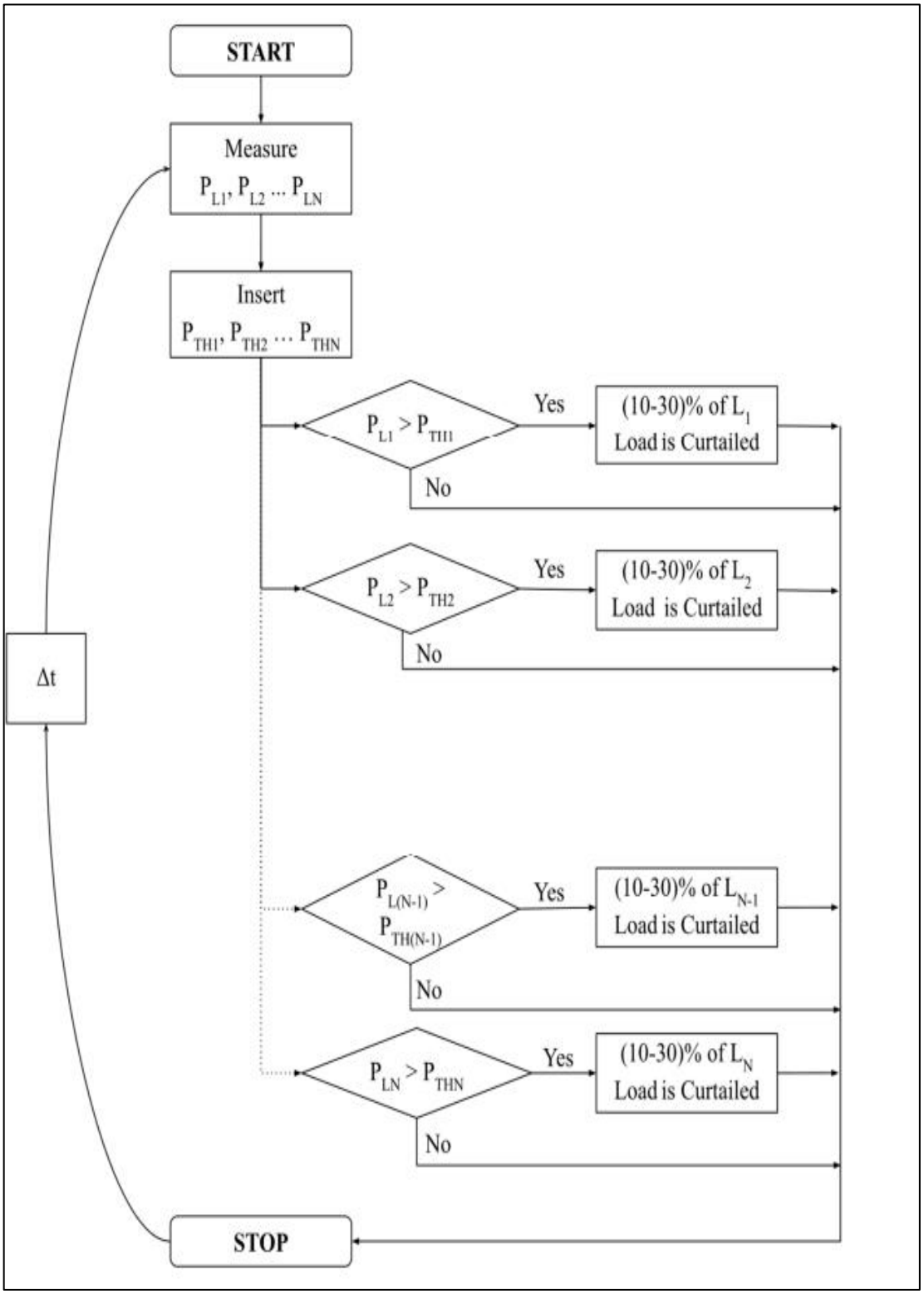

Figure B.6

P.u power of PV systems

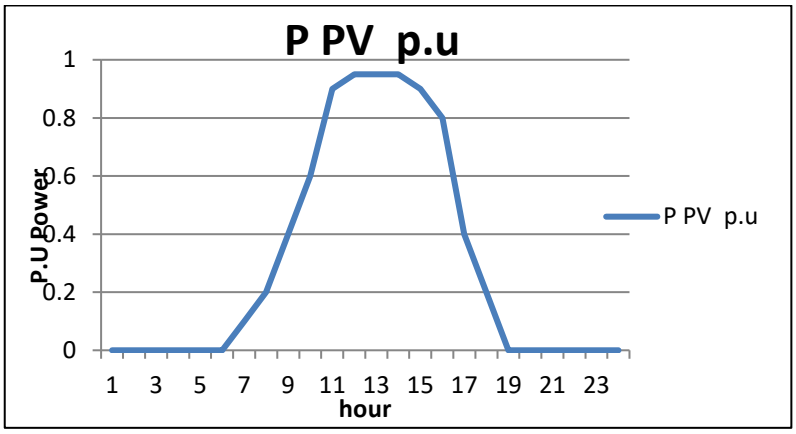

Figure B.7

P.u busses voltages of base case

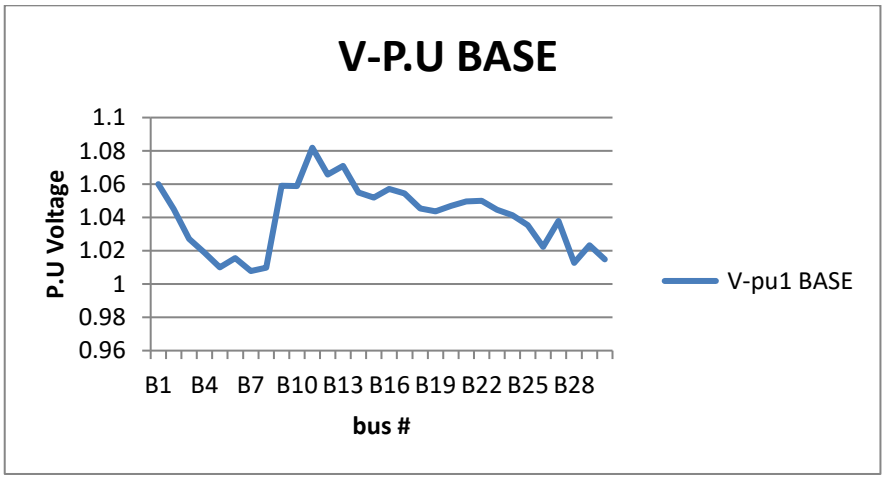

Figure B.8

Bus 30 voltage monitor in base case

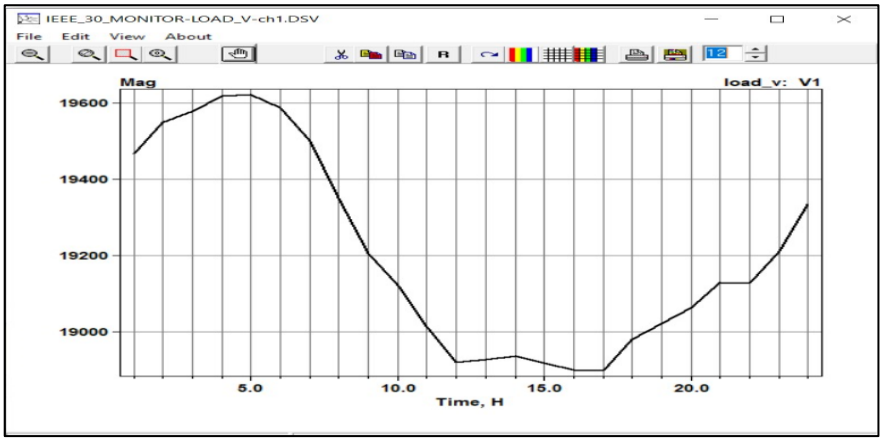

Figure B.9

24-H Daily load shape

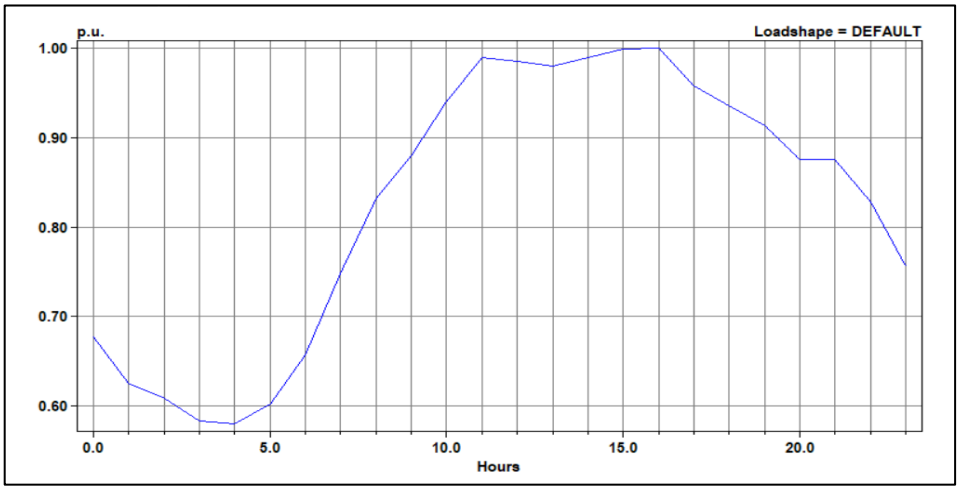

Figure B.10

PV system connected to the grid

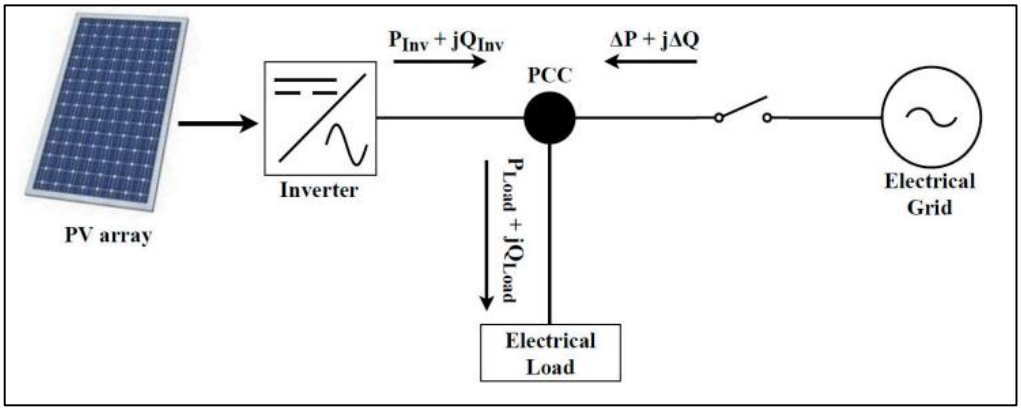

Figure B.11

Load flow representation without PV

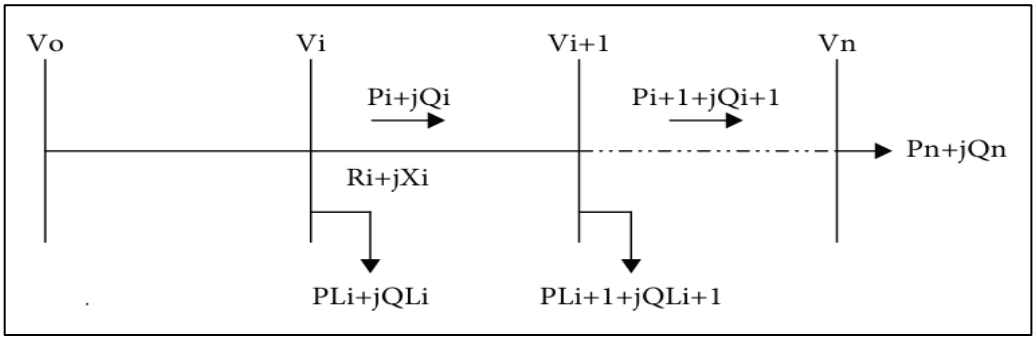

Figure B.12

Load flow representation with PV

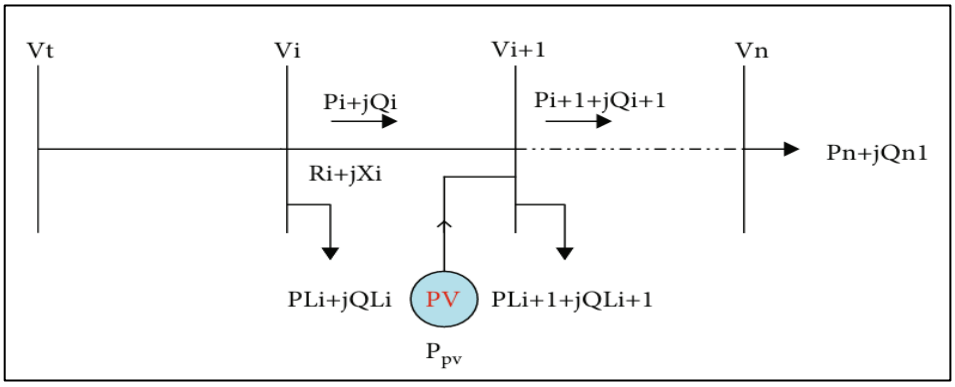

Figure B.13

Bus voltages before and after the PV addition

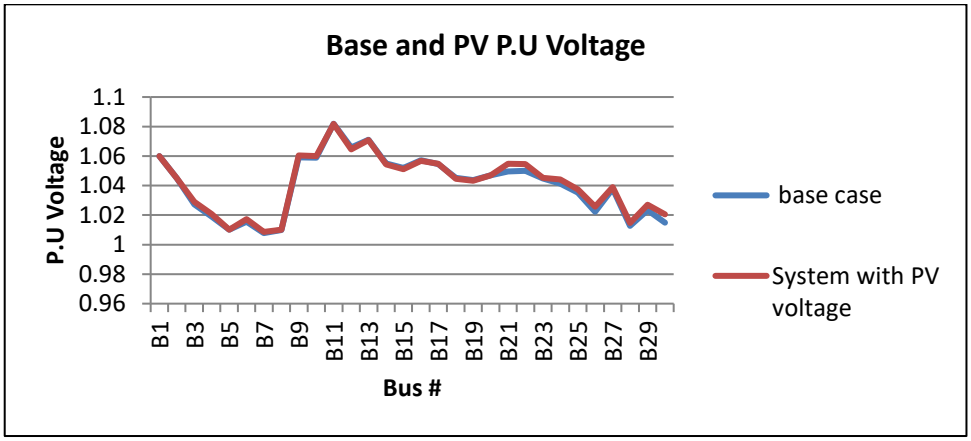

Figure B.14

P.u voltage busses with and without DLC

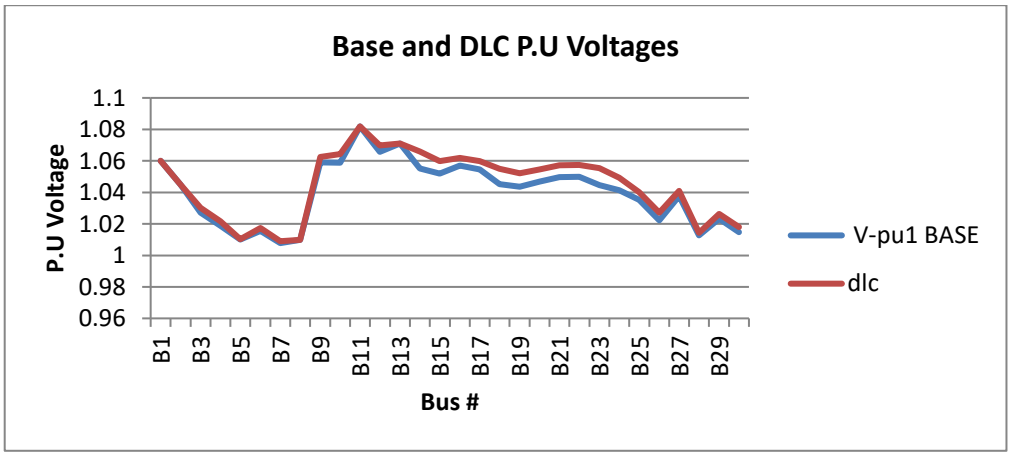

Figure B.15

Bus 23 power monitor with and without DLC

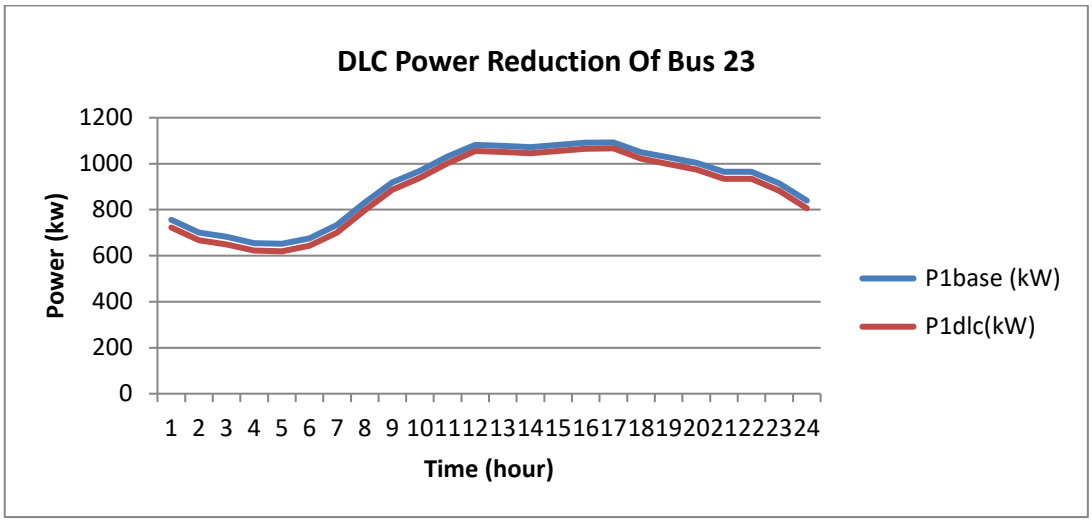

Figure B.16

P.u voltage busses with DLC and with PV system

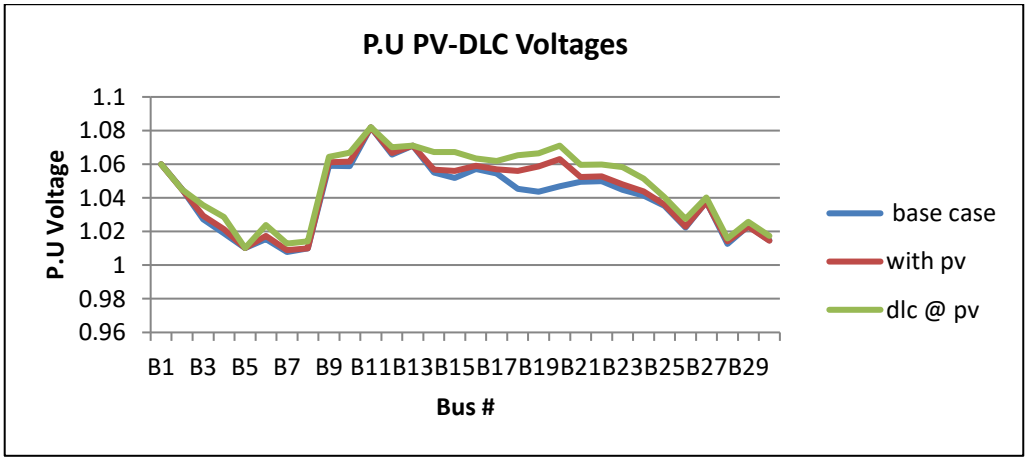

Figure B.17

Bus voltages before and after CVR

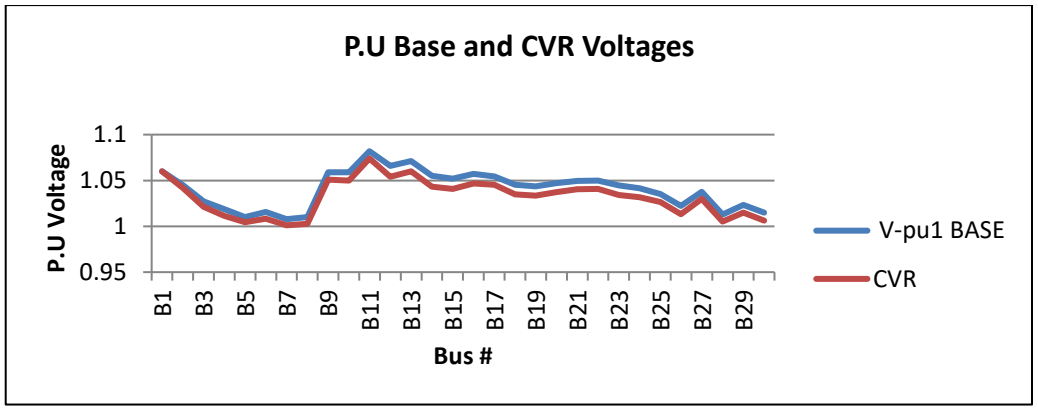

Figure B.18

Bus 30 voltage profile of bus 30 all over the day before and after CVR

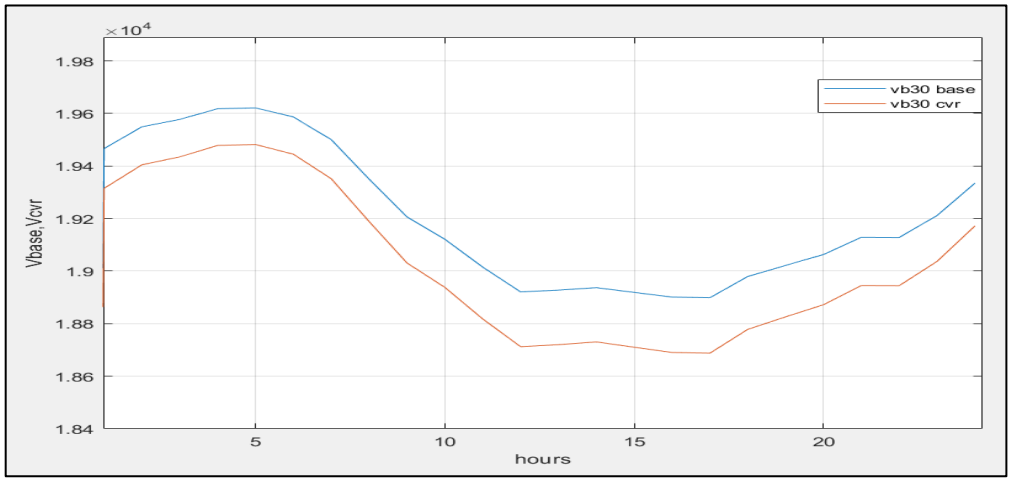

Figure B.19

Buses voltages after applying CVR with addition of PV system

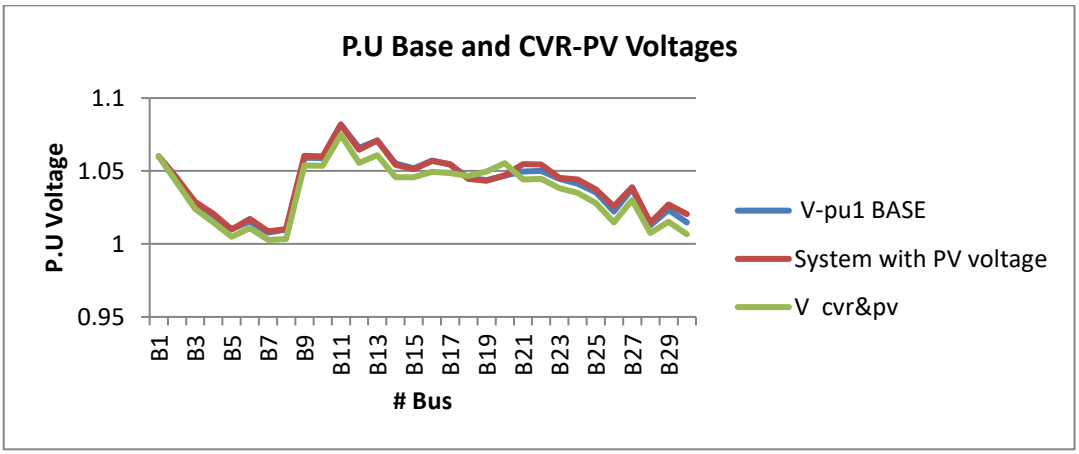

Figure B.20

Bus 30 daily voltage profile after applying CVR and PV and before.

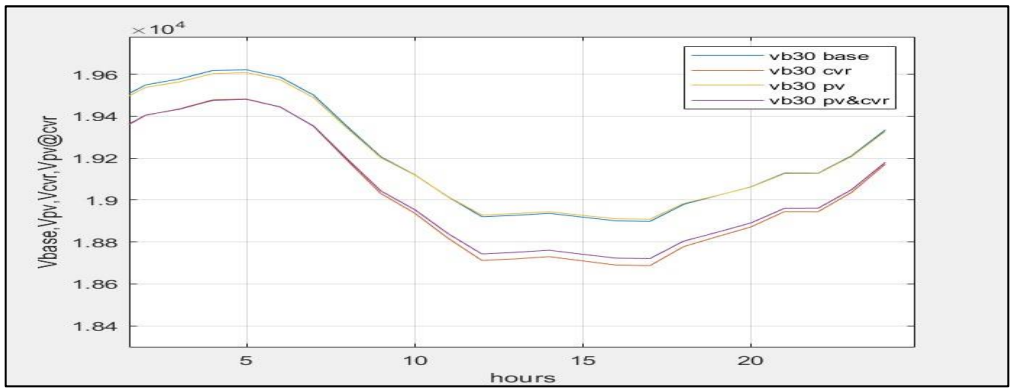

Figure B.21

Bus 30 24-h load profile before and after TOU

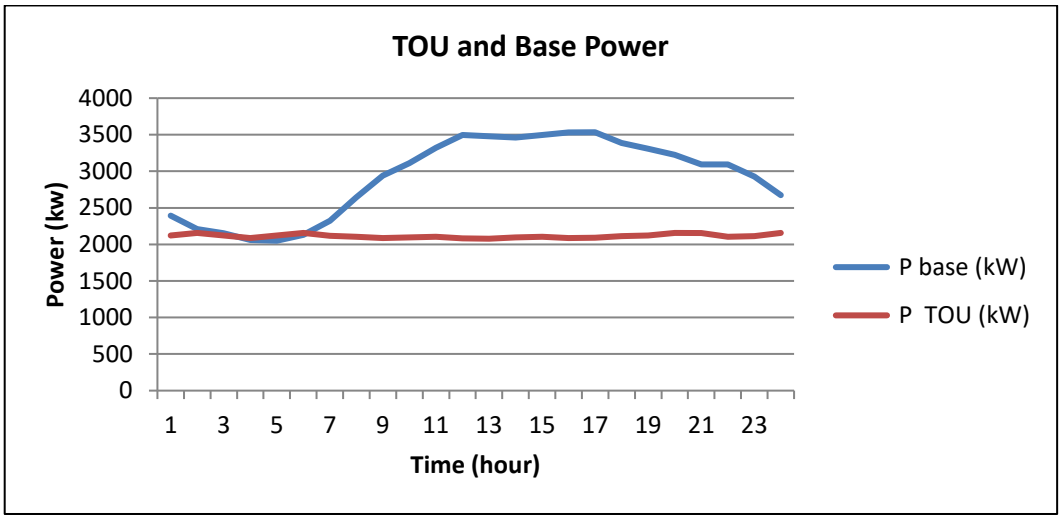

Figure B.22

Buses voltages after applying TOU

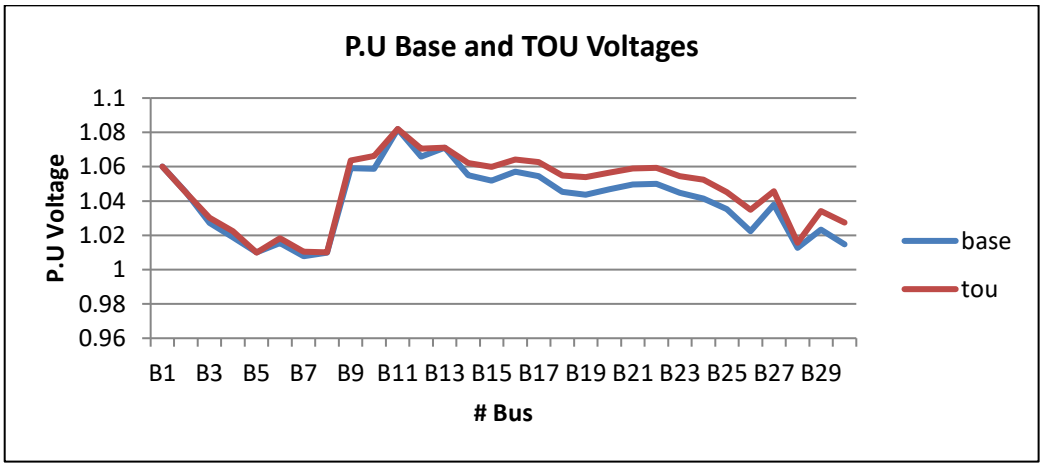

Figure B.23

Buses voltages after applying TOU with addition pf PV system

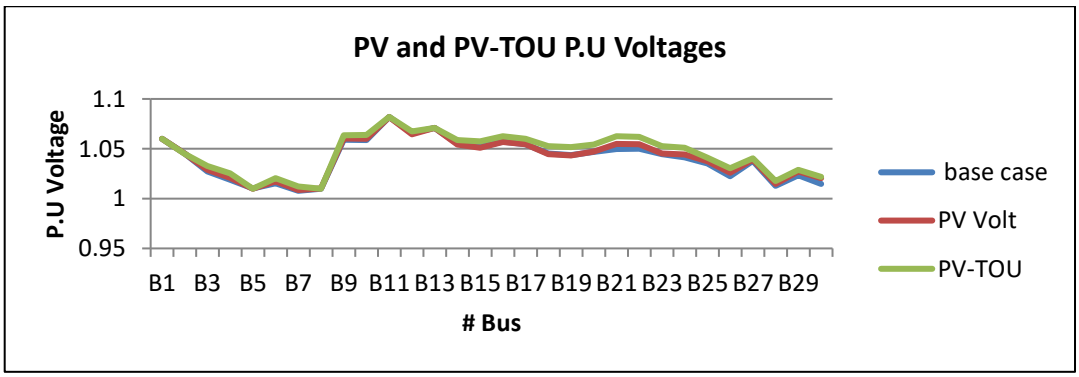

Figure B.24

Power losses in many PV penetration levels

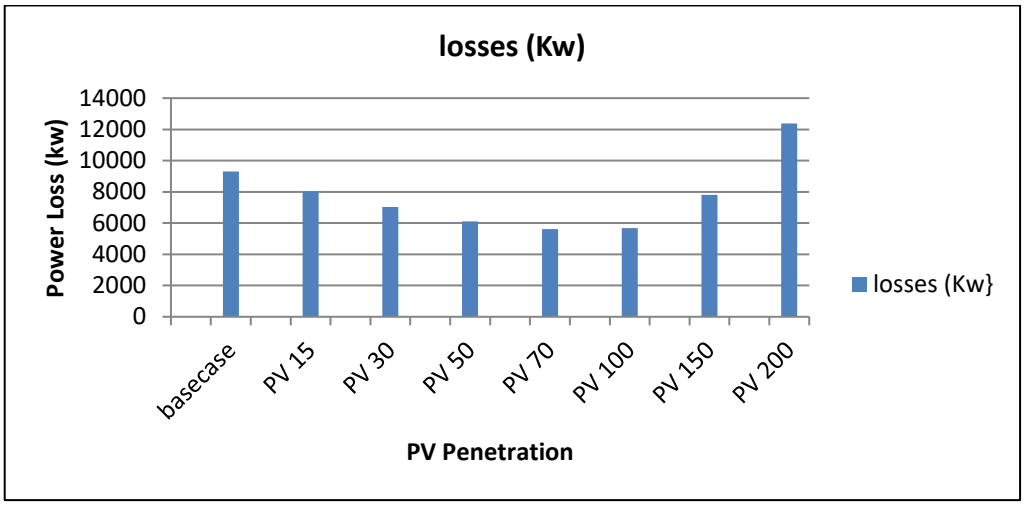

Figure B.25

V.R of many PV penetration levels

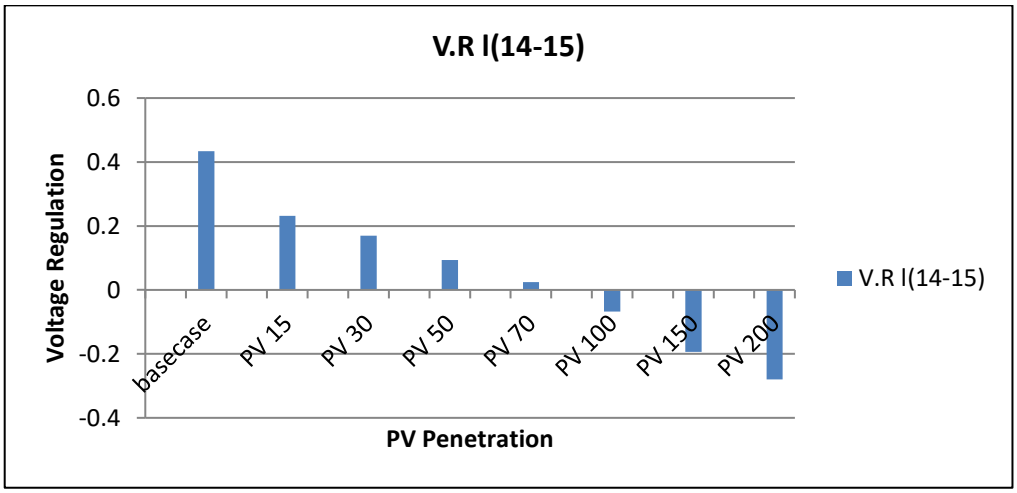

Figure B.26

Bus 3 voltages at many PV penetration levels with base case voltage

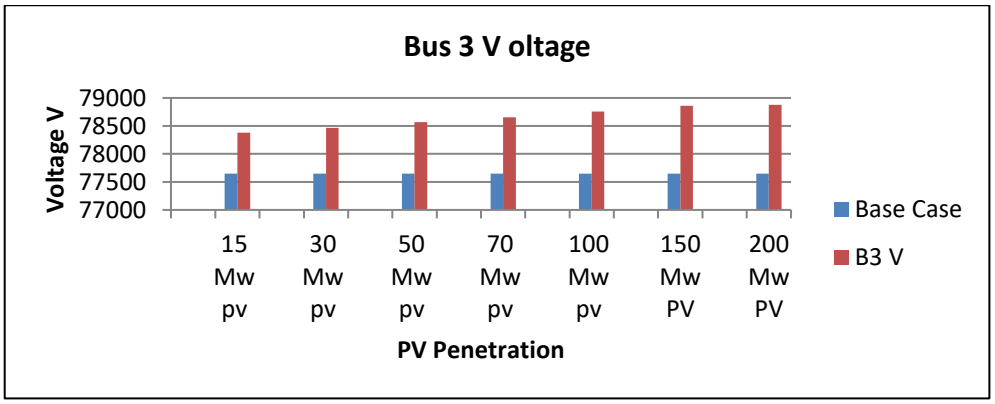

Figure B.27

Bus 23 voltages at many PV penetration levels with base case voltage

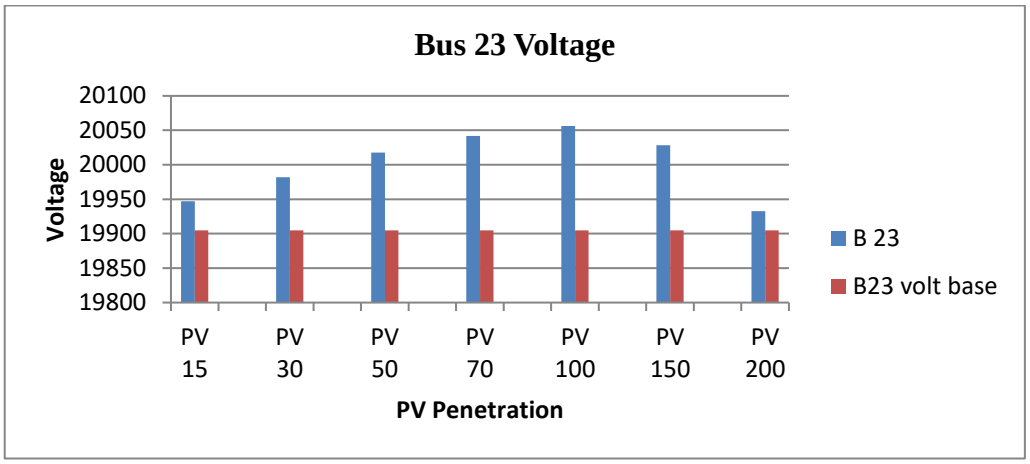

Figure B.28

Bus 18 voltages at many PV penetration levels with base case voltage

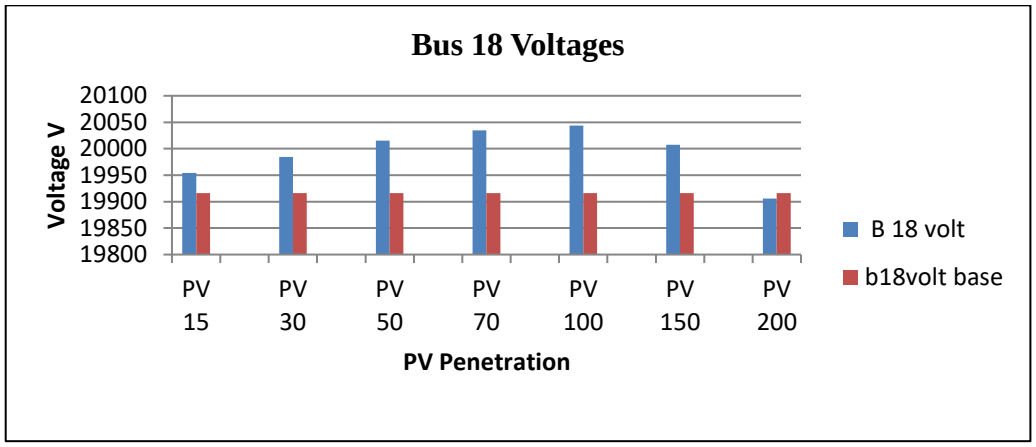

Figure B.29

Line B15-18 currents at many PV penetration levels with the base case

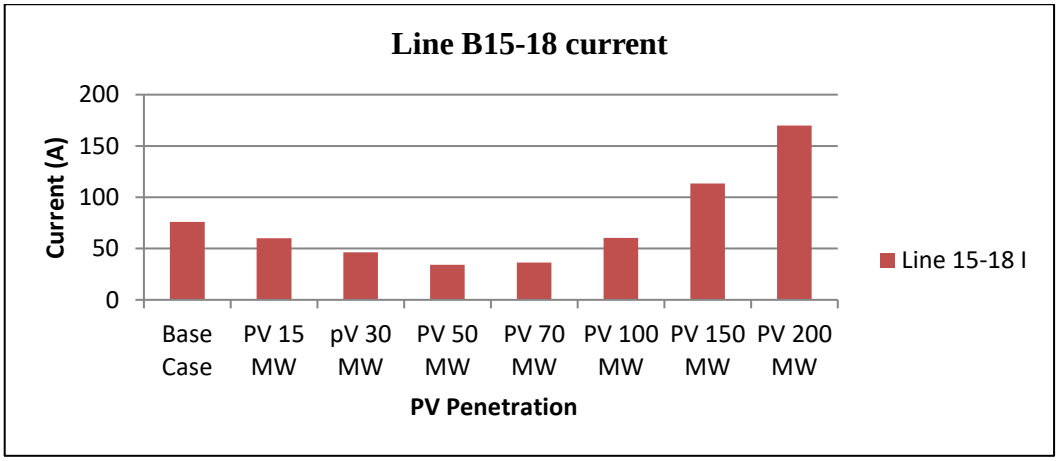

Figure B.30

Line B19-20 currents at many PV penetration levels with base case

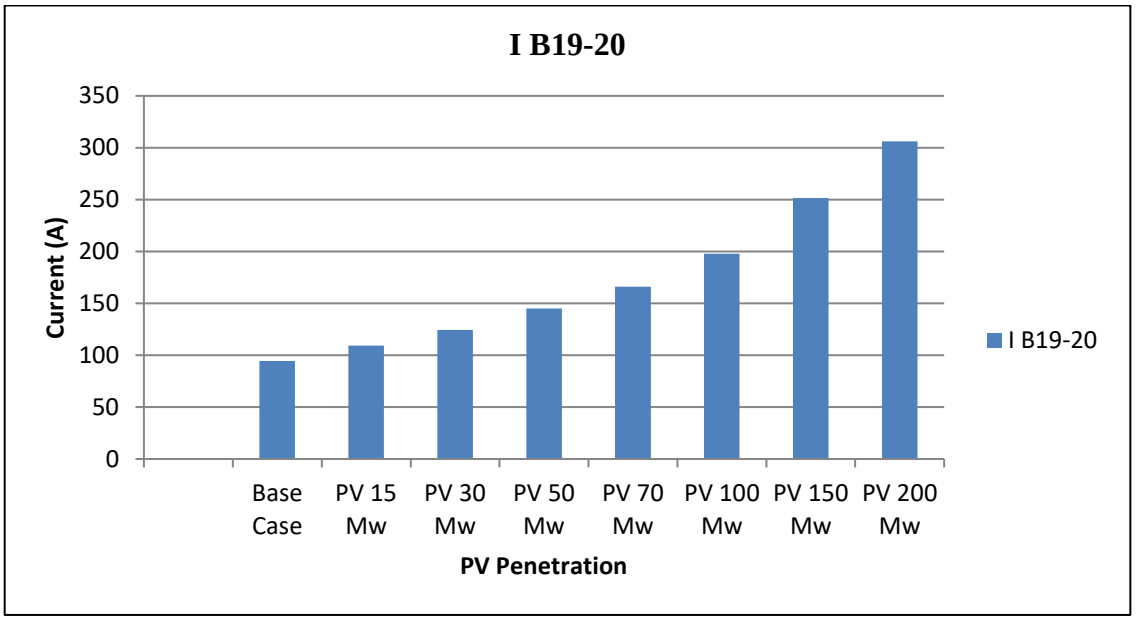

Figure B.31

Network losses in many PV penetration level with and without DSM

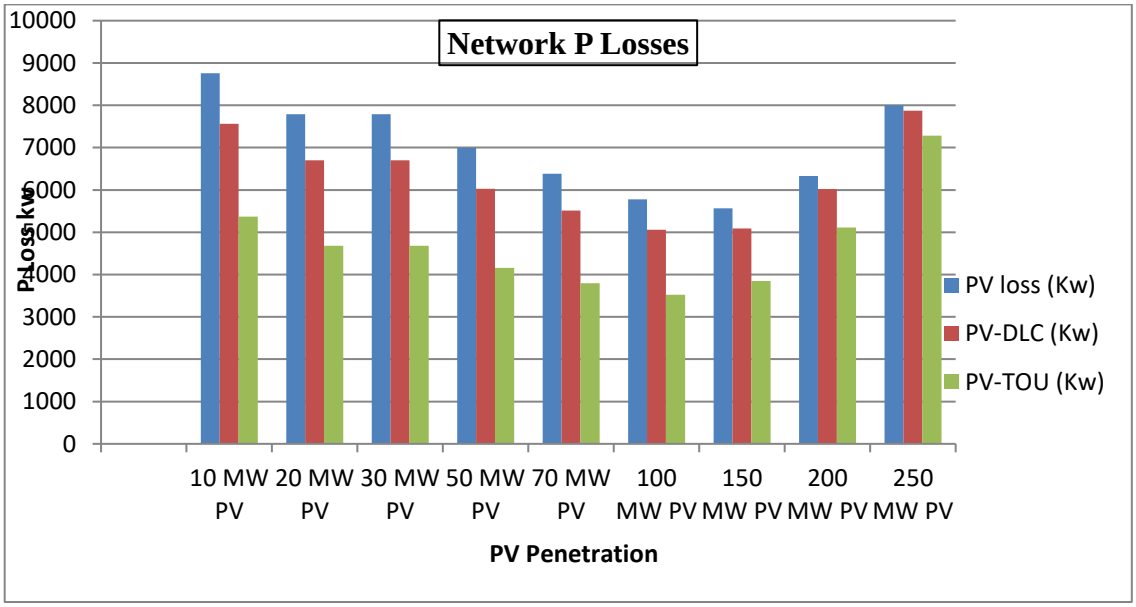

Figure B.32

Line 10-20 current in many PV penetration level with and without DSM.

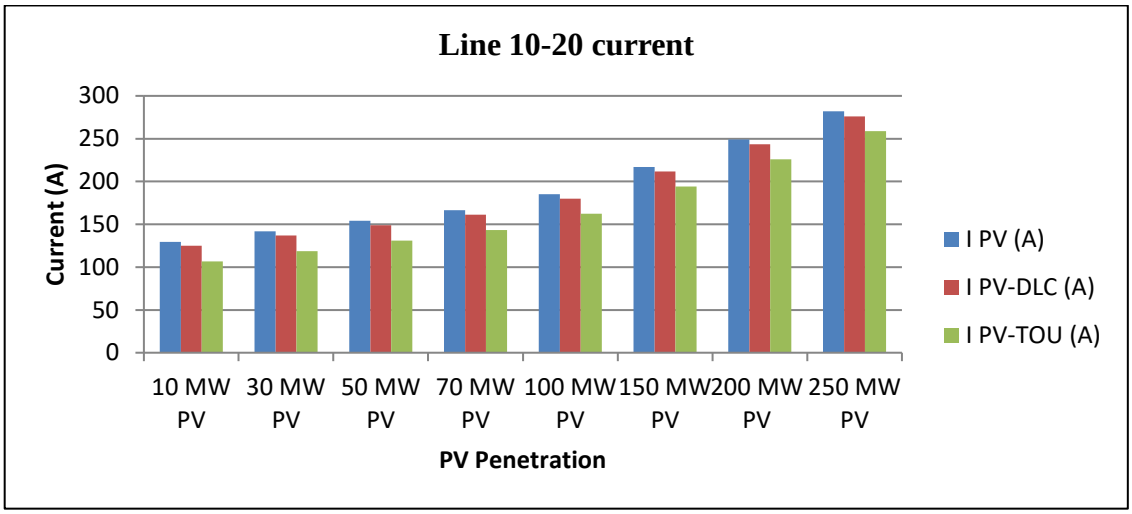

Figure B.33

Network losses in many PV penetration levels with and without DLC-TOU simultaneously

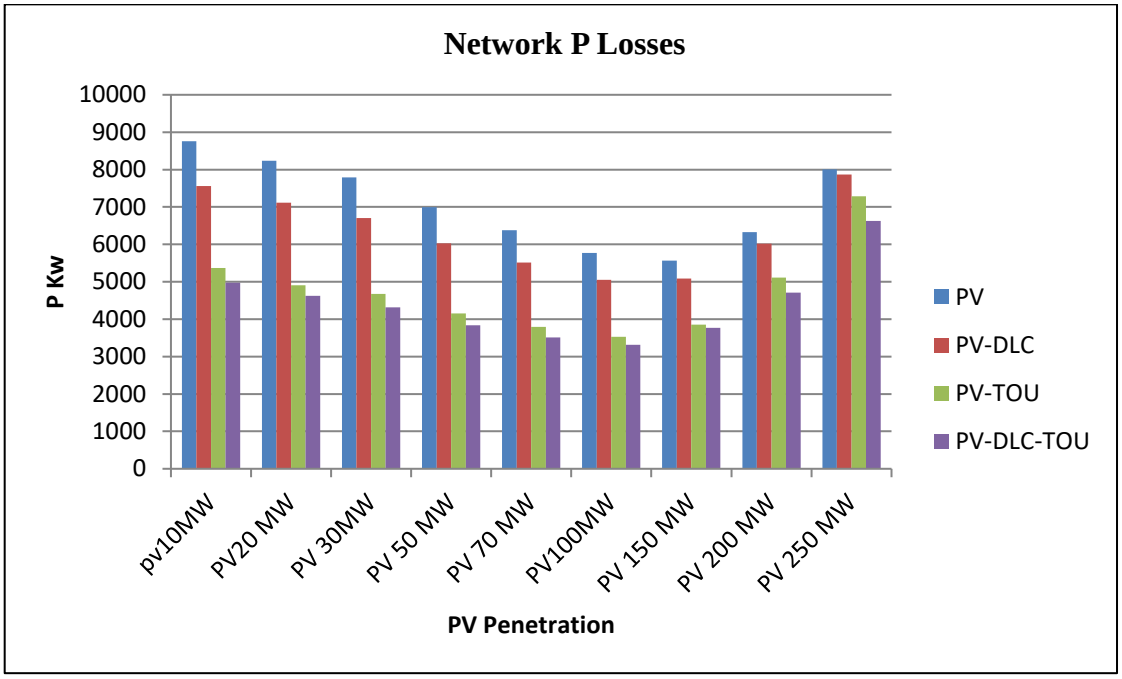

Figure B.34

Buses voltages after applying CVR with DLC-TOU simultaneously system with 250 MW PV

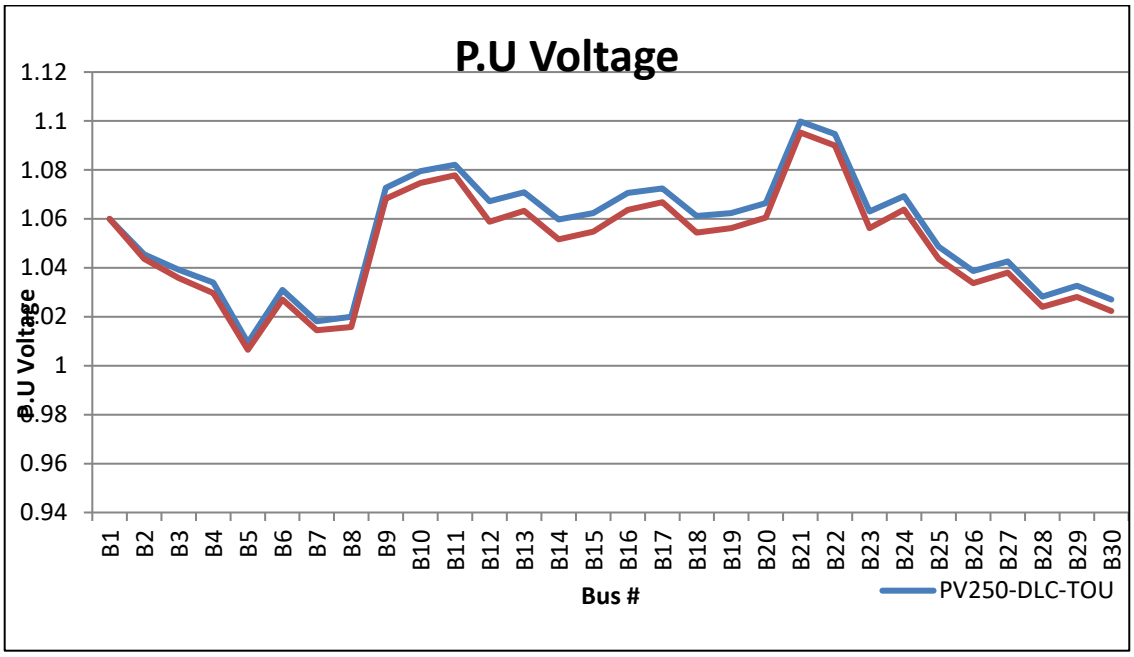

Appendix C

Ieee 30-Bus System Data and Parameters

Transmission line characteristics of IEEE30-Bus System

Line	From Bus	To Bus	R (p.u.)	X (p.u.)	Tap Ratio	Rating (p.u)
1	1	2	0.0192	0.0575		0.300
2	1	3	0.0452	0.1852	0.9610	0.300
3	2	4	0.0570	0.1737	0.9560	0.300
4	3	4	0.0132	0.0379		0.300
5	2	5	0.0472	0.1983		0.300
6	2	6	0.0581	0.1763		0.300
7	4	6	0.0119	0.0414		0.300
8	5	7	0.0460	0.0116		0.300
9	6	7	0.0267	0.0820		0.300
10	6	8	0.0120	0.0420		0.300
11	6	9	0.0000	0.2080		0.300
12	6	10	0.0000	0.5560		0.300
13	9	11	0.0000	0.2080		0.300
14	9	10	0.0000	0.1100	0.9700	0.300
15	4	12	0.0000	0.2560	0.9650	0.65
16	12	13	0.0000	0.1400	0.9635	0.65
17	12	14	0.1231	0.2559		0.32
18	12	15	0.0662	0.1304		0.32
19	12	16	0.0945	0.1987		0.32
20	14	15	0.2210	0.1997		0.160
21	16	17	0.0824	0.1932		0.160
22	15	18	0.1070	0.2185		0.160
23	18	19	0.0639	0.1292	0.9590	0.160
24	19	20	0.0340	0.0680		0.32
25	10	20	0.0936	0.2090		0.32
26	10	17	0.0324	0.0845	0.9850	0.32
27	10	21	0.0348	0.0749		0.300
28	10	22	0.0727	0.1499		0.300
29	21	22	0.0116	0.0236		0.300
30	15	23	0.1000	0.2020		0.160
31	22	24	0.1150	0.1790		0.300
32	23	24	0.1320	0.2700	0.9655	0.160
33	24	25	0.1885	0.3292		0.300
34	25	26	0.2544	0.3800		0.300
35	25	27	0.1093	0.2087		0.300
36	28	27	0.0000	0.3960		0.300
37	27	29	0.2198	0.4153	0.9810	0.300
38	27	30	0.3202	0.6027		0.300
39	29	30	0.2399	0.4533		0.300
40	8	28	0.0636	0.2000	0.9530	0.300
41	6	28	0.0169	0.599		0.300

BUS LOADS:

P,Q Load characteristic of IEEE30-Bus System

Bus	P [pu]	Q [pu]
2	0.217	0.127
3	0.024	0.012
4	0.076	0.016
5	0.942	0.190
7	0.228	0.109
8	0.300	0.300
10	0.058	0.020
12	0.112	0.075
14	0.062	0.016
15	0.082	0.025
16	0.035	0.018
17	0.090	0.058
18	0.032	0.009
19	0.095	0.034
20	0.022	0.007
21	0.175	0.112
23	0.032	0.016
24	0.087	0.067
26	0.035	0.023
29	0.024	0.009
30	0.106	0.019

Bus Data In IEEE30-Bus System

Bus No.	Bus Voltage		Generation		Load	
	Magnitude (P.U)	Phase angles (Degrees)	Real MW	Reactive MVAR	Real MW	Reactive MVAR
1	1.0500	0.0	138.48	-2.79	0.0	0.0
2	1.0338	-2.7339	57.56	2.47	21.7	12.7
3	1.0313	-4.6815	0.0	0.0	2.4	1.2
4	1.0263	-5.6077	0.0	0.0	7.6	1.6
5	1.0058	-8.9930	24.56	22.57	94.2	19.0
6	1.0208	-6.4547	0.0	0.0	0.0	0.0
7	1.0069	-8.0244	0.0	0.0	22.8	10.9
8	1.0230	-6.4733	35.0	34.84	30.0	30.0
9	1.0332	-8.0300	0.0	0.0	0.0	0.0
10	1.0183	-9.9268	0.0	0.0	5.8	2.0
11	1.0913	-6.1345	17.93	30.78	0.0	0.0
12	1.0399	-9.4036	0.0	0.0	11.2	7.5
13	1.0883	-8.2049	16.91	37.83	0.0	0.0
14	1.0236	-10.3086	0.0	0.0	6.2	1.6
15	1.0179	-10.3600	0.0	0.0	8.2	2.5
16	1.0235	-9.90280	0.0	0.0	3.5	1.8
17	1.0144	-10.1356	0.0	0.0	9.0	5.8
18	1.0057	-10.9253	0.0	0.0	3.2	0.9
19	1.0017	-11.0615	0.0	0.0	9.5	3.4
20	1.0051	-10.8310	0.0	0.0	2.2	0.7
21	1.0061	-10.4047	0.0	0.0	17.5	11.2
22	1.0069	-10.3936	0.0	0.0	0.0	0.0
23	1.0053	-10.7221	0.0	0.0	3.2	1.6
24	0.9971	-10.8465	0.0	0.0	8.7	6.7
25	1.0086	-10.9074	0.0	0.0	0.0	0.0
26	0.9908	-11.3345	0.0	0.0	3.5	2.3
27	1.0245	-10.6624	0.0	0.0	0.0	0.0
28	1.0156	-6.86710	0.0	0.0	0.0	0.0
29	1.0047	-11.8893	0.0	0.0	2.4	0.9
30	0.9932	-12.7699	0.0	0.0	10.6	1.9

Line Data In IEEE30-Bus System

Line No	Between Buses	Line impedance		Half Line Charging Susceptance per unit
		R per unit	X per unit	
1	1 – 2	0.0192	0.0575	0.0528
2	1 – 3	0.0452	0.1652	0.0408
3	2 – 4	0.0570	0.1737	0.0368
4	3 – 4	0.0132	0.0379	0.0084
5	2 – 5	0.0472	0.1983	0.0418
6	2 – 6	0.0581	0.1763	0.0374
7	4 – 6	0.0119	0.0414	0.0090
8	5 – 7	0.0460	0.1160	0.0204
9	6 – 7	0.0267	0.0820	0.0170
10	6 – 8	0.0120	0.0420	0.0090
11	6 – 9	0.0	0.2080	0.0
12	6 – 10	0.0	0.5560	0.0
13	9 – 10	0.0	0.1100	0.0
14	4 – 12	0.0	0.2560	0.0
15	12 – 14	0.1231	0.2559	0.0
16	12 – 15	0.0662	0.1304	0.0
17	12 – 16	0.0945	0.1987	0.0
18	14 – 15	0.2210	0.1997	0.0
19	16 – 17	0.0524	0.1923	0.0
20	15 – 18	0.1073	0.2185	0.0
21	18 – 19	0.0639	0.1292	0.0
22	19 – 20	0.0340	0.0680	0.0
23	10 – 20	0.0936	0.2090	0.0
24	10 – 17	0.0324	0.0845	0.0
25	10 – 21	0.0348	0.0749	0.0
26	10 – 22	0.0727	0.1499	0.0
27	21 – 22	0.0116	0.0236	0.0
28	15 – 23	0.1000	0.2020	0.0
29	22 – 24	0.1150	0.1790	0.0
30	23 – 24	0.1320	0.2700	0.0
31	24 – 25	0.1885	0.3292	0.0
32	25 – 27	0.1093	0.2087	0.0
33	28 – 27	0.0	0.3960	0.0
34	27 – 29	0.2198	0.4153	0.0
35	27 – 30	0.3202	0.6027	0.0
36	29 – 30	0.2399	0.4533	0.0
37	8 – 28	0.0636	0.2000	0.4028
38	6 – 28	0.0169	0.0599	0.0130
39	9 – 11	0.0	0.2080	0.0
40	12 – 13	0.0	0.1400	0.0
41	25 – 26	0.2544	0.3800	0.0

Line Power Limits for branches in IEEE30-Bus System

Line	MW Limit (pu)
1 – 2	1.0400
1 – 3	1.0400
2 – 4	0.5200
3 – 4	1.0400
2 – 5	1.0400
2 – 6	0.5200
4 – 6	0.7200
5 – 7	0.5600
6 – 7	1.0400
6 – 8	0.2560
6 – 9	0.5200
6 – 10	0.2560
9 – 10	0.5200
4 – 12	0.5200
12 – 14	0.2560
12 – 15	0.2560
12 – 16	0.2560
14 – 15	0.1280
16 – 17	0.1280
15 – 18	0.1280
18 – 19	0.1280
19 – 20	0.2560
10 – 20	0.2560
10 – 17	0.2560
10 – 21	0.2560
10 – 22	0.2560
21 – 22	0.2560
15 – 23	0.1280
22 – 24	0.1280
23 – 24	0.1280
24 – 25	0.4800
25 – 27	0.1280
28 – 27	0.5200
27 – 29	0.1280
27 – 30	0.1280
29 – 30	0.1280
8 – 28	0.2560
6 – 28	0.2560
9 – 11	0.5200
12 – 13	0.5200
25 – 26	0.1280

Appendix D

Code and Tools Used for Simulation

The main circuit (RUN)

```
clear
// Standard IEEE 30-Bus Transmission System Test Case

Compile Masterd.DSS

! The compile builds the circuit model and sets the voltage bases

! sometimes this model needs more than the default 15 iterations
Set maxiterations=500

set mode = daily
set stepsize = 1h
set number = 24
new monitor.losses3  element= line.1-3  terminal=1 mode=9


!new monitor.powers1 element= Circuit.IEEE_30 terminal=1 ppolar=no mode=1
new monitor.powers2 element= load.B2  terminal=1 ppolar=no mode=1
new monitor.powers3 element= load.B3  terminal=1 ppolar=no mode=1
new monitor.powers4 element= load.B4  terminal=1 ppolar=no mode=1
new monitor.powers5 element= load.B5 terminal=1 ppolar=no mode=1
new monitor.powers6 element= Transformer.6-9 terminal=1 ppolar=no mode=1
new monitor.powers7 element= load.B7 terminal=1 ppolar=no mode=1
new monitor.powers8 element= load.B8 terminal=1 ppolar=no mode=1
new monitor.powers9 element= Transformer.6-9 terminal=2 ppolar=no mode=1
new monitor.powers10 element= load.B10 terminal=1 ppolar=no mode=1
new monitor.powers11 element= Transformer.9-11 terminal=2 ppolar=no mode=1
new monitor.powers12 element= load.B12  terminal=1 ppolar=no mode=1
new monitor.powers13 element= Transformer.12-13 terminal=2 ppolar=no mode=1
new monitor.powers14 element= load.B14 terminal=1 ppolar=no mode=1
new monitor.powers15 element= load.B15 terminal=1 ppolar=no mode=1
new monitor.powers16 element= load.B16 terminal=1 ppolar=no mode=1
new monitor.powers17 element= load.B17 terminal=1 ppolar=no mode=1
new monitor.powers18 element= load.B18 terminal=1 ppolar=no mode=1
new monitor.powers19 element= load.B19 terminal=1 ppolar=no mode=1
new monitor.powers20 element= load.B20 terminal=1 ppolar=no mode=1
new monitor.powers21 element= load.B21 terminal=1 ppolar=no mode=1
!new monitor.powers22 element= B22 terminal=1 ppolar=no mode=1
new monitor.powers23 element= load.B23 terminal=1 ppolar=no mode=1
new monitor.powers24 element= load.B24 terminal=1 ppolar=no mode=1
!new monitor.powers25 element= B25 terminal=1 ppolar=no mode=1
new monitor.powers26 element= load.B26 terminal=1 ppolar=no mode=1
new monitor.powers27 element= Transformer.28-27  terminal=2 ppolar=no mode=1
new monitor.powers28 element= Transformer.28-27  terminal=1 ppolar=no mode=1
new monitor.powers29 element= load.B29 terminal=1 ppolar=no mode=1
```

Generators:

```
! Generator Definitions

New Generator.B2  Bus1=B2  kV= 132 kW=40000 Model=3 Vpu=1.045 Maxkvar=50000 Minkvar=-40000 !  kvar=50000

! The following buses just have a voltage target and kvar limits defined.
! The kW value is defined as zero, but this is illegal in the OpenDSS Generator model
! So we just put a small value (1 kW) here and use model 3 to regulate the bus.

New Generator.B5  Bus1=B5  kV= 132 kW=1     Model=3 Vpu=1.01  Maxkvar=40000 Minkvar=-40000 !  kvar=37000
New Generator.B8  Bus1=B8  kV= 132 kW=1     Model=3 Vpu=1.01  Maxkvar=40000 Minkvar=-10000 !  kvar=37300
New Generator.B11 Bus1=B11 kV= 11  kW=1     Model=3 Vpu=1.082 Maxkvar=24000 Minkvar=-6000  !  kvar=16200
New Generator.B13 Bus1=B13 kV= 11  kW=1     Model=3 Vpu=1.071 Maxkvar=24000 Minkvar=-6000  !  kvar=10600
```

Loads

```
New Load.B2  Bus1=B2  kV=132 kW=21700 kvar=12700 vminpu=0.9 vmaxpu=1.10   daily = default


New Load.B3  Bus1=B3  kV=132 kW=2400  kvar=1200  vminpu=0.9 vmaxpu=1.10   daily = default
New Load.B4  Bus1=B4  kV=132 kW=7600  kvar=1600  vminpu=0.9 vmaxpu=1.10   daily = default

New Load.B5  Bus1=B5  kV=132 kW=94200 kvar=19000 vminpu=0.9 vmaxpu=1.10   daily = default
New Load.B7  Bus1=B7  kV=132 kW=22800 kvar=10900 vminpu=0.9 vmaxpu=1.10   daily = default
New Load.B8  Bus1=B8  kV=132 kW=30000 kvar=30000 vminpu=0.9 vmaxpu=1.10   daily = default
New Load.B10 Bus1=B10 kV=33  kW=5800  kvar=2000  vminpu=0.9 vmaxpu=1.10   daily = default
New Load.B12 Bus1=B12 kV=33  kW=11200 kvar=7500  vminpu=0.9 vmaxpu=1.10   daily = default
New Load.B14 Bus1=B14 kV=33  kW=6200  kvar=1600  vminpu=0.9 vmaxpu=1.10   daily = default
New Load.B15 Bus1=B15 kV=33  kW=8200  kvar=2500  vminpu=0.9 vmaxpu=1.10   daily = default
New Load.B16 Bus1=B16 kV=33  kW=3500  kvar=1800  vminpu=0.9 vmaxpu=1.10   daily = default
New Load.B17 Bus1=B17 kV=33  kW=9000  kvar=5800  vminpu=0.9 vmaxpu=1.10   daily = default
New Load.B18 Bus1=B18 kV=33  kW=3200  kvar=900   vminpu=0.9 vmaxpu=1.10   daily = default
New Load.B19 Bus1=B19 kV=33  kW=9500  kvar=3400  vminpu=0.9 vmaxpu=1.10   daily = default
New Load.B20 Bus1=B20 kV=33  kW=2200  kvar=700   vminpu=0.9 vmaxpu=1.10   daily = default
New Load.B21 Bus1=B21 kV=33  kW=17500 kvar=11200 vminpu=0.9 vmaxpu=1.10   daily = default
New Load.B23 Bus1=B23 kV=33  kW=3200  kvar=1600  vminpu=0.9 vmaxpu=1.10   daily = default
New Load.B24 Bus1=B24 kV=33  kW=8700  kvar=6700  vminpu=0.9 vmaxpu=1.10   daily = default
New Load.B26 Bus1=B26 kV=33  kW=3500  kvar=2300  vminpu=0.9 vmaxpu=1.10   daily = default
New Load.B29 Bus1=B29 kV=33  kW=2400  kvar=900   vminpu=0.9 vmaxpu=1.10   daily = default
New Load.B30 Bus1=B30 kV=33  kW=10600 kvar=1900  vminpu=0.9 vmaxpu=1.10   daily = default
```

Lines

```
! Line definitions

! Note, the line data are given in pu. However, the OpenDSS works in Ohms
! The per unit values are converted to ohms using 100 MVA base and the voltage base of the first bus
! No capacitance was defined for the 33 and 11 kv lines.

New line.1-2   Bus1=B1  Bus2=B2  R1=3.345408 X1=10.0188   R0=10.036224 X0=30.0564    C1=803.793907242183 C0=267.931302414061 Length=1
New line.1-3   Bus1=B1  Bus2=B3  R1=7.875648 X1=28.784448 R0=23.626944 X0=86.353344  C1=621.113473778051 C0=207.037824592684 Length=1
New line.2-4   Bus1=B2  Bus2=B4  R1=9.93168  X1=30.265488 R0=29.79504  X0=90.796464  C1=560.219995956673 C0=186.739998652224 Length=1
New line.3-4   Bus1=B3  Bus2=B4  R1=2.299968 X1=6.603696  R0=6.899904  X0=19.811088  C1=127.876303424893 C0=42.6254344749642 Length=1
New line.2-5   Bus1=B2  Bus2=B5  R1=8.224128 X1=34.551792 R0=24.672384 X0=103.655376 C1=636.336843233395 C0=212.112281077798 Length=1
New line.2-6   Bus1=B2  Bus2=B6  R1=10.123344 X1=30.718512 R0=30.370032 X0=92.155536  C1=569.35401762988  C0=189.784672543293 Length=1
New line.4-6   Bus1=B4  Bus2=B6  R1=2.073456 X1=7.213536  R0=6.220368  X0=21.640608  C1=137.010325098099 C0=45.6701083660331 Length=1
New line.5-7   Bus1=B5  Bus2=B7  R1=8.01504  X1=20.21184  R0=24.04512  X0=60.63552   C1=310.556736889025 C0=103.518912296342 Length=1
New line.6-7   Bus1=B6  Bus2=B7  R1=4.652208 X1=14.28768  R0=13.956624 X0=42.86304   C1=258.797280740854 C0=86.2657602469515 Length=1
New line.6-8   Bus1=B6  Bus2=B8  R1=2.09088  X1=7.31808   R0=6.27264   X0=21.95424   C1=137.010325098099 C0=45.6701083660331 Length=1
New line.12-14 Bus1=B12 Bus2=B14 R1=1.340559 X1=2.786751  R0=4.021677  X0=8.360253   C1=0              C0=0              Length=1
New line.12-15 Bus1=B12 Bus2=B15 R1=0.720918 X1=1.420056  R0=2.162754  X0=4.260168   C1=0              C0=0              Length=1
New line.12-16 Bus1=B12 Bus2=B16 R1=1.029105 X1=2.163843  R0=3.087315  X0=6.491529   C1=0              C0=0              Length=1
New line.14-15 Bus1=B14 Bus2=B15 R1=2.40669  X1=2.174733  R0=7.22007   X0=6.524199   C1=0              C0=0              Length=1
New line.16-17 Bus1=B16 Bus2=B17 R1=0.570636 X1=2.094147  R0=1.711908  X0=6.282441   C1=0              C0=0              Length=1
New line.15-18 Bus1=B15 Bus2=B18 R1=1.168497 X1=2.379465  R0=3.505491  X0=7.138395   C1=0              C0=0              Length=1
New line.18-19 Bus1=B18 Bus2=B19 R1=0.695871 X1=1.406988  R0=2.087613  X0=4.220964   C1=0              C0=0              Length=1
New line.19-20 Bus1=B19 Bus2=B20 R1=0.37026  X1=0.74052   R0=1.11078   X0=2.22156    C1=0              C0=0              Length=1
New line.10-20 Bus1=B10 Bus2=B20 R1=1.019304 X1=2.27601   R0=3.057912  X0=6.82803    C1=0              C0=0              Length=1
New line.10-17 Bus1=B10 Bus2=B17 R1=0.352836 X1=0.920205  R0=1.058508  X0=2.760615   C1=0              C0=0              Length=1
New line.10-21 Bus1=B10 Bus2=B21 R1=0.378972 X1=0.815661  R0=1.136916  X0=2.446983   C1=0              C0=0              Length=1
New line.10-22 Bus1=B10 Bus2=B22 R1=0.791703 X1=1.632411  R0=2.375109  X0=4.897233   C1=0              C0=0              Length=1
New line.21-22 Bus1=B21 Bus2=B22 R1=0.126324 X1=0.257004  R0=0.378972  X0=0.771012   C1=0              C0=0              Length=1
New line.15-23 Bus1=B15 Bus2=B23 R1=1.089    X1=2.19978   R0=3.267     X0=6.59934    C1=0              C0=0              Length=1
New line.22-24 Bus1=B22 Bus2=B24 R1=1.25235  X1=1.94931   R0=3.75705   X0=5.84793    C1=0              C0=0              Length=1
New line.23-24 Bus1=B23 Bus2=B24 R1=1.43748  X1=2.9403    R0=4.31244   X0=8.8209     C1=0              C0=0              Length=1
New line.24-25 Bus1=B24 Bus2=B25 R1=2.052765 X1=3.584988  R0=6.158295  X0=10.754964  C1=0              C0=0              Length=1
New line.25-26 Bus1=B25 Bus2=B26 R1=2.770416 X1=4.1382    R0=8.311248  X0=12.4146    C1=0              C0=0              Length=1
New line.25-27 Bus1=B25 Bus2=B27 R1=1.190277 X1=2.272743  R0=3.570831  X0=6.818229   C1=0              C0=0              Length=1
New line.27-29 Bus1=B27 Bus2=B29 R1=2.393622 X1=4.522617  R0=7.180866  X0=13.567851  C1=0              C0=0              Length=1
New line.27-30 Bus1=B27 Bus2=B30 R1=3.486978 X1=6.563403  R0=10.460934 X0=19.690209  C1=0              C0=0              Length=1
New line.29-30 Bus1=B29 Bus2=B30 R1=2.612511 X1=4.936437  R0=7.837533  X0=14.809311  C1=0              C0=0              Length=1
New line.8-28  Bus1=B8  Bus2=B28 R1=11.081664 X1=34.848   R0=33.244992 X0=104.544   C1=651.560212688739 C0=217.186737562913 Length=1
New line.6-28  Bus1=B6  Bus2=B28 R1=2.944656 X1=10.436976 R0=8.833968  X0=31.310928  C1=197.903802919477 C0=65.9679343064923 Length=1
```

Transformers:

```
! Since no transformer rating data exist in the Common Data Forma
! all transformer are defined as begin 100 MVA, the system base
! Thus, the conversion of impedances is simple: just multiply by 100 to get percent

! The tap in the original data is assumed to apply to the first winding.

! Transformers are modeled with their actual turns ratios

! The OpenDSS defaults to Yg-Yg connection. Since we don't have to worry about
! floating Delta windings, the PPM_antifloat property is set to 0.

! All transformer branches are defined with R=0. This is accomplished by
! setting %Loadloss=0

! Although OpenDSS can handle 3-winding transformers the model here
! follows the model in the old data set by defining 3 separate transformers to an
! intermediate bus with a 1 kV voltage rating.  Since there is nothing connected
! there, you could actually use any voltage you wish.

New Transformer.6-9 kVAs=[100000 100000] XHL=20.8 PPM=0
~ Wdg=1 R=0 kV=132 Bus=B6 Tap=0.978
~ Wdg=2 R=0 kV=1 Bus=B9
~ %loadloss=0
New Transformer.6-10 kVAs=[100000 100000] XHL=55.6 PPM=0
~ Wdg=1 R=0 kV=132 Bus=B6 Tap=0.969
~ Wdg=2 R=0 kV=33 Bus=B10
~ %loadloss=0
New Transformer.9-11 kVAs=[100000 100000] XHL=20.8 PPM=0
~ Wdg=1 R=0 kV=1 Bus=B9 Tap=1
~ Wdg=2 R=0 kV=11 Bus=B11
~ %loadloss=0
New Transformer.9-10 kVAs=[100000 100000] XHL=11 PPM=0
~ Wdg=1 R=0 kV=1 Bus=B9 Tap=1
~ Wdg=2 R=0 kV=33 Bus=B10
~ %loadloss=0
New Transformer.4-12 kVAs=[100000 100000] XHL=25.6 PPM=0
~ Wdg=1 R=0 kV=132 Bus=B4 Tap=0.932
~ Wdg=2 R=0 kV=33 Bus=B12
~ %loadloss=0
New Transformer.12-13 kVAs=[100000 100000] XHL=14 PPM=0
~ Wdg=1 R=0 kV=33 Bus=B12 Tap=1
~ Wdg=2 R=0 kV=11 Bus=B13
~ %loadloss=0
New Transformer.28-27 kVAs=[100000 100000] XHL=39.6 PPM=0
~ Wdg=1 R=0 kV=132 Bus=B28 Tap=0.968
~ Wdg=2 R=0 kV=33 Bus=B27
~ %loadloss=0
```

CVR implementation:

```
clearall
clear

Compile Masterd.DSS


solve

! The compile builds the circuit model and sets the voltage bases

! sometimes this model needs more than the default 15 iterations
Set maxiterations=100


New Line.Linex Bus1=B12.1.2.3 Bus2=H.1.2.3

New REACTOR.Jumper phases=1 Bus1=H.1  Bus2=Bx.2  R=0 X=0.0001
New Transformer.Auto1 X12=1 Phases=1 Windings=2
~ wdg=1 Bus=Bx.1.0 kV=19 kVA=50
~ wdg=2 Bus=Bx.1.2 kV=1.9 kVA=50 Maxtap=1.0 Mintap=-1.0
~ %loadloss=.1

New Load.Loadx Phases=1 Bus1=Bx.1.0 kW=1500 PF=.9 kV=19
Set voltagebases=[132,33,11,1]
calcvoltagebases



New REGCONTROL.Reg1 transformer=Auto1 winding=2 bus=H  ptratio=60 vreg=300  band =3
~ maxtapchange=1
Set maxcontroliter=250
regcontrol.reg1.vreg=250

|
```

DLC implementation:

```
New Load.B2  Bus1=B2  kV=132 kW=21700 kvar=12700 vminpu=0.9 vmaxpu=1.10  model =2  daily = default
New Load.B3  Bus1=B3  kV=132 kW=1680  kvar=1200 vminpu=0.9 vmaxpu=1.10   model =2   daily = default
New Load.B4  Bus1=B4  kV=132 kW=5320  kvar=1600  vminpu=0.9 vmaxpu=1.10    model =2  daily = default

New Load.B5  Bus1=B5  kV=132 kW=94200 kvar=19000 vminpu=0.9 vmaxpu=1.10   model = 2   daily = default
New Load.B7  Bus1=B7  kV=132 kW=22800 kvar=10900 vminpu=0.9 vmaxpu=1.10   model = 2  daily = default
New Load.B8  Bus1=B8  kV=132 kW=30000 kvar=30000 vminpu=0.9 vmaxpu=1.10  model = 2 daily = default
New Load.B10 Bus1=B10 kV=33  kW=5220 kvar=2000  vminpu=0.9 vmaxpu=1.10  model = 2  daily = default
New Load.B12 Bus1=B12 kV=33  kW=11200 kvar=7500  vminpu=0.9 vmaxpu=1.10  model = 2  daily = default
New Load.B14 Bus1=B14 kV=33  kW=4340  kvar=1600  vminpu=0.9 vmaxpu=1.10   model = 2  daily = default
New Load.B15 Bus1=B15 kV=33  kW=8200  kvar=2500  vminpu=0.9 vmaxpu=1.10   model = 2  daily = default
New Load.B16 Bus1=B16 kV=33  kW=3500  kvar=1800  vminpu=0.9 vmaxpu=1.10 model = 2   daily = default
New Load.B17 Bus1=B17 kV=33  kW=9000  kvar=5800  vminpu=0.9 vmaxpu=1.10 model = 2   daily = default
New Load.B18 Bus1=B18 kV=33  kW=3200  kvar=900   vminpu=0.9 vmaxpu=1.10  model = 2  daily = default
New Load.B19 Bus1=B19 kV=33  kW=9500  kvar=3400  vminpu=0.9 vmaxpu=1.10 model = 2  daily = default
New Load.B20 Bus1=B20 kV=33  kW=1540  kvar=700   vminpu=0.9 vmaxpu=1.10   model = 2 daily = default
New Load.B21 Bus1=B21 kV=33  kW=14000 kvar=11200 vminpu=0.9 vmaxpu=1.10  model = 2 daily = default
New Load.B23 Bus1=B23 kV=33  kW=3200  kvar=1600  vminpu=0.9 vmaxpu=1.10 model =2 daily = default
New Load.B24 Bus1=B24 kV=33  kW=6090  kvar=6700  vminpu=0.9 vmaxpu=1.10  model = 2 daily = default
New Load.B26 Bus1=B26 kV=33  kW=2450  kvar=2300  vminpu=0.9 vmaxpu=1.10  model = 2 daily = default
New Load.B29 Bus1=B29 kV=33  kW=1680  kvar=900   vminpu=0.9 vmaxpu=1.10  model = 2 daily = default
New Load.B30 Bus1=B30 kV=33  kW=7420 kvar=1900  vminpu=0.9 vmaxpu=1.10  model = 2  daily = default
```

TOU implementation:

```
new loadshape.tou npt=24 interval=1
 ~ mult = { .6 .61 .6 .59 .6 .61 .599  .595 .59 .593 .595 .589 .588 .593 .595 .59 .592 .598 .6 .61 .61 .595 .598 .61 }


New Load.B2  Bus1=B2  kV=132 kW=21700 kvar=12700 vminpu=0.9 vmaxpu=1.10    daily = tou


New Load.B3  Bus1=B3  kV=132 kW=2400  kvar=1200  vminpu=0.9 vmaxpu=1.10    daily =  tou
New Load.B4  Bus1=B4  kV=132 kW=7600  kvar=1600  vminpu=0.9 vmaxpu=1.10    daily =  tou

New Load.B5  Bus1=B5  kV=132 kW=94200 kvar=19000 vminpu=0.9 vmaxpu=1.10   daily =  tou
New Load.B7  Bus1=B7  kV=132 kW=22800 kvar=10900 vminpu=0.9 vmaxpu=1.10   daily =  tou
New Load.B8  Bus1=B8  kV=132 kW=30000 kvar=30000 vminpu=0.9 vmaxpu=1.10   daily =  tou
New Load.B10 Bus1=B10 kV=33  kW=5800  kvar=2000  vminpu=0.9 vmaxpu=1.10    daily =  tou
New Load.B12 Bus1=B12 kV=33  kW=11200 kvar=7500  vminpu=0.9 vmaxpu=1.10    daily =  tou
New Load.B14 Bus1=B14 kV=33  kW=6200  kvar=1600  vminpu=0.9 vmaxpu=1.10    daily =  tou
New Load.B15 Bus1=B15 kV=33  kW=8200  kvar=2500  vminpu=0.9 vmaxpu=1.10    daily =  tou
New Load.B16 Bus1=B16 kV=33  kW=3500  kvar=1800  vminpu=0.9 vmaxpu=1.10    daily =  tou
New Load.B17 Bus1=B17 kV=33  kW=9000  kvar=5800  vminpu=0.9 vmaxpu=1.10    daily =  tou
New Load.B18 Bus1=B18 kV=33  kW=3200  kvar=900   vminpu=0.9 vmaxpu=1.10    daily =  tou
New Load.B19 Bus1=B19 kV=33  kW=9500  kvar=3400  vminpu=0.9 vmaxpu=1.10    daily =  tou
New Load.B20 Bus1=B20 kV=33  kW=2200  kvar=700   vminpu=0.9 vmaxpu=1.10    daily =  tou
New Load.B21 Bus1=B21 kV=33  kW=17500 kvar=11200 vminpu=0.9 vmaxpu=1.10   daily =  tou
New Load.B23 Bus1=B23 kV=33  kW=3200  kvar=1600  vminpu=0.9 vmaxpu=1.10    daily =  tou
New Load.B24 Bus1=B24 kV=33  kW=8700  kvar=6700  vminpu=0.9 vmaxpu=1.10    daily =  tou
New Load.B26 Bus1=B26 kV=33  kW=3500  kvar=2300  vminpu=0.9 vmaxpu=1.10    daily =  tou
New Load.B29 Bus1=B29 kV=33  kW=2400  kvar=900   vminpu=0.9 vmaxpu=1.10    daily =  tou
New Load.B30 Bus1=B30 kV=33  kW=10600 kvar=1900  vminpu=0.9 vmaxpu=1.10    daily =  tou
```

PV Implementation

```
! PV system definitions
// P-T curve is per unit of rated Pmpp vs temperature
// This one is for a Pmpp stated at 25 deg
New XYCurve.MyPvsT npts=4 xarray=[0 25 75 100] yarray=[1.2 1.0 0.8 0.6]
// efficiency curve is per unit eff vs per unit power
New XYCurve.MyEff npts=4 xarray=[.1 .2 .4 1.0] yarray=[.86 .9 .93 .97]
// per unit irradiance curve (per unit if "irradiance" property)
New Loadshape.MyIrrad npts=24 interval=1 mult=[0 0 0 0 0 0 0.1 0.2 0.3 0.5 0.8 0.9 1.0 1.0 0.99 0.9 0.7 0.4 0.1 0 0 0 0 .8]
// 24-hr temp shape curve
New Tshape.MyTemp npts=24 interval=1 temp=[25 25 25 25 25 25 25 25 35 40 45 50 60 60 55 40 35 30 25 25 25 25 25 25]
// **** plot tshape object=mytemp
// take the default line
// pv definition
New PVSystem.PV phases=3 bus1=B21.1.2.3 kV=33 kva=20000 irrad=.8  Pmpp=20000 wattpriority=yes
~ temperature=25 PF=1  effcurve=Myeff  P-TCurve=MyPvsT   model=1
~ Daily=MyIrrad TDaily=MyTemp  %cutin=0.1 %cutout=0.1

! Let the openDSS estimate the voltage bases
Set maxiterations=500

! Let the openDSS estimate the voltage bases
Set Voltagebases=[132, 33, 11, 1]    ! legal bases for this problem
```

Master code :

```
Clear   ! always have this as the first line before defining a new circuit

New Circuit.IEEE_30

! Define a really stiff 132 kV source for the slack bus
! (continue editing the VSOURCE object created by the New Circuit command)
~ BasekV=132  Bus1=B1   pu=1.06  MVASC3=5000000  5000000

! Define the circuit elements
Redirect Lines.DSS
!redirect pypypy.dss
Redirect Transformers.DSS

Redirect looods.DSS

Redirect Capacitors.DSS

Redirect Generators.DSS

!set mode = daily
!set stepsize = 1h
!set number = 24


! Let the openDSS estimate the voltage bases
Set Voltagebases=[132, 33, 11, 1]    ! legal bases for this problem
Calcvoltagebases



solve
```

Modeling 1-Phase Regulators as AutoTransformers

Single-phase voltage regulators are actually autotransformers. Since the beginning of DSS in 1997, we have traditionally modeled regulators as conventional, but low-impedance, two-winding transformers and controlled one of the windings with a RegControl device. The is the same approach we use for substation LTC models. This is easier than constructing an autotransformer by connecting the windings in a special way and, for the most part, it gives the same answer for distribution system analysis purposes.

There have been a few cases where it would have been advantageous to model line regulators as autotransformers. While we found workarounds for those cases, we have taken another look at modeling the regulators as autotransformers. This document describes one approach.

The problem is not that OpenDSS cannot model autotransformers. While there is no built-in autotransformer model (yet), you can construct an autotransformer by connecting the windings of 1-phase transformers appropriately. The problem, until recently, was that the RegControl element was not capable of properly controlling the tap position correctly. As of version 7.6.3 build 20, (version 7.6.3.20) this has been remedied and this document illustrates how to use the model.

The script in Figure 1 has been uploaded to the website under the Test folder. The script file name is **TestAuto.DSS**.

Figure 2 shows a schematic diagram of this simple test circuit. It consists of a 12.47 kV 3-phase source connected to the default SourceBus. Then there is a short line (default OpenDSS Line model) between SourceBus and the bus at the high-side of the regulator, Hbus.

One restriction in OpenDSS is that all conductors at a circuit element terminal must be connected to the same bus. They can be connected to different *nodes* at the bus, but they must be connected to the same bus. The autotransformer connection requires that winding 1 and winding 2 of the transformer share a node in common – where the series winding is connected to the common winding. So we have at least a couple of choices for making the autotransformer connection:

1. Connect both windings to the same bus with the node connections defined to make up the proper autotransformer connection between the series and common winding.
2. Connect the windings to different buses and use a short jumper (a Reactor element) to create the tie between the series and common windings.

Either option will work. For this example, we use the first option and connect both windings of the Transformer element to Xbus. To make things a little cleaner, a jumper is used to connect node 1 of Hbus to node 1 of Xbus. Thus it effectively appears that the regulator is between Hbus and Xbus. The jumper is a Reactor element with an impedance of 0 +j0.0001 ohms.

The transformer Auto1 has two windings: 1) the main (common) winding rated 7.2 kV and 2) the series winding rated 1/10 of that, or 0.72 kV. This give a nominal regulation range of +/- 10% as is common for standard step voltage regulators. By default, the transformer is assumed to have 32 taps from Mintap to Maxtap. For a standard two-winding transformer, Mintap defaults to 0.90 and Maxtap defaults to 1.10 to achieve the desired range from 10% buck to 10% boost. With the autotransformer model, we intend to use the entire Winding 2 as our tap winding. The tap range is defined from Mintap=-1.0 to

Appendix E

CVR Implementation by Autotransformers

Maxtap=1.0. Assuming the base (common) winding is rated at 1.0-pu voltage, this combination gives the same regulation range as the two-winding LTC-type transformer model we have been using traditionally.

```
Clear

// Script to Test RegControl on a transformer configured as an autotransformer

New Circuit.TestAuto
~ BasekV=12.47

New Line.Line1 Bus1=SourceBus.1.2.3 Bus2=Hbus.1.2.3

New REACTOR.Jumper  phases=1 Bus1=Hbus.1  Bus2=Xbus.2  R=0  X=0.0001

New Transformer.Auto1 Xl2=1 Phases=1 Windings=2
~ wdg=1 Bus=Xbus.1.0  kV=7.2   kVA=50
~ wdg=2 Bus=Xbus.1.2 kV=0.72  kVA=50  Maxtap=1.0 Mintap=-1.0
~ %loadloss=.1

New Load.Load1 Phases=1 Bus1=Xbus.1.0  kW=100 PF=.9 kV=7.2

Set voltagebases=[12.47]
calcvoltagebases

New REGCONTROL.Reg1 transformer=Auto1 winding=2 bus=Xbus.1  ptratio=60  vreg=125
~ maxtapchange=1

Set maxcontroliter=30

solve

Show Currents Elements
Show Voltage LN Nodes

Show Eventlog
show taps
```

Figure 1. Script for Autotransformer Test Case (TestAuto.DSS)

The impedance of Transformer.Auto1 is defined as 1% on a 50 kVA base. This brings up one difference between this modeling approach and the two-winding LTC-type transformer approach. The auto transformer components are designed to transformer 50 kVA, which allows the autotransformer to regulate about 500 kVA of load at 10% raise or lower. For a two-winding model, we would have defined the impedance as approximately 0.1% and the transformer kVA = 500 to make an equivalent model.

Note the polarity of the two windings (see the script and the diagram). This will be important for understanding the example where we actually get a voltage rise across the first winding.

One change that had to be made to the Transformer and RegControl element models is to allow for the null tap position where the winding 2 tap = 0. Negative tap positions were never a problem with the OpenDSS transformer model, but zero was. When the Regcontrol proposes a zero tap value, the Transformer automatically replaces that with a small non-zero value.

Also, note that the RegControl device is only permitted to make one tap change per control iteration.

This is not necessary, but was done in the example so we could verify that the model was working correctly.

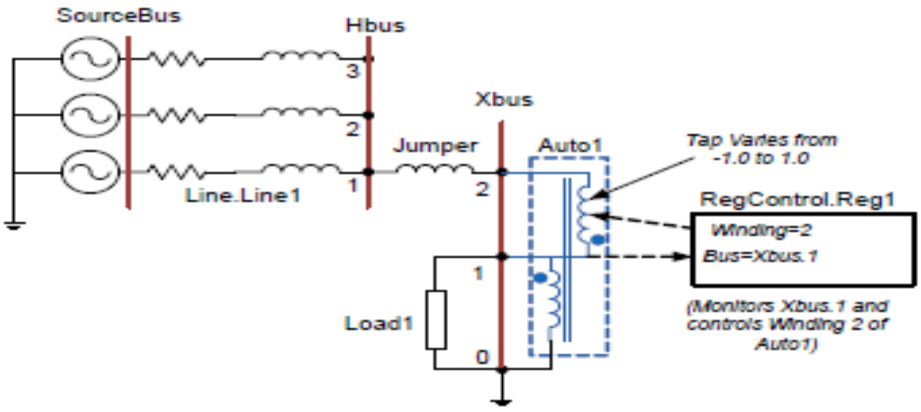

Figure 2. Autotransformer Test Circuit Schematic

The final "trick" to making this work is to have the RegControl monitor a bus voltage instead of the transformer's winding 2 voltage. In the normal OpenDSS model, the RegControl monitors the *winding* voltage. This is sufficient for the two-winding LTC-type transformer equivalent of the regulator, but the series winding voltage of the autotransformer will not necessarily correspond to the voltage we want the regulator to control. Fortunately, the RegControl has the option to monitor a selected bus voltage using the Bus property. This feature is more common used to model voltage regulation schemes that get voltage signals from remote locations. In this case we are having the RegControl monitor node Xbus.1, which is local to the regulator.

The RegControl controls winding 2 of the autotransformer (the series winding). Its algorithm adjusts the tap (one step at a time in this case) until the voltage being monitored falls within the band specified by the Vreg and Band properties.

> *Note: It is possible in this case that we could have told the RegControl that it was connected to Winding 1 and set the TapWinding property to winding 2. Thus, it would attempt to achieve the target voltage across winding 1 by adjusting taps on winding 2. However, this was not tested.*

SOLUTION

The solution summary from the test script is shown in Figure 3. It indicates there were 9 adjustments of the taps. The power flow is very easy to solve, so it only took two iterations per tap step.

```
Control Mode =STATIC
Total Iterations = 18
Control Iterations = 9
Max Sol Iter = 2
```

Figure 3. Solution Summary

You can see what is happening during the solution process by executing the **Show Eventlog** command. This is shown in Figure 4. That initial tap for the autotransformer winding 2 is 1.0, creating a 10% rise (see polarity of the series winding). So it must move the tap down to lower the voltage to the desired 125 V on a 120 V base (PTratio = 60). Each tap change is 0.0625 pu (5/8%), which is typical. When the process gets to tap position 0.5 (0.72 * 0.5 = 0.36 kV), the control objective is met. That is, the series winding adds about 360 V to the incoming 7196 V to get 7574.5 V. The resulting L-N voltage solution is shown in Figure 5.

The resulting voltage is 1.0521 pu = 126.25 V, which is within half the bandwith of 3 V specified for the regulation target. Note that if we had started off from a lower tap position and had to raise the tap to achieve the objective, the solution would have been different. With a 3 V bandwidth, it is common for there to be 3 valid solutions for a tapchanging regulator depending on the initial tap position. The present OpenDSS RegControl device stops changing the tap when the voltage enters the band. Other algorithms might try to get closer to the center of the band.

```
Hour=0, Sec=0, ControlIter=1, Element=Regulator.xotol, Action= CHANGED -1 TAPS TO 0.9375.
Hour=0, Sec=0, ControlIter=2, Element=Regulator.xotol, Action= CHANGED -1 TAPS TO 0.875.
Hour=0, Sec=0, ControlIter=3, Element=Regulator.xotol, Action= CHANGED -1 TAPS TO 0.8125.
Hour=0, Sec=0, ControlIter=4, Element=Regulator.xotol, Action= CHANGED -1 TAPS TO 0.75.
Hour=0, Sec=0, ControlIter=5, Element=Regulator.xotol, Action= CHANGED -1 TAPS TO 0.6875.
Hour=0, Sec=0, ControlIter=6, Element=Regulator.xotol, Action= CHANGED -1 TAPS TO 0.625.
Hour=0, Sec=0, ControlIter=7, Element=Regulator.xotol, Action= CHANGED -1 TAPS TO 0.5625.
Hour=0, Sec=0, ControlIter=8, Element=Regulator.xotol, Action= CHANGED -1 TAPS TO 0.5.
```

Figure 4. Event Log for Solution

```
NODE-GROUND VOLTAGES BY BUS & NODE

Bus          Node     V (kV)      Angle       p.u.     Base kV

SOURCEBUS    1        7.1988 /_     0.0     0.9999      12.470
   -         2        7.1995 /_  -120.0    0.99999      12.470
   -         3        7.1996 /_   120.0          1      12.470
EBUS  ....   1         7.196 /_     0.0     0.9995      12.470
   -         2         7.201 /_  -120.0     1.0002      12.470
   -         3        7.1993 /_   120.0    0.99996      12.470
XBUS  ....   1        7.5745 /_     0.0     1.0521      12.470
   -         2         7.196 /_     0.0     0.9995      12.470
```

Figure 5. Voltage solution

CVR CASE

Now, let's do something interesting with the model. Let's assume we want to go from regulating the voltage high at 125 V to adopting a conservation voltage reduction (CVR) approach and regulating to 118 V.

Figure 6 shows the script, event log, and tap report for moving from the present solution at 125 V to 118 V. First the Vreg property of RegControl.Reg1 is changed to 118 by the script command

```
regcontrol.reg1.vreg=118
```

Any property in OpenDSS can be changed using this syntax. This invokes the property editor for the named device and changes the value of the specified property. You can change multiple properties once the property editor is invoked for the specified circuit element, for example:

```
regcontrol.reg1.vreg=118 delay=25
```

After changing the Vreg property to 118, another power flow solution is made (solve). The resulting tap changes can be seen in the event log as shown in Figure 6.

```
regcontrol.reg1.vreg=118
solve
show eventlog

Hour=0, Sec=0, ControlIter=1, Element=Regulator.xvtol, Action= CHANGED -1 TAPS TO 0.9375.
Hour=0, Sec=0, ControlIter=2, Element=Regulator.xvtol, Action= CHANGED -1 TAPS TO 0.875.
Hour=0, Sec=0, ControlIter=3, Element=Regulator.xvtol, Action= CHANGED -1 TAPS TO 0.8125.
Hour=0, Sec=0, ControlIter=4, Element=Regulator.xvtol, Action= CHANGED -1 TAPS TO 0.75.
Hour=0, Sec=0, ControlIter=5, Element=Regulator.xvtol, Action= CHANGED -1 TAPS TO 0.6875.
Hour=0, Sec=0, ControlIter=6, Element=Regulator.xvtol, Action= CHANGED -1 TAPS TO 0.625.
Hour=0, Sec=0, ControlIter=7, Element=Regulator.xvtol, Action= CHANGED -1 TAPS TO 0.5625.
Hour=0, Sec=0, ControlIter=8, Element=Regulator.xvtol, Action= CHANGED -1 TAPS TO 0.5.
Hour=0, Sec=0, ControlIter=1, Element=Regulator.xvtol, Action= CHANGED -1 TAPS TO 0.4375.
Hour=0, Sec=0, ControlIter=2, Element=Regulator.xvtol, Action= CHANGED -1 TAPS TO 0.375.
Hour=0, Sec=0, ControlIter=3, Element=Regulator.xvtol, Action= CHANGED -1 TAPS TO 0.3125.
Hour=0, Sec=0, ControlIter=4, Element=Regulator.xvtol, Action= CHANGED -1 TAPS TO 0.25.
Hour=0, Sec=0, ControlIter=5, Element=Regulator.xvtol, Action= CHANGED -1 TAPS TO 0.1875.
Hour=0, Sec=0, ControlIter=6, Element=Regulator.xvtol, Action= CHANGED -1 TAPS TO 0.125.
Hour=0, Sec=0, ControlIter=7, Element=Regulator.xvtol, Action= CHANGED -1 TAPS TO 0.0625.
Hour=0, Sec=0, ControlIter=8, Element=Regulator.xvtol, Action= CHANGED -1 TAPS TO 0.
Hour=0, Sec=0, ControlIter=9, Element=Regulator.xvtol, Action= CHANGED -1 TAPS TO -0.0625.


CONTROLLED TRANSFORMER TAP SETTINGS

Name            Tap       Min       Max      Step  Position
xvtol       -0.06250 -1.00000   1.00000   0.06250        -1
```

Figure 6. Script and Event Log for Move from 125 V to CVR Mode, 118 V

Since the regulator needs to lower the voltage to the new set point, it taps down through tap 0 until it ends up one tap below neutral, or the null tap. This yields the voltages shown in Figure 7.

The voltage at the regulated bus (Xbus.1) is 0.9933 pu = 119.2 V. This is 1.2 V above the desired set point of 118 V, but is less than 1.5 V (half the3 V bandwidth). So it is an acceptable solution.

EPRI ELECTRIC POWER RESEARCH INSTITUTE

```
NODE-GROUND VOLTAGES BY BUS & NODE

Bus         Node     V (kV)     Angle       p.u.    Base kV

SOURCEBUS 1         7.1988 /_     0.0     0.9999     12.470
    -       2         7.1995 /_ -120.0    0.99999     12.470
    -       3         7.1996 /_  120.0          1     12.470
EBUS  .... 1          7.196 /_     0.0    0.99951     12.470
    -       2          7.201 /_ -120.0     1.0002     12.470
    -       3         7.1993 /_  120.0    0.99996     12.470
XBUS  .... 1         7.1513 /_     0.0     0.9933     12.470
    -       2          7.196 /_     0.0    0.99951     12.470
```

Figure 7. Voltage Solution for CVR Mode

```
clearall
clear

Compile Masterd.DSS


solve

! The compile builds the circuit model and sets the voltage bases

! sometimes this model needs more than the default 15 iterations
Set maxiterations=100


New Line.Linex Bus1=B12.1.2.3 Bus2=H.1.2.3

New REACTOR.Jumper phases=1 Bus1=H.1  Bus2=Bx.2  R=0 X=0.0001
New Transformer.Auto1 X12=1 Phases=1 Windings=2
~ wdg=1 Bus=Bx.1.0 kV=19 kVA=50
~ wdg=2 Bus=Bx.1.2 kV=1.9 kVA=50 Maxtap=1.0 Mintap=-1.0
~ %loadloss=.1

New Load.Loadx Phases=1 Bus1=Bx.1.0 kW=1500 PF=.9 kV=19
Set voltagebases=[132,33,11,1]
calcvoltagebases


New REGCONTROL.Reg1 transformer=Auto1 winding=2 bus=H  ptratio=60 vreg=300  band =3
~ maxtapchange=1
Set maxcontroliter=250
regcontrol.reg1.vreg=250
```

جـامعـــة النجاح الوطنية
كليـــة الدراســـات العليـــا

تأثير إدارة الطلب على الاجراءات المطبقة من قبل الشركات الكهربائية والتي تستخدم لتحسين شبكات التوزيع التي تتضمن الانظمة الكهروضوئية

إعداد
ملكة مصطفى عبد الرحيم حنحن

إشراف
د. معين عمر

قدمت هذه الرسالة استكمالا لمتطلبات الحصول على درجة الماجستير في هندسة القوى الكهربائية، من كلية الدراسات العليا، في جامعة النجاح الوطنية، نابلس- فلسطين.
2025

تأثير إدارة الطلب على الاجراءات المطبقة من قبل الشركات الكهربائية والتي تستخدم لتحسين شبكات التوزيع التي تتضمن الانظمة الكهروضوئية

إعداد

ملكة مصطفى عبد الرحيم حنحن

إشراف

د. معين عمر

الملخص

تناقش هذه الرسالة تأثير استراتيجيات إدارة جانب الطلب (DSM) على تحسين أداء أنظمة التوزيع في ظل التكامل الكبير لأنظمة الطاقة الشمسية الكهروضوئية (PV). تم إجراء دراسة حالة باستخدام برنامج OpenDSS وتطبيق شبكة الاختبار (IEEE-30). حيث تم دمج نظام كهروضوئي بقدرة 50 ميجاواط عند العقدة 21، وأظهرت النتائج انخفاضًا في إجمالي الفواقد الكهربائية في خطوط النقل من 9308.34 كيلوواط إلى 7742.83 كيلوواط.

في الوقت نفسه، تناولت الدراسة تأثير تطبيق استراتيجيات مختلفة لإدارة جانب الطلب على تحسين جودة الشبكة بعد إدخال النظام الكهروضوئي. حيث أدت استراتيجية التحكم المباشر في الأحمال (DLC) إلى خفض الفواقد إلى 5365.5 كيلوواط، بينما حققت استراتيجية التسعير حسب وقت الاستخدام (TOU) تقليلًا أكبر، حيث انخفضت الفواقد إلى 3736.9 كيلوواط. بالإضافة إلى ذلك، ساهمت استراتيجية خفض الجهد الكهربائي (CVR) في تحسين مستويات الجهد عبر الشبكة، حيث انخفض الجهد عند العقدة 21 من 1.0524 وحدة نسبية إلى 1.0442 وحدة نسبية، وعند العقدة 11 من 1.0819 وحدة نسبية إلى 1.0748 وحدة نسبية.

كشفت دراسة قدرة الاستيعاب أن زيادة مشاركة أنظمة الخلايا اشمسية تُسهم مبدئيًا في تقليل الفواقد الكهربائية، حيث لوحظت تخفيضات كبيرة عند مستويات مشاركة 15 ميجاواط، 30 ميجاواط، 50 ميجاواط، و70 ميجاواط، مع فواقد تقارب 9830 كيلوواط، 8000 كيلوواط، 7000 كيلوواط، و5800 كيلوواط على التوالي.

إلا أن تجاوز قدرة استيعاب 70 ميجاواط أدى إلى زيادة الفواقد، حيث وصلت إلى 7900 كيلوواط عند مستوى اختراق 150 ميجاواط، وتجاوزت 12200 كيلوواط عند مستوى اختراق 200 ميجاواط.

أثبتت الدراسة أن استراتيجيات إدارة جانب الطلب تسهم بشكل فعّال في الحد من هذه الفواقد حتى مع ارتفاع مستويات المشاركة. على سبيل المثال، خفضت استراتيجية التحكم المباشر في الأحمال الفواقد إلى حوالي 6000 كيلوواط، بينما خفضتها استراتيجية التسعير حسب وقت الاستخدام إلى 5000 كيلوواط عند قدرة استيعاب 200 ميجاواط. تبرز هذه النتائج الدور الحيوي لاستراتيجيات إدارة جانب الطلب في تعزيز كفاءة وموثوقية تشغيل أنظمة التوزيع في ظل التكامل الكبير لأنظمة الطاقة الكهروضوئية.

الكلمات المفتاحية: ادارة جانب الطلب (DSM)، الخلايا الكهروضوئية (PV)، التحكم المباشر بالطلب (DLC)، خفض الجهد الحفظي (CVR)، التسعير حسب وقت الاستخدام (TOU).